Figure 24. A) Ultimaker 2+ 3D picture. B) PLA molds fabricated by 3D printing.

3.2.3 Oxygen plasma equipment

An oxygen plasma processing apparatus referred to as an oxygen plasma cleaner or plasma etcher, serves as a pivotal device within a diverse array of scientific, industrial, and research contexts to cleanse, modify, or etch surfaces by utilizing a low-pressure O_2 gas plasma. This intricate process entails the deliberate generation of a controlled plasma environment, where O_2 molecules undergo dissociation into constituent atoms and ions. These reactive entities subsequently engage with the target surface to engender specific and predetermined outcomes.

This apparatus finds application across three distinct applications: removing organic residues from substrates, activating surfaces, and etching process. The latter two applications, with their pronounced implications for microfabrication, are particularly noteworthy. Notably, this thesis did not encompass any etching process, a technique that enables the precise formation of intricate patterns, designs, or features on a substrate while simultaneously conserving select areas via the targeted material removal. In the manufacturing phase of this research, the application of oxygen

plasma treatment served to induce alterations in the chemical attributes of PDMS, enhancing its hydrophilic affinity and facilitating adhesion to the adhesive side of the vinyl material. To proceed with an oxygen plasma treatment, several steps must be done for having an optimal surface activation:

Vacuum phase: evacuation of the chamber, a low-pressure environment is established. In the context of the utilized oxygen plasma, a vacuum level of 0.2 millibar is requisite for the successful initiation of this phase (Figure 25B).

Gas Introduction and Stabilization: O_2 gas is introduced into the vacuum chamber. The process entails a stabilization period, necessitating the synchronization of O_2 flow and vacuum forces. Based on laboratory experiments, an equilibrium at 0.3 millibar is discerned to manifest optimal operational conditions.

Radio frequency or microwave excitation and plasma generation: Plasma generation hinges upon the infusion of energy into the O_2 gas via either Radio frequency or microwave energy. This is affected by an oscillating electric field that augments the energy state of electrons, propelling them into heightened activity. Consequent interactions between these energetic electrons and O_2 molecules precipitate molecular dissociation, generating a composite amalgam of O_2 atoms, oxygen ions (O^+), and electrons, ultimately giving rise to a partially ionized gas (Figure 25C).

Ventilation Phase: Upon the culmination of surface activation, the radiofrequency activation is ended, O_2 supply curtailed, and air progressively reintroduced into the chamber (Figure 25D).

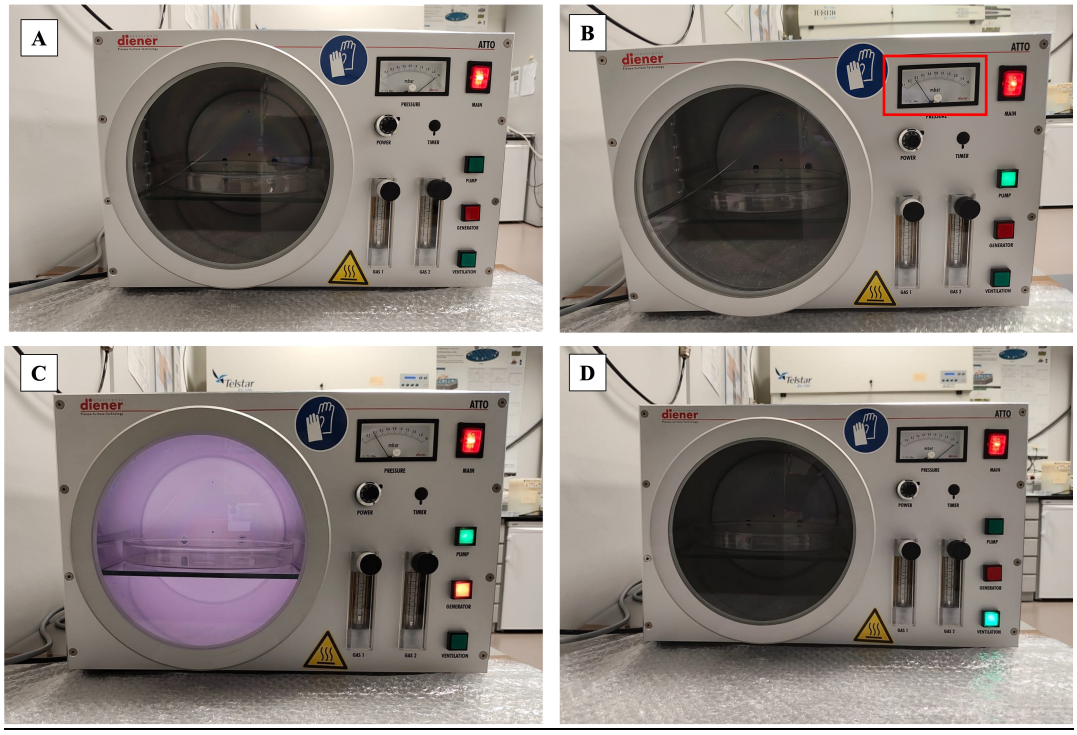

Figure 25. A) Oxygen plasma treatment and its most relevant stages: vaccum (B), plasma generation (C) and ventilation (D)

The equipment used for this thesis is a plasma device (Atto, Diener). Before conducting the plasma activation of PDMS, a chamber cleaning protocol is executed to eliminate any potential organic residues left inside the equipment's chamber from previous activation processes.

3.2.4 Autoclave

An autoclave is a device used for sterilization, which kills or eliminates all forms of microbial life, including bacteria, viruses, and spores. Autoclaves are commonly used in various fields, including medical, laboratory, pharmaceutical, and industrial settings, to ensure that equipment, instruments, and materials are free from potentially harmful microorganisms. The equipment subjects the items to high-pressure saturated steam at elevated temperatures. The combination of heat and moisture effectively destroys or inactivates the microorganisms on the surfaces and inside the items being sterilized. The steps involved in the autoclaving sterilization process are:

Loading: The items suitable for sterilization are placed inside the autoclave chamber. Since the autoclaving process can reach maximum temperatures of 134ºC, it cannot introduce elements or materials that are not able to withstand this temperature, being more critical in the case of plastics that can melt.

Sealing: The autoclave chamber is sealed tightly to prevent steam escape and maintain the pressure necessary for sterilization.

Air removal: Before initiating the sterilization cycle, air must be removed from the chamber and within the items. The presence of air can hinder effective steam penetration and heat transfer.

Steam injection and pressurization: Water is heated to generate steam, which is then injected into the chamber. As steam is introduced, the pressure inside the autoclave chamber increases. This elevated pressure raises the boiling point of water, allowing the steam to reach temperatures higher than the boiling point of water at atmospheric pressure.

Sterilization phase: The chamber temperature is maintained at a specific level, typically around 121-134ºC for a predetermined period, not less than 20 minutes. This combination of high temperature and pressure effectively kills microbial organisms, spores, and other contaminants.

Cooling: After the sterilization and drying phases are complete, the chamber is allowed to cool down gradually before it is safe to open. Rapid cooling can cause thermal shock to the materials and compromise their integrity.

Even if autoclaves are highly effective in killing most types of microorganisms, they may not eliminate certain types of prions, some viruses, and some bacterial spores, which have high resistance to heat and pressure. In such cases, additional sterilization methods or precautions may be necessary.

3.2.5 Perfusion pumps

Two types of pumps, perfusion pumps and peristaltic pumps, can be used to generate a continuous flow through a microfluidic devie. Perfusion pumps utilize mechanical or electronic mechanisms to deliver fluids with precision at a consistent and controlled flow rate, finding everyday use in applications requiring accurate and continuous fluid delivery such as tissue perfusion and drug testing. Offering uninterrupted and smooth fluid flow, they are crucial for stable experimental conditions necessitating precise infusion rates across extended durations. These pumps bestow researchers with exceptional control overflow rates, which is particularly advantageous for exacting fluid delivery in experiments. With their ability to deliver low-pulsatility fluid, perfusion pumps are well-suited for delicate tissues, sensitive cell cultures, and scenarios demanding consistent and smooth flow. Employed extensively in physiological, pharmacological, and tissue culture research, drug testing, and medical procedures, perfusion pumps play a critical role in maintaining continuous and precise fluid delivery. Notably, these pumps are characterized by their complexity and sophistication, often entailing higher costs attributable to their precision and advanced attributes.

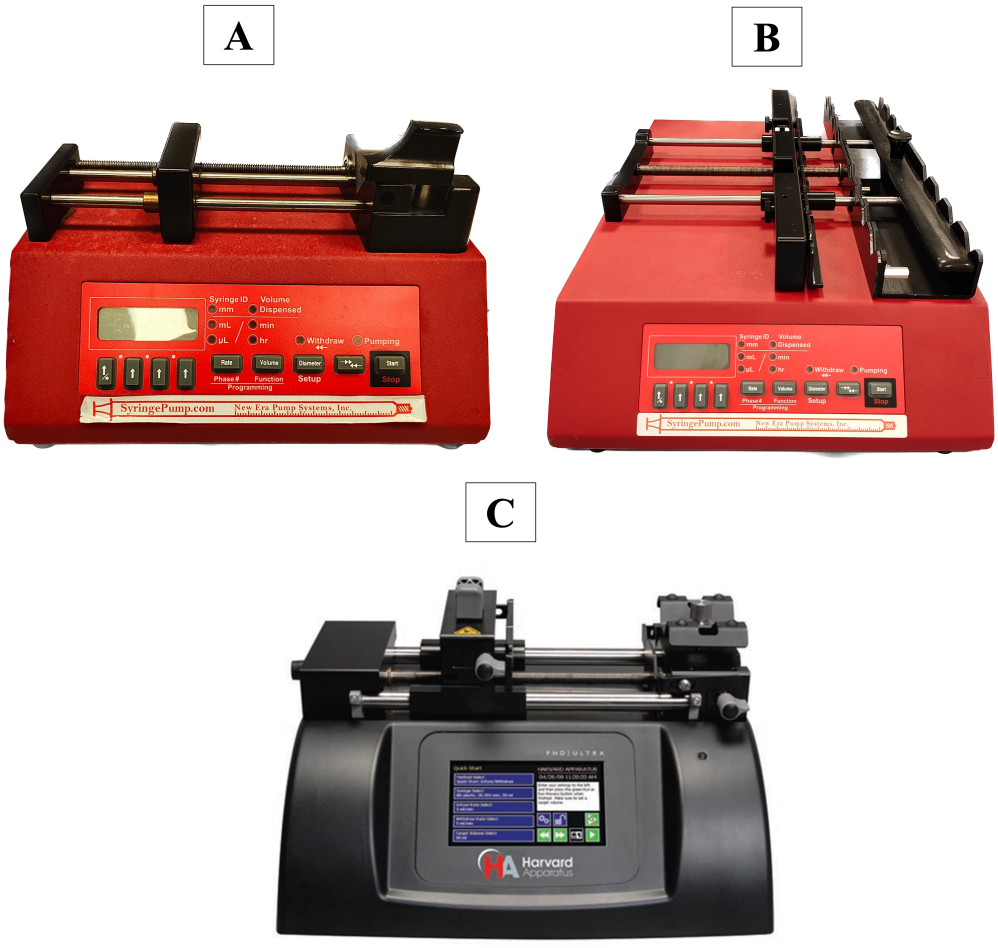

Figure 26. Syringe pump pictures: A) NE-300 syringe pump, B) NE-1800 syringe pump,, C) PHD Ultra syringe pump.

On the other hand, peristaltic pumps employ rotating rollers or pins to compress and release a flexible tube, engendering a pulsatile flow of fluid through its squeezing and propulsive action within the tube. This inherent pulsatility, derived from the cyclical compression and release of the tube, may make these pumps unsuitable for endeavors requiring continuous flow or those susceptible to pulsation. Despite their capacity to control flow rates, peristaltic pumps exhibit less precision than perfusion pumps, potentially requiring more frequent monitoring and calibration. This propensity for pulsatile flow, limiting their suitability for consistent applications, also informs their adaptability, rendering them particularly adept at tasks such as fluid transfer, chemical dosing, and container filling, primarily where uninterrupted flow holds secondary importance.

Considering the characteristics of both devices, this thesis has worked with perfusion pumps, precisely 12 syringe pumps of the NE-300 model (Figure 26A) for single syringe pump perfusion, one NE-1800 syringe pump with a capacity of eight syringes (Figure 26B), and a PHD Ultra syringe pump (Figure 26C). These microfluidic alternatives have been chosen because the volumes are minimal in some of the applications, and flow rates are relatively low, with a working range between 0.1 μL/min to 2 μL/min, being the best equipment to work with these workflows, since most of the peristaltic pumps cannot work correctly at such low rates in a precise way. Furthermore, OOC devices host cells inside, and high pulsatility poses a risk of damage to the cells, either by jeopardizing their integrity or by causing cells to be dragged off the chip. A final feature of perfusion pumps that is a benefit when working with these devices is the reduced risk of contamination. Perfusion pumps often use sterile, single-use fluid paths, storing the culture media in an airtight container such as a syringe, reducing the risk of cross-contamination between experiments and ensuring the integrity of biological samples.

3.2.6 Gassed incubator

A cell incubator is a specialized piece of laboratory equipment designed to provide a controlled environment for the growth, maintenance, and experimentation of living cells. It creates a stable and consistent atmosphere of temperature, humidity, and gas composition, allowing researchers to cultivate and study cells under conditions that closely mimic the physiological environment.

Incubators can maintain a precise and stable temperature. The temperature value is set in 37°C but it can be different in case of which is the standard body temperature of mammals but can be different in case of a non-mammalian cell culture. It is worthy to mention that these incubators are made to reach a temperature target, but they can barely dissipate the inner temperature if it is above the set value. Incubators ensure uniform temperature distribution throughout the chamber, minimizing temperature variations that could affect cell growth and experimental reproducibility.

Specialized gassed incubators for cell culture allow a particular feature, the administration and control of carbon dioxide levels, making them particularly useful for cell lines that require specific CO_2 concentrations to maintain the appropriate pH of the cell culture medium. The GOFB laboratories had two 108L (Memmert) capacity gassed incubators (Figure 27A).

While there are temperature and gas sensors (more specifically CO_2 sensors for incubators suitable for cell culture) there is no humidity control within these devices. Humidity is a relevant factor in the cultures to prevent desiccation and maintain optimal growth conditions, but it acquires a bigger role in the PDMS-vinyl-glass microfluidic chips developed in this doctoral thesis. The volumes of the fluidic compartments of the chips vary from 80 to 135 µL of total volume. A loss of volume due to the evaporation phenomenon if there is not a correct humidity in the culture environment has a great impact, being able to completely empty the chambers of the chips thanks to the gas permeability that PDMS possesses. For this reason, it is essential to ensure humidity conditions whenever working with OOC devices. Throughout the thesis, the perfusion pumps were initially housed inside the incubator, as were the other components of the microfluidic system (Figure 27B). This configuration was used in Chapters 4 and 5. In contrast, in Chapter 6, the perfusion pumps were moved outside the incubator to accommodate more chips running simultaneously, taking advantage of the additional space inside the incubator and allowing a higher amount of perfusion pumps outside (Figure 27C).

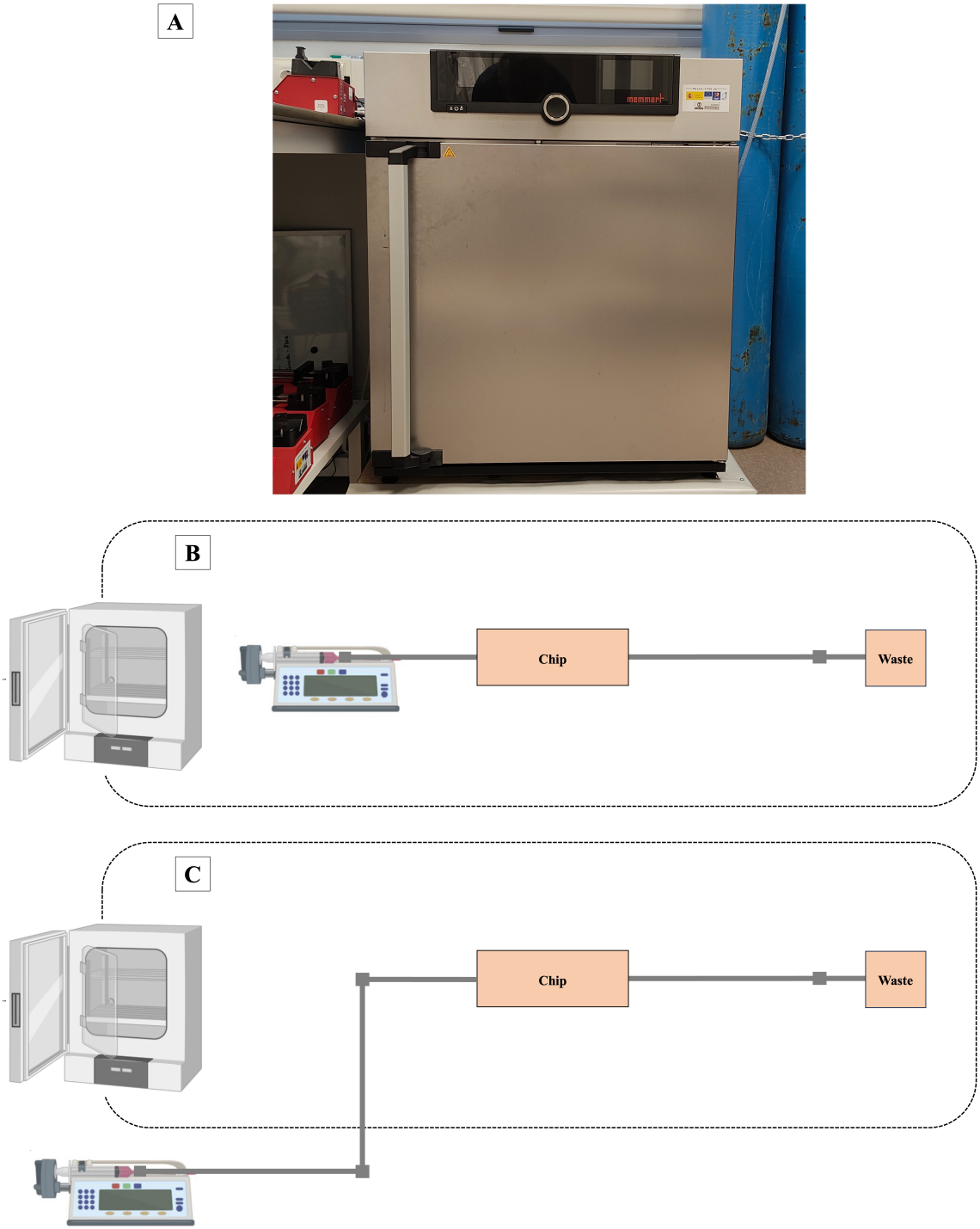

Figure 27. A) 108L Memmert gassed incubator. B) First microfluidic setup diagram, showing the entire fluidic platform inside the incubator, including the syringe pump. C) Second microfluidic diagram with the peristaltic pump located outside the incubator.

3.2.7 Optical imaging equipment

Microscopes are indispensable tools for the routine assessment of cell and tissue cultures. Throughout the development of this thesis, microscopy imaging has been the primary method

employed to assess cell distribution and viability in all conducted experiments using several microscopes.

In Chapter 4, image acquisition was carried out using a phase-contrast Nikon Eclipse TiS microscope equipped with an automated motorized XYZ stage controller and a DSFi1 camera (Nikon). This setup allowed for precise image merging, facilitating image superimposition, and indicating the lateral boundaries of the observed area.

Chapter 5 involved the use of two microscopes: the Olympus BX51 direct fluorescence microscope and the Leica DMI3000 B inverted fluorescence microscope, each paired with its respective camera, the Olympus DP70 and DFC 340 FX. The Olympus BX51 was employed for imaging samples cultured in OOC devices, while the Leica DMI3000 microscope was utilized for observing and capturing images of the control culture plates.

In Chapter 6, four microscopes were employed for image capture. The Leica DMi1 and Miotic SE2000 microscopes were used for daily monitoring of cultures. The Dmi1 microscope featured an MC170HD camera for image acquisition. In one phase of the thesis, when the capture program was non-operational, Figures 74,75 and 76 were captured by photographing the screen display. The Leica DMI3000 B microscope acquired fluorescence images in sections 6.2, 6.3.1, and 6.3.2. During the international stay at the University of Hull, two microscopes were used, one being the same SE2000 model. Figures presented without a scale bar in section 6.3.3 were captured using a smartphone through the binoculars of this microscope. Finally, the Olympus CKX43 microscope with the EP50 camera was employed for obtaining high-quality photographs. The specifications of every equipment are listed in Table 7.

Model	Manufacturer	Type	Camera	Camera manufacturer	Thesis sections
Eclipse TiS	Nikon	Phase-contrast	DsFi1	Nikon	Chapter 4
BX51	Olympus	Direct fluorescence	DP70	Olympus	Chapter 5
DMI3000	Leica	Inverted fluorescence	DFC 340 FX	Leica	Chapters 5,6
DMi1	Leica	Inverted	MC170 HD	Leica	Chapter 6
SE2000	Miotic	Inverted	None		Chapter 5, 6
CKX43	Olympus	Inverted	EP50	Olympus	Chapter 6

Table 7. Microscopes used throughout the doctoral thesis.

3.2.8 Laminar flow cabinet

A laminar flow cabinet, also known as a laminar flow hood, is a piece of laboratory equipment designed to provide a controlled, sterile, and particle-free working environment for tasks that require a clean and aseptic workspace. It is commonly used in various scientific, medical, and industrial settings where a sterile environment is crucial to prevent contamination and maintain the integrity of experiments or processes. The main feature of this equipment is a high-efficiency particulate air (HEPA) filter, which removes particles and microorganisms from the air. This filtered air is recirculated inside the cabinet with a unidirectional flow that to prevent airborne contaminants from entering the workspace. The airflow can be vertical, avoiding that any element introduced into the cabinet is expelled to the outside of the cabinet without being filtered, or horizontally, without allowing any external element to get inside the cabinet.

Vertical flow cabinets are used for cell culture protocols, such as cell culture manipulation and microbiological and virological work, where it is crucial to maintain a sterile environment to avoid cross-contamination-aseptic techniques. Equally important is the well-functioning of the cabinets for the operator, as it protects from biological samples, which can be hazardous. Horizontal flow cabinets are commonly used for sample preparation tasks, where a clean and

particle-free environment is needed to prevent contamination of samples or reagents, or for tasks that involve non-biological materials, such as handling powders, chemicals, and electronic components, where protection from external particles is essential.

Figure 28. Telstar Bio II Advance Plus 3 model picture.

Another method of classifying cabinets is according to the materials that can be worked with inside them. Class I protects the user and surrounding environment, but no protection for the sample being manipulated. Class II protects the user, environment, and sample. It is important to remark that flow cabinets do not protect against harmful chemical vapors or gases. The cabinet used throughout most of the thesis was the Telstar Bio II Advance Plus 3 model (Figure 28). This cabinet has UV lamps integrated in the Hood chamber to kill or inactivate any microorganism to maintain a sterile contamination free environment inside the cabinet. Ethanol is sprayed on the surfaces after ultraviolet exposure to ensure the sterility of the cabinet. Spraying ethanol on any objects or tools introduced into the cabinet for work with cell cultures, such as 1000, 200, and 10 µL pipettes, pipette tips, tube racks, syringes, and more, is also necessary.

3.3 CELL CULTURE BIOLOGICAL SAMPLES

The fabricated chips in this thesis have been used to regenerate three study models: an invertebrate neuronal model, a mouse hippocampal brain slice model, and a skin model mainly using human cells. In order to understand the particularities of each culture, it is essential to know the origin of

each biological sample. It can be made a distinction between primary cell/tissue culture and cell line cultures.

Primary cultures are those in which the sample, either cells or tissues, have been isolated directly from a target organism maintaining its characteristics such as cell morphology and functionality. This characteristic of primary cultures defines their performance in vitro cultures. The origin of the primary cells implies having a more realistic model where cells capture the cellular diversity present in the original tissue, which can be advantageous for studying tissue-specific responses, and they also keep a genetic heterogeneity.

Primary cultures have a more significant challenge in obtaining a stable culture over a prolonged time due to their limited lifespan. Primary cells allow a limited and finite number of cell divisions; once this limit is surpassed, they enter a state of senescence or cell death. Furthermore, primary cells can be more difficult to culture than immortalized cell lines since they have not undergone extensive manipulation or transformation in a laboratory setting. In contrast, cell lines are derived from primary cells but have been cultured for multiple generations, often undergoing genetic and phenotypic changes that can make them easier to maintain and grow in culture. Ethical issues are the last drawback that does not exist with commercial cell lines. Ethical approval and consent from the individual will likely be required when the origin of the primary cells are human beings.

Cell lines, as discussed above, are characterized by having been transformed to become immortal, allowing them to divide indefinitely having longer lifespan. This feature makes cellular lines the best option for long-term studies rather than primary cultures due to their greater genetic and phenotypic stability, allowing cell characteristics to be maintained over multiple splits with greater consistency.

During the development of the doctoral thesis, it has been possible to work with both types of cultures. On the one hand, the neuron-on-a-chip and brain slice-on-a-chip bioapplications are based on primary cultures obtaining the samples by dissection protocols. For the SOC bioapplication, commercial cell lines have consistently been employed, with the exception of one cell type. All the characteristics of the biological samples cultured on the chips are shown below.

Animal models remain essential in neuroscience for their ability to provide a controlled environment and opportunities for invasive procedures that are often infeasible or unethical in humans. The complexity of the human brain necessitates simplified models to study basic principles, disease mechanisms, and potential therapies. While alternative methods are explored, animal models are crucial in advancing our understanding of the brain and its functions. For this reason, animals of *Schistocerca gregaria* (desert locus) and *Mus musculus* (mouse) were euthanized to develop neuron-on-a-chip and brain slice-on-a-chip models. All necessary biosafety measures for handling and humanely sacrificing the animals received approval from the bioethics

committee of the Research Ethics Committee at the Universidad Politécnica de Madrid. These procedures adhered rigorously to the welfare guidelines outlined by the European Commission for experimental animals (Directive 2010/63/EU, Directive 86/609/EEC).

3.3.1 *Schistocerca gregaria* neurons – extraction and culture conditions

Schistocerca gregaria, commonly known as desert locusts, is an animal model being used as a approximation of neuronal systems because the size of neurons is larger than in mammals, facilitating culture monitoring. The animals were fed wheatgrass in a cage under a 12:12-hour light:dark cycle.

The experiments performed in this thesis have required the sacrifice and dissection of several desert locusts. For each culture, 12 ganglia were extracted from the frontal ganglion of the locusts, containing about 100 neurons per ganglion. After dissection of the individuals, ganglia were then forced to pass through the tip of a 1 mL pipette to mechanically dissociate the neurons and subjected to enzymatic treatment with a collagenase/dispase mixture 2 mg/ml (Roche, Indianapolis, USA) to cause dissociation of the neurons and the connections already established between them. Finally, a solution of 150 µL of dissociated neurons was obtained in Leibovitz's L-15 medium supplemented with L-glutamine (2,5 mM, Sigma Aldrich/Merck) and 0.01% penicillin-streptomycin (Pen/Strep) (Biological Industries).

3.3.2 CD-1 mice – brain slice obtention and culture conditions

CD-1 mice (*Mus musculus*), an outbred mouse stock commonly employed in toxicology, pharmacology, and fundamental biomedical research, exhibit genetic diversity akin to wild mice and possess a larger body size than many other laboratories mouse strains, making them particularly advantageous for experiments requiring substantial tissue samples or surgical procedures. The last characteristic was a differential factor in selecting this mouse strain to obtain larger, more consistent brain samples.

Seven-day-old male CD-1 mice were obtained from a breeding colony situated in CTB. These mice were housed under controlled conditions, including a 12-hour light:12-hour dark cycle, a temperature maintained at 22°C ± 1°C, and unrestricted access to food and water. Upon euthanasia and decapitation, their brains were promptly extracted and submerged in ice cold Dulbecco's Modified Eagle Medium (DMEM) high glucose (Gibco) medium. Brain slices were dissected, ensuring the removal of the choroid plexus and meninges; this process was conducted under the guidance of a dissecting microscope. The dissected brains were transversely sectioned into 400 µm thick slices using a VWR tissue chopper (Stoelting). For long term culture, the media

used was DMEM-high glucose supplemented with 20% Horse Serum heat-inactivated (Gibco) and 1% antibiotic and antimycotic solution (Thermo Fisher Scientific).

3.3.3 CV-1 cell line – culture conditions

The CV-1 cell line is a fibroblast cell line isolated from the kidney of the African green monkey (*Cercopithecus aethiops sabaeus*). It was first isolated in 1952 by Harry Eagle and Robert Koprowski from the kidney cells of an African green monkey that had been infected with poliovirus. CV-1 cells are of the adherent growth type, requiring attachment to a surface for growth and proliferation, resulting in an elongated morphology (Figure 29). This cell line is immortalized, allowing indefinite division of cells in culture. CV-1 cell line played a pioneering role in testing dual-chamber chips to evaluate the ability of adherent cells to adhere to candidate membranes.

For the culture of these cells, the culture medium used was DMEM (Gibco), supplemented with L-glutamine (2 mM), 10% fetal bovine serum (FBS) (Gibco) and 1% Pen/Strep (Gibco) reagent.

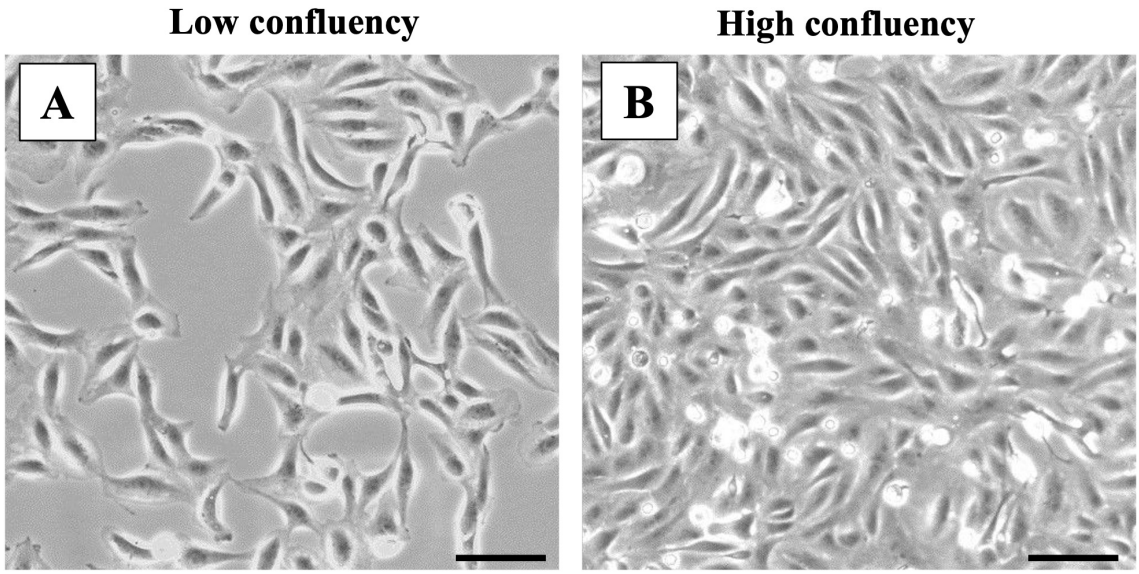

Figure 29. Pictures of a CV-1 culture in low and high confluency. Extracted from Cell Lines Service (cls.shop). Scale bars represent 100 µm.

3.3.4 Primary human fibroblast (PHF) cells - culture conditions

In the development of the SOC model, human fibroblast cell lines were also evaluated to create a skin model composed entirely of human-origin cells. One of the alternatives involved the use of human primary fibroblasts (PHF) provided by the Tissue Engineering and Regenerative Medicine group of the Universidad Carlos III de Madrid. Primary cells resemble in vivo human cells more

closely than cells cultured in a laboratory environment. This quality enhances the understanding of normal human cell biological processes and allows the study of a broader range of diseases that cannot be adequately investigated using lab-cultured cells.

The culture medium for these cells consisted of DMEM-F12 (PAN Biotech), which is DMEM supplemented with L-glutamine, HEPES buffer (15 mM), and $NaHCO_3$ (1.2 g/L). The medium was enriched with 10% FBS (Gibco) and 1% Pen/Strep antibiotic.

3.3.5 HFF-1 cell line - culture conditions

HFF-1 cells are human fibroblasts isolated from normal human foreskin pooled from two individuals. These cells constitute an immortal cell line, enabling them to multiply indefinitely in culture, and they typically exhibit a spindle-shaped morphology, a hallmark of fibroblast cells. HFF-1 cells have diverse applications, including their use in cancer research. They serve as a valuable model for investigating the stromal component of tumors, examining interactions between this stroma and cancer cells, and conducting experiments on cancer cell invasion and migration.

For cell culture, HFF-1 cells are grown in DMEM – high glucose (containing 4,5g/L of D-glucose, L-glutamine, sodium pyruvate, sodium bicarbonate, and phenol red, Sigma Life Science). The medium is supplemented with Pen/Strep (1%), L-glutamine (1%), and 10% unfiltered, heat-deactivated FBS (10%).

3.3.6 HaCaT cell line - culture conditions

The HaCaT cell line comprises immortalized human keratinocytes derived from adult human skin. Keratinocytes represent the predominant cells in the epidermis, forming the primary protective barrier of an organism. Typically, HaCaT cells display an epithelial-like morphology characterized by a polygonal “brick” shape, with a tendency to form monolayers when cultured (Figure 30). HaCaT cells are commonly cultivated in Petri dishes or culture flasks and can be cultured in various media; being the most frequent DMEM supplemented with FBS.

For experimentation, HaCaT cells were cultured using two distinct media compositions. In the experiments conducted in the CTB, they were cultured in DMEM-F12 medium (PAN Biotech) supplemented with FBS (10%) and Pen/Strep (1%). In contrast, the culture medium employed in Hull consisted of DMEM with L-glutamine (1%), $CaCl_2$ (2.8 mM), FBS (10%), and Pen/Strep (1%).

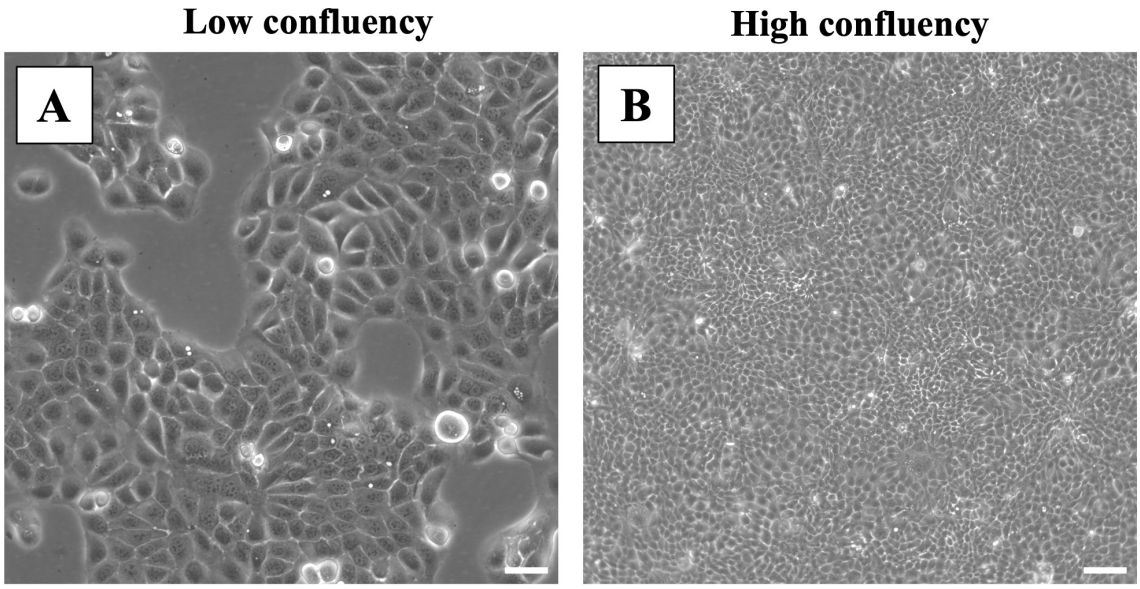

Figure 30. Pictures of a HaCaT culture in low and high confluency. Extracted from ATCC (atcc.org). Scale bars represent 100 µm.

3.3.7 U937 cell line - culture conditions

U937 is a human cell line originating from the pleural effusion of a patient with histiocytic lymphoma. They are derived from monoblastic cells, which are a type of white blood cell precursor. This cell line has been used extensively in research to study the biology of monocytes and macrophages. This is possible due to the ability to differentiate U937 cells by exposing stimuli such as phorbol esters like phorbol 12-myristate 13-acetate (PMA) into a more mature macrophage-like phenotype. U937 cells typically have a round, oval morphology with a single nucleus in the undifferentiated state (Figure 31). After differentiation, they exhibit a more adherent and extended morphology.

U937 cells are suspension cells, and therefore, the culture medium employed consists of RPMI (PAN Biotec) complemented with L-glutamine (1 mM), Pen/Strep (1%), and FBS (5%).

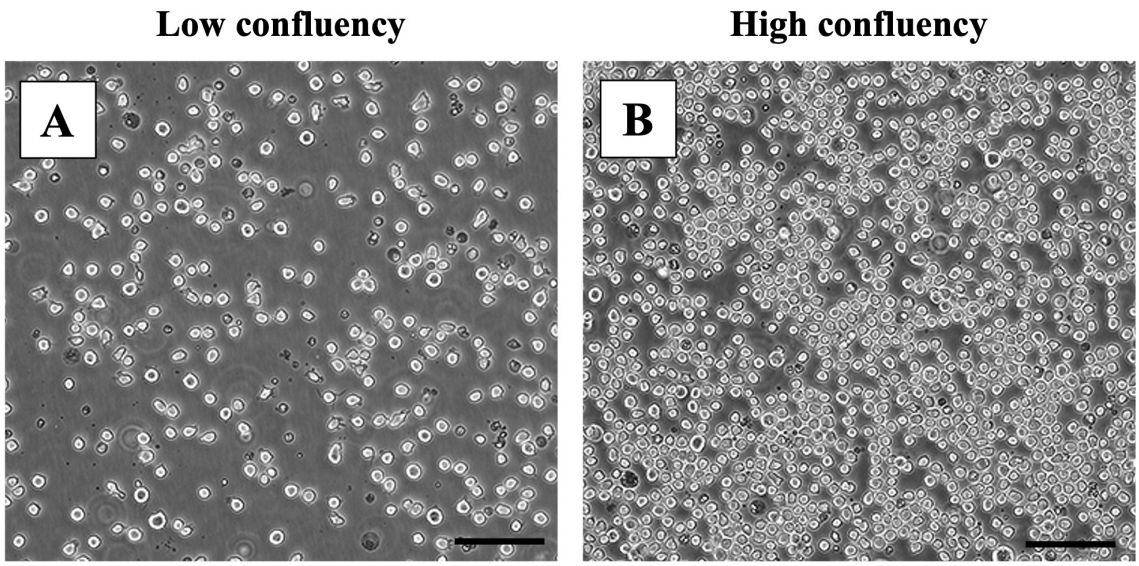

Figure 31. Pictures of a U937 culture in low and high confluency. Extracted from ATCC (atcc.org). Scale bars represent 100 µm.

3.3.8 Jurkat cell line - culture conditions

Jurkat cells, derived from a patient with acute T cell leukemia, are a representative model for exploring the biology and functions of T lymphocytes. These cells exhibit a typical lymphocytic appearance, characterized by a small, round morphology and a single nucleus (Figure 32).

Their extensive use in research has contributed to our understanding of T lymphocyte biology and their roles in immune responses to infections and cancer. Jurkat cells can differentiate into various T helper lymphocytes, cytotoxic T lymphocytes, and natural killer cells, enabling researchers to explore the influence of diverse factors on T lymphocyte differentiation and function.

These cells naturally reside in the bloodstream and are categorized as suspension cells. Their culture medium consists of RPMI (Gibco) supplemented only with filtered FBS (10%).

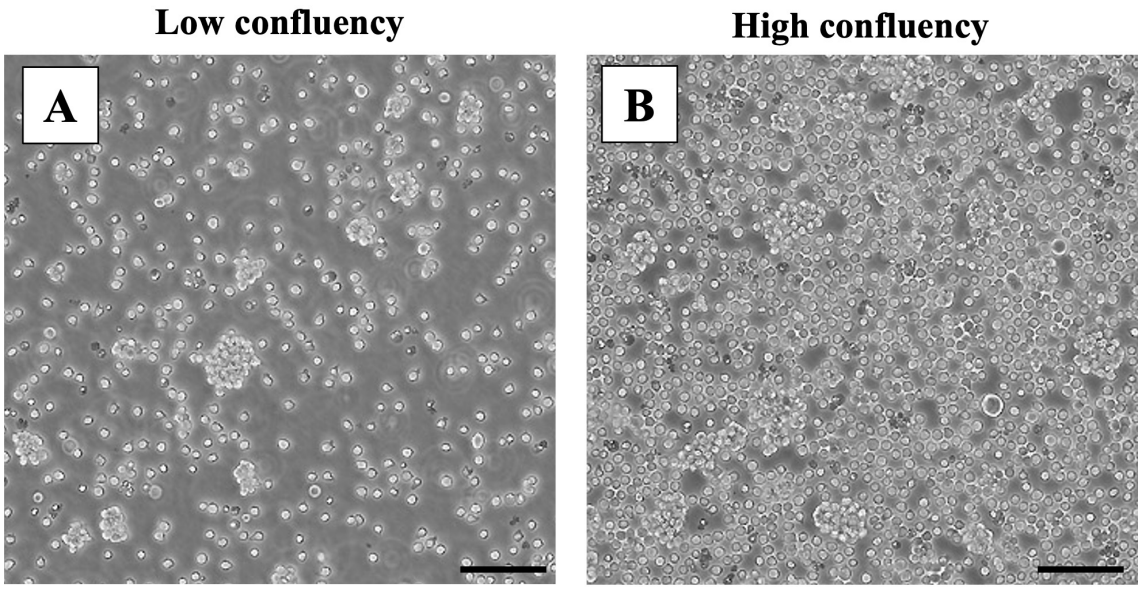

Figure 32. Pictures of a Jurkat culture in low and high confluency. Extracted from ATCC (atcc.org). Scale bars represent 100 µm.

3.3.9 SK-MEL-28 cell line - culture conditions

The SK-MEL-28 is an immortalized cell derived from melanocytes found in the skin tissue of a 51-year-old male patient with malignant melanoma.

SK-MEL-28 cells are a widely used model for studying melanoma biology due to their human origin and ease of culturing in laboratory settings. These cells can differentiate into various cell types, including melanocytes, dendritic cells, and inflammatory cells. Researchers have extensively utilized SK-MEL-28 in studies focused on melanoma biology, drug development, vaccine testing, and gene therapy efficacy against melanoma.

Similar to other cells found in epithelial tissue, SK-MEL-28 cells are adherent, requiring attachment to a surface for growth (Figure 33). The culture medium used for SK-MEL-28 cells is the same as that used for HaCaT and PHF cells: DMEM-F12 medium (PAN Biotech) supplemented with 10% FBS and 1% Pen/Strep.

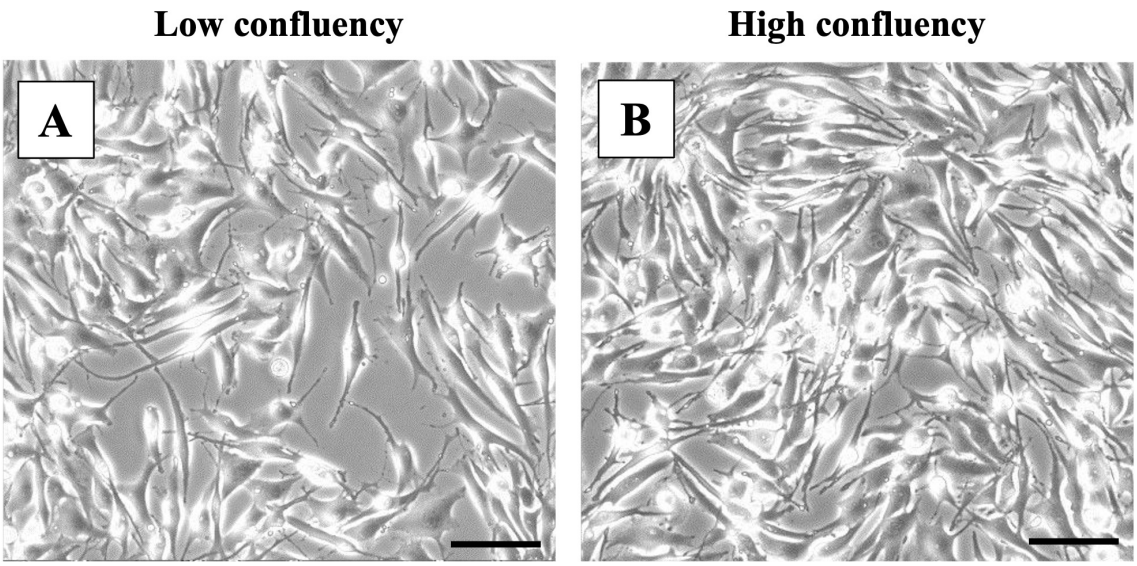

Figure 33. Pictures of SK-MEL-28 culture in low and high confluency. Extracted from Cell Lines Service (cls.shop). Scale bars represent 100 μm.

3.4 CELL CULTURE VIABILITY AND CONFLUENCY ANALYSIS

Depending on the type of cells being cultured in each of the applications, different values of temperature, CO_2 supply (or its absence), culture media, culture volumes and specific flow rates are required. In the same way there are different methodologies depending on the culture method and the components of the microfluidic chips to evaluate the viability and confluence of the cultures. In this subheading it is specified the culture conditions in the three different models that have been developed, since each case requires specific conditions.

3.4.1 Neuron-on-a-chip culture evaluation

The viability and confluence study conducted in this application was based on acquiring images of the entire culture area to assess cell migration and development of connections between neurons, ultimately resulting in the formation of a complex neural network over time. After the experimental phase, all images underwent analysis using an image segmentation algorithm implemented in MatLab (Gourley et al., 2002). This algorithm was employed to analyze the positioning of neurons and the evolution of the neural network in each image.

To comprehensively monitor the network's development, a longitudinal assessment was conducted, focusing on several commonly studied graph parameters:

1. The total number of connected nodes: This parameter provided valuable insights into the overall extent of connectivity within the network, indicating the number of interconnected nodes.

2. The average clustering coefficient: This metric delved into the density of local network connections, highlighting the degree to which nodes within proximity were densely linked. It served as a measure of the network's tendency to form tightly connected clusters.
3. The shortest path length: This parameter was computed with the largest connected component of the network. It quantified the topological distance between nodes, shedding light on how far nodes were from each other within the network.

The leverage clustering coefficient and shortest path length are key factors to elucidate the balance between local and long-distance connectivity dynamics within the evolving network.

3.4.2 Brain slice-on-a-chip viability evaluation by fluorescence staining

The brain slice-on-a-chip experiment is based on adapting traditional interphase cultures in a microfluidic chip. Brain slices with a thickness of 400 μm were transferred to both microfluidic chips and P24 culture plates, maintaining both cultures in cell incubators at 37ºC with 5% CO_2 with humidity. The brain sections were placed over a PC membrane and the brain slices were placed over a commercial PTFE membrane insert.

The viability study to evaluate the condition of the brain slices was done with the fluorescent dye Oregon Green Bapta 488 (Thermo Fisher). The calcium indicator dye stock solution at 5mM was prepared mixing a solution of 20% (weight/volume) Pluronic F-127 in absolute dimethylsulphoxide (DMSO). A final volume of 50 μL of OGB solution (20 μM) was administered per chip as well as the control slices. Both the chip sections and the well plate slices were incubated for one hour in the gassed incubator. After this period, the transwells hosting the brain sections were transferred to a new well to reduce background fluorescence. In case of the brain slice-on-a-chips an incubation flow rate of 0.1 μL/min was established to ensure proper dye penetration into the chip.

Throughout the imaging process, the chip remained sealed, enabling real-time analysis of the slices within the chips. Pictures were acquired using both a direct fluorescence microscope, specifically the Olympus BX51 and an inverted fluorescence microscope, the Leica DMI3000 B.

3.4.3 Skin-on-a-chip culture and viability evaluation

Seven different cell types were used to recreate the skin-on-a-chip model: three different fibroblasts variants, CV-1 cells, HPF cells, and HFF cells, plus three other cell types, HaCaT cells, SK-MEL cells, U937 cells, and Jurkat cells. A large number of combinations of co-cultures have been performed in order to achieve the most viable skin model.

The evaluation of cell viability and confluence has been performed with three different markers. The first one is the Oregon Breen Bapta 488, replicating the concentration and volumes indicated for the mouse brain sections: 50 µL of a 20 µM solution. The new ones, CMFDA and CMTPX, were used to check the distribution of cells in the co-cultures performed on the chip, each cell type being labeled with a different marker.

CellTracker Green CMFDA and CellTracker Red CMTPX (Thermo Fisher Scientific) fluorescent dyes are designed to permeate cell membranes and undergo intracellular transformations, resulting in cell-impermeant, fluorescent products that are retained through multiple cell generations. These dyes are inherited by daughter cells but not transferred to neighboring cells within a population. Both dyes offer prolonged fluorescence for at least 72 hours, characterized by stability, low toxicity at working concentrations, robust retention within cells, and vivid fluorescence under physiological pH conditions. The excitation and emission spectra are 492/517 nm for green CMFDA tracker and 577/602 nm for CMTPX dye, being sufficiently distant to visualize each emission signal on different microscope filters. Unlike the OGFB dye, the technical specifications of these two reagents emphasize the transmission of the fluorescent signal to the daughter cells. This feature was irrelevant in the culture of mouse brain slices since the tissue sample is a nerve tissue that will gradually lose its morphology, and the cells do not have a high division rate. However, signal transfer in the SOC model acquires great importance as the cells that make up the culture will be dividing continuously, and therefore, CMFDA and CMTPX dyes allow us to study the distribution of cells in a confined area, and whether one cell type is predominant over others.

The two reagents are stocked in 50 µg vials of lyophilized sample. The final working concentration is 1µM. Because of that, a stock solution of 1 mM CMFDA and CMTPX must be prepared by dissolving the 50 µg in 20 µL of DMSO, which can be stored at -20°C. When it is necessary to administer one of the dyes, a new final working solution of 1 µM has to be prepared in DMEM-12 medium, which is the culture media employed for the HFF-HaCaT-SK-MEL co-culture.

The working solutions of CMFDA and CMTPX can be administered to adherent cells cultured on a surface or when cells are in suspension before seeding. This versatility in cell labeling is a great advantage, as the cells cultured on the chip membranes can be labeled first, and then the second cell type of interest can be seeded before seeding.

3.5 SOFTWARE DESIGN

Every layout made in this thesis was novel and designed by the student. To accomplish this task, the Universidad Politécnica de Madrid has access to and licenses for several design programs,

including Autodesk programs. Among these, AutoCAD has been used for creating 2D designs, and Solid Edge for the 3D modeling chip designs.

AutoCAD is a widely used computer-aided design software developed by Autodesk. It is a versatile tool for creating precise, detailed 2D drawings, designs, and other 2D representations. Its extensive range of drawing tools, measurement capabilities, and drafting features simplifies the process of creating scaled and intricate designs.

Solid Edge is another software computer-aided design software developed by Siemens Digital Industries Software, for 3D design applications. It serves as a comprehensive platform to create, visualize, and simulate complex three-dimensional mechanical and industrial designs. The software offers a wide range of tools and features that enable the creation of detailed and accurate 3D models of mechanical parts and assemblies if needed. It also supports parametric modeling, which establishes relationships between components, ensuring that design changes are seamlessly incorporated throughout the model. This program was employed to create 3D reconstructions of the OOCs and to generate 3D designs that were manufactured using Ultimaker M2 3D printing.

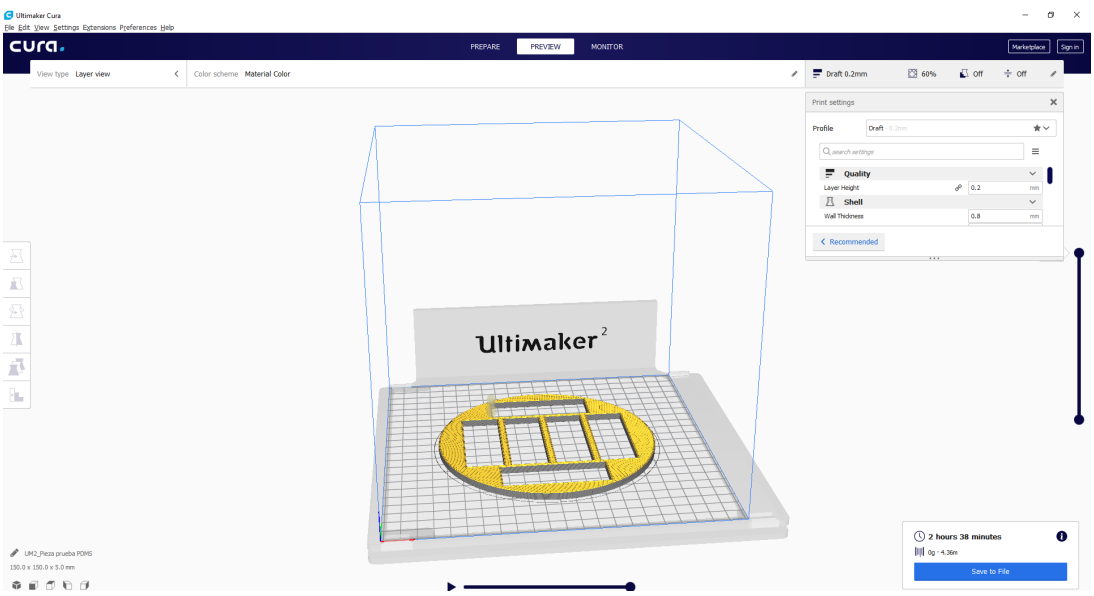

Figure 34. Screenshot of the Ultimaker4.1.0 program..

To convert the STL layout files into the printer's native format, the Ultimaker 4.1.0 program must be used for this purpose (Figure 34). This software permits the selection of various printing parameters, including extrusion material, filament thickness, quantity of 3D parts filling, and more. Temperature parameters are automatically determined once the extrusion material is selected.

The last software employed was Summa Winplot program, which was used to load layouts for cutting on the plotter (Figure 35). Although the technical data sheet of the equipment specifies

.dxf format (the standard one for 2D design) is compatible with the program, it was impossible to open files in this format. Because of this, it was necessary to convert the .dxf to .ai files that could be opened correctly in the software. The only parameter that can be adjusted using Summa Winplot is the number of cuts per design; the rest are configured directly on the equipment's touchscreen.

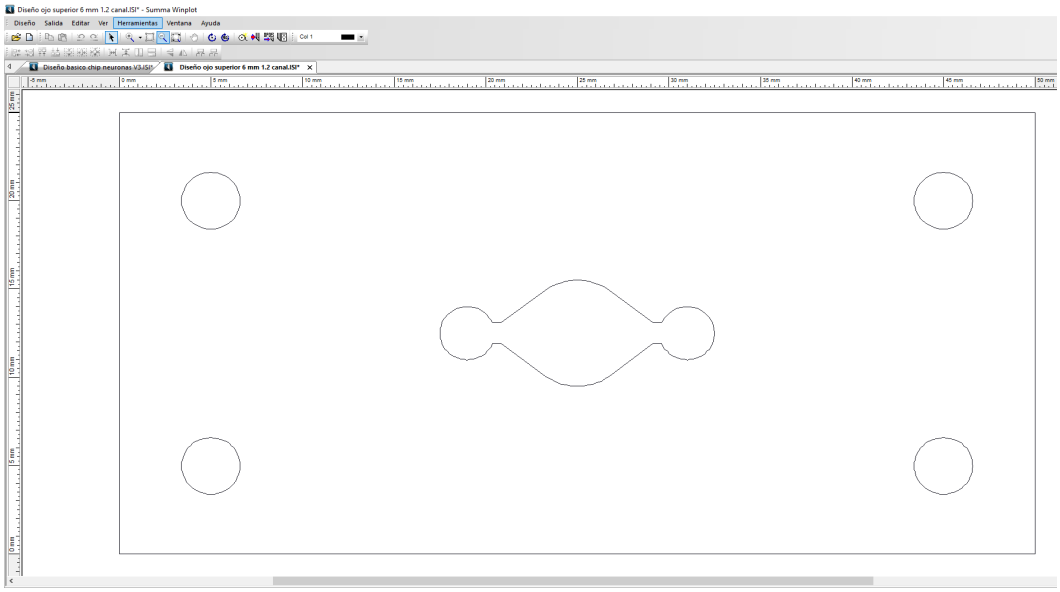

Figure 35. Screenshot of the Summa Winplot program.

4 NEURONAL CIRCUITS ON A CHIP

The first microfluidic chips of this thesis were designed to recreate a neuron-on-a-chip device in collaboration with Biological Networks group located in the CTB. One of the research lines of this group is the analysis of the formation and evolution of neural networks, mainly in invertebrates. These studies are conducted using MEAs, unique devices featuring a network of electrodes for studying nerve impulse transmission through neurons. The methodology used by this group consists of culturing the neurons of *Schistocerca gregaria* locusts in culture plates or on MEAs and monitoring the evolution of the culture by microscopic imaging. Subsequently, an analysis of the position of the neurons and the network formed is performed using computer software.

Neuron culture presented several challenges. The primary issue was the uneven distribution of neurons on the culture surface. To optimize the study of neuronal networks, reducing the distance between cells is essential, concentrating the cell population within a specific 5 mm area on the culture surface or MEAs. When pipetting cells onto the culture surface, the droplets containing neurons often spread beyond the desired area. This dispersion results in increased cell-to-cell distances, reducing cell density per unit area.

The second challenge is related to the culture conditions of neurons, especially desert locust neurons. It is essential to supplement the culture medium with hemolymph extracted from the locusts to promote the formation of connections between neurons. However, this process faces several limitations. These include the limited volume of sample that can be extracted from each individual, the skill and expertise required for the extraction procedure, and the quality of the extracted hemolymph. In addition, a critical issue arises because of melanin, a molecule contained in the hemolymph, which is produced by the neurons themselves. The accumulation of melanin can be cytotoxic due to the activity of phenol oxidase, potentially harming cells. This circumstance imposes constraints on the duration of neuronal network studies.

The use of the microfluidic chip in this bioapplication aims to enhance culture conditions. Firstly, it allows to delimitste the culture area within the microfluidic chamber's geometry, concentrating all neurons within a specific, defined area. Secondly, it provides greater control over the culture

microenvironment by facilitating the perfusion of the culture medium, thereby preventing the accumulation and excessive exposure of hemolymph to the cells.

This application is ideal for the first testing of a new OOC, as it only requires a single flow within the chip with relatively simple geometry (Figure 36).

The objectives of this chapter are:

- To establish a fabrication methodology for microfluidic chips made from PDMS, glass, and vinyl compatible with cell culture.
- To design a chip capable of accurately defining the cell seeding area, addressing the limitations associated with traditional plate cultures.
- To conduct a comparative study between the neuron-on-a-chip developed for this bioapplication and the culture plates. The aim is to assess whether there is an improvement in neuronal network formation, stability, and long-term maintenance.

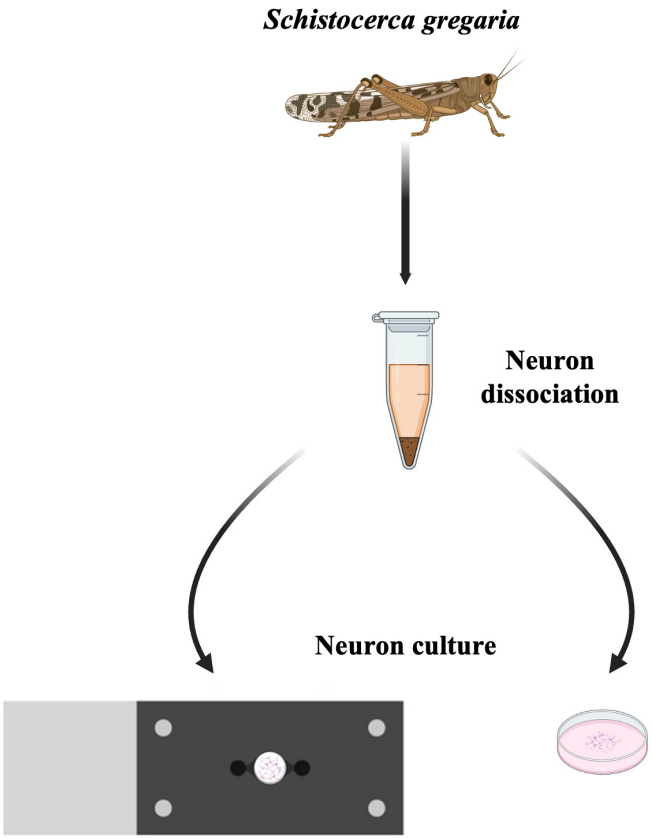

Figure 36. A representative workflow scheme of Chapter 4, starting with the dissection of Schistocerca gregaria ganglia, followed by the dissociation of neurons and their subsequent seeding in neuron-on-a-chip devices and culture plates to compare the evolution of the culture. Created with Biorender.com

4.1 SINGLE-CHAMBER CHIP

The chip designed for the study of neural networks must meet specific criteria:

- It should enable clear and sharp cell observation under a microscope, as the analysis software needs to track cell migration over time and detect connections formed between neurons.
- The chip must withstand standard sterilization procedures applied to materials used in cell culture, such as autoclaving, ethanol washing, and exposure to UV radiation.
- The chip's surface must be compatible with the biofunctionalization process required for proper cell adhesion, preventing cells from being washed away by fluid flow.

In terms of fluidic chamber design, the chip layout must incorporate a central circular seeding region, and it is essential to minimize the dead volume between the inlet and outlet ports leading to this circular area. This reduction is critical because the cell solution will be introduced through the inlet port, and without minimizing dead volume, there is a risk that some neurons might be excluded from the central circular area. Three prototypes were manufactured and tested to fulfill these requirements. The specifications of these prototypes are shown in Table 8.

Chip version	**Prototype 1**	**Prototype 2**	**Prototype 3**	**Prototype 4**	
Layout	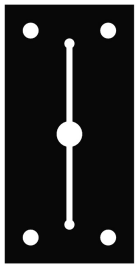	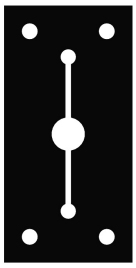	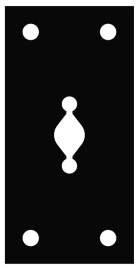	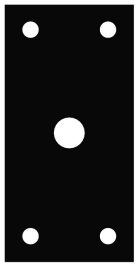	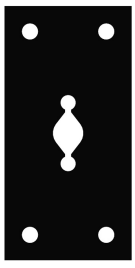
Vinyl thickness	2000 µm	1500 µm	1500 µm	75 µm	1200 µm
Chip volumen	119.46 µL	104.97 µL	73.95 µL	2.12 µL	63.10 µL
Dead volume	80.19 µL	62.56 µL	22.71 µL	-	18.17 µL
Channel size	1.1 mm	1.1 mm	1.2 mm	-	1.2 mm

Table 8. Specifications of the neuron-on-a-chip prototypes.

4.1.1 Design of the microfluidic chip.

The final microfluidic chip developed for this application was designed with an eye-like shape combining two vinyl layouts and a capacity of 83.4 µL. The first layout defined the geometry of the microfluidic compartment (Figure 37B) with eight 150-µm-thick cuts, and the second layout (Figure 37C) introduced a single 75-µm-thick vinyl cut with circular geometry to avoid cell dragging. Both designs featured four circles, each measuring 3.2 mm in diameter. This setup allowed to fit the vinyls into the alignment tool accurately.

Specific considerations influenced the choice of this layout. A crucial requirement was to have a central circular observation area of approximately 5 millimeters in diameter, as requested by the collaborating group. To account for the slight imperfections in vinyl alignment during manual placement, a 6 mm diameter circle was defined in the central area of the vinyls instead of 5 mm. This adjustment ensured that the final manually obtained dimension would be closer to the desired 5 mm diameter. This compact geometry composed of two vinyls is intended to minimize the dead volume within the microfluidic channels connecting the tubes to the central circular zone and ensure a uniform flow distribution, preventing cell retention in the central zone, which has a higher exposure to the perfused flow.

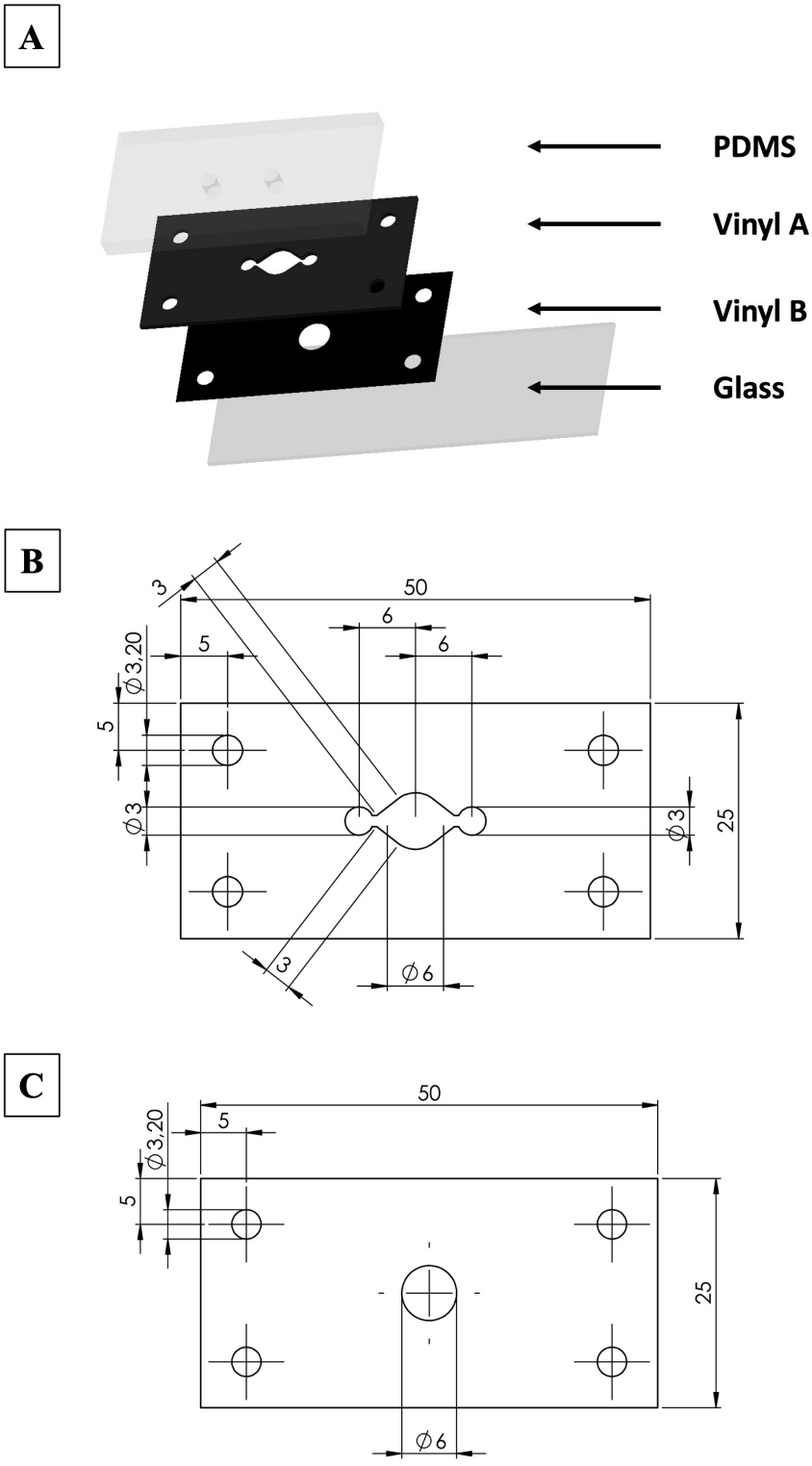

Figure 37. A) Exploded view of the neuron-on-a-chip device. B) Upper layout dimensioned. C) Lower layout dimensioned. The units of the layouts are represented in mm. Image A is extracted from (Herreros et al., 2021).

There is another reason for using this specific layout, and it is closely related to the study methodology. In order to analyze the position of the neurons, their migration on the surface, the formation of connections between them, and cell clustering, it is necessary to capture images of

the culture under a microscope and then compare these images. In the image capture software, it is manually defined the upper, lower, left, and right boundaries of the area to be photographed. The presence of black vinyl around the microfluidic chamber serves a critical purpose here. The boundaries are not fixed in traditional plate cultures where cells are not confined to a specific area. This means there are no consistent visual references from one day to the next, and consequently, the dimensions of these images may fluctuate daily, potentially introducing complexities into computerized analysis and impeding the software's capacity to interpret and compare the images effectively. The uniformly black outline of the microfluidic chamber delimitated by a circular geometry served as a stable and unmistakable reference point. This situation assists the software in identifying well-defined illuminated regions, which are the areas subjected to analysis.

4.1.2 Fabrication of the microfluidic device.

The neuron-on-a-chip device comprises a single-chamber microfluidic chip constructed from PDMS, glass, and vinyl. The chip's base consists of a standard glass slide (75 x 25 mm). While there were no specific restrictions on the dimensions of this glass component during the chip's design, conventional class slides where chosen as a bottom layer due to the analysis method employed in the study. Building the chip on a component that fits the microscope's stage is advantageous to ensure precise imaging under the microscope, thereby reducing the risk of inadvertent chip movement during image acquisition. Prior to attaching the vinyl to the glass, the glass slide undergoes a thorough cleaning process with acetone, isopropanol, and distilled water.

In parallel, PDMS blocks were fabricated following the protocol described in section 3.1.1. The base-curing agent ratio was 10:1.5, and the final block dimensions were 50 x 25 x 3 mm (length, width, and height). Once the PDMS blocks had cured, they were removed from the PLA mold. After that, two holes, each with a diameter of 2 mm, were created in each block. These holes served as ports for the inlet and outlet tubes and provided access to the microfluidic compartment using a 1000 µL pipette.

4.1.2.1 Neuron-on-a-chip fabrication process

Vinyl cuts are employed to define both the microfluidic chamber and the channels' geometry. The desired thickness for the microfluidic component of the chip was 1275 µm, necessitating the use of 9 vinyl cuts These cuts were obtained using a mechanical plotter. After the cutting process, the vinyl cuts are ready to be overlapped. In order to glue the vinyl cuts one on top of the other in an aligned way, a PLA alignment tool with four columns is used as a guide.

The overlapping process proceeds as follows:

1. A protective paper is positioned on the aligner's base, onto which the adhesive side of the first vinyl will be adhered.
2. Vinyl cuts are inserted into the guides through the circular notches at each vinyl cut's corners. Using a pair of tweezers, gently slide the ends of the vinyl cuts towards the bottom of the guide. When the vinyl is about to make contact with the protective paper at the base, smooth the surface of the cut with a lancet, making horizontal movements to prevent the formation of bubbles. This process is repeated this for every vinyl cut until reaching the penultimate one.
3. A double-sided vinyl is applied with the same design as the last one onto the second last vinyl cut.
4. The last vinyl cut is flipped so that its glossy side faces the double-sided vinyl, exposing its adhesive side.
5. Lastly, the exposed adhesive side is covered with an additional protective paper. This prevents dirt from adhering and preserves its adhesive properties.
6. After completing this step, a unified vinyl layer is obtained, which can be handled as a single entity. This layer must be removed from the alignment tool and stuck to the glass slide. To achieve this, the lower protective paper should be carefully peeled off, and the vinyl must be aligned with the glass surface applying manual pressure will secure the vinyl onto the glass.
7. The glass-vinyl piece is positioned on a hot plate and subjected to a heat treatment at 80 degrees Celsius for 30 minutes, accompanied by applying pressure using a weighted plate (5 kg) on top of the assembly. This protocol enhances the fluidity of the vinyl adhesive. Consequently, when vertical pressure is applied, it reinforces the adhesion between the vinyl and the glass, resulting in a smooth surface. Following this process, the vinyl-glass component is ready for sealing with PDMS.

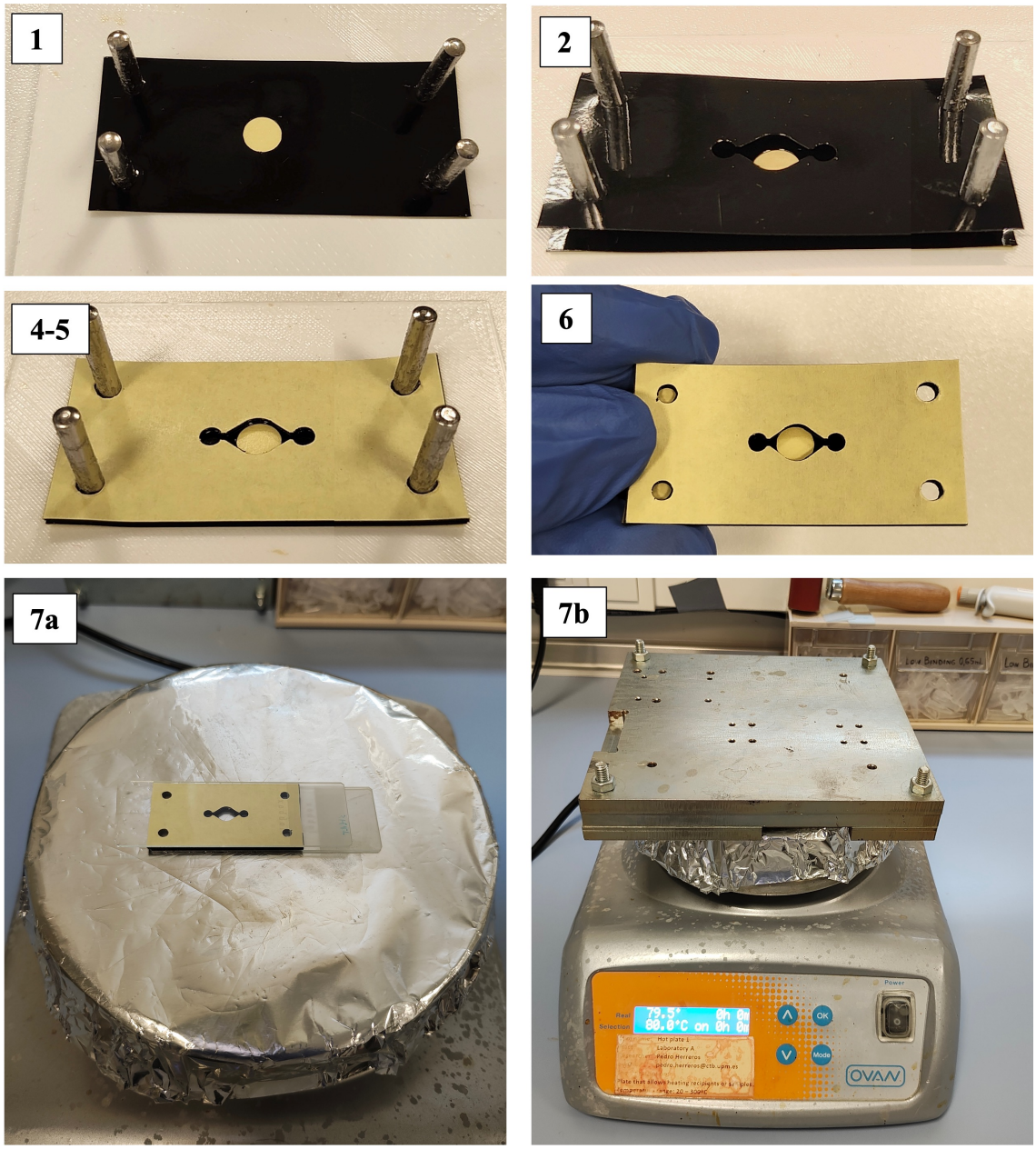

Figure 38. Neuron-on-a-chip fabrication procedure. The labeling of the images corresponds to the steps explained in section 4.1.1.1.

4.1.2.2 Chip assembly.

The last step of the chip fabrication process is the assembly between the PDMS block and the glass-vinyl piece. In order to bond the PDMS block to the upper vinyl, PDMS must be exposed to an oxygen plasma treatment. This method is employed to modify the material's chemical properties, making it more hydrophilic. In the context of the research presented in this thesis, an oxygen plasma treatment is applied to the PDMS block to facilitate its bonding with the last vinyl, where the adhesive side is exposed externally. Attempts to bond the PDMS to the glossy side of PDMS sheets proved ineffective, hence the need for the adhesive side of the last vinyl to be exposed during the overlapping process. The oxygen plasma process was conducted under 50

Watts (W) conditions for 120 seconds. After this treatment, the PDMS block is placed onto the vinyl by pressing it firmly and ensuring the removal of any air bubbles that may become trapped between the vinyl and PDMS.

4.1.3 Microfluidic chip post-fabrication processes

After the chip manufacturing process, the OOCs were not yet suitable for cell culture use. While LOC devices have versatile applications, OOC systems aim to replicate specific organs or tissues. This bioapplication requires additional requirements for compatibility with cell culture. The foremost requirement is sterility. An incorrect sterilization process in these devices can lead to the proliferation of microorganisms, such as bacteria or fungi inside the microfluidic chamber, hindering the growth and maintenance of the desired cells.

While it is possible to mitigate contamination by incorporating antibiotics or antifungals into the culture medium, complete sterility is essential. In order to achieve this, an autoclaving process is employed to sterilize the chips developed in this application. PDMS, vinyl, and glass can resist this treatment, simplifying sterilization. Once autoclaved, the chips are ready to use inside a laminar flow cabinet.

The cells to be cultured on the chips, invertebrate neurons, lack the intrinsic ability to adhere to glass surfaces, which are the substrates upon which the neurons will be seeded. A biofunctionalization process of the chip must be done to facilitate neuron adhesion. This process was carried out in collaboration with the Biological Networks group, which possesses prior experience in biofunctionalizing glass plates for their own cultures.

The biofunctionalization solution consisted of a mixture containing Concanavalin-A (0.2 mg L-1) (Sigma Aldrich) and poly-D-lysine (0.016 mg L-1) (molecular weight 70k-150k, Sigma Aldrich), resulting in a final solution volume of 70 μL. This solution was pipetted through the inlet port and maintained at 37°C for 2 hours. After this incubation period, the chips underwent a thorough washing process with 3 mL of distilled water and were subjected to 30 minutes of UV light sterilization to ensure the sterility of the chip's external surfaces. After the fabrication and post-fabrication stages, the chip is ready to be seeded (Figure 39).

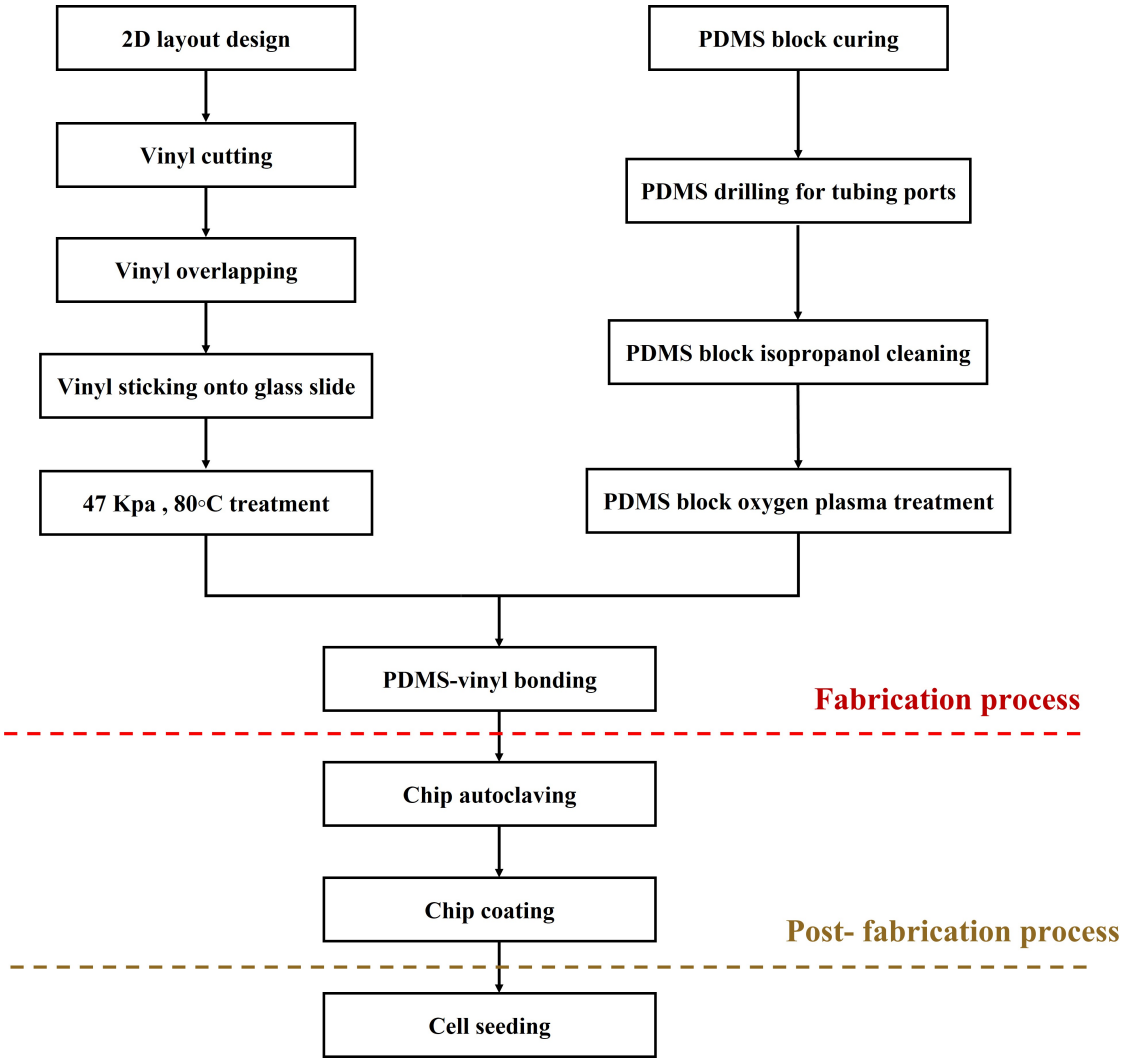

Figure 39. Workflow of the neuron-on-a-chip manufacturing and post-fabrication process.

4.1.4 Layout modification and optimization

The final prototype employed in this study underwent an optimization process involving the testing of various microfluidic geometries until the final design was achieved. The initial design (prototype 1) featured a central circular area measuring 6 mm in diameter, connected to rectangular microfluidic channels with a width of 1.2 mm. This preliminary version underwent the autoclaving and biofunctionalization procedures as previously described.

An alternative sample injection method was proposed during the early stages of chip development instead of pipetting the sample. This method involved directly injecting the biofunctionalization solution and the cells into the central circular chamber. This injection approach was considered for its potential to use less sample volume. The initial test was conducted using L-15 culture medium, the same medium used for neuron culture. Figure 40 illustrates the successful puncture, with no observable leakage in the region where the PDMS was penetrated. The puncture was executed using a 1 mL syringe equipped with a 21G gauge needle.

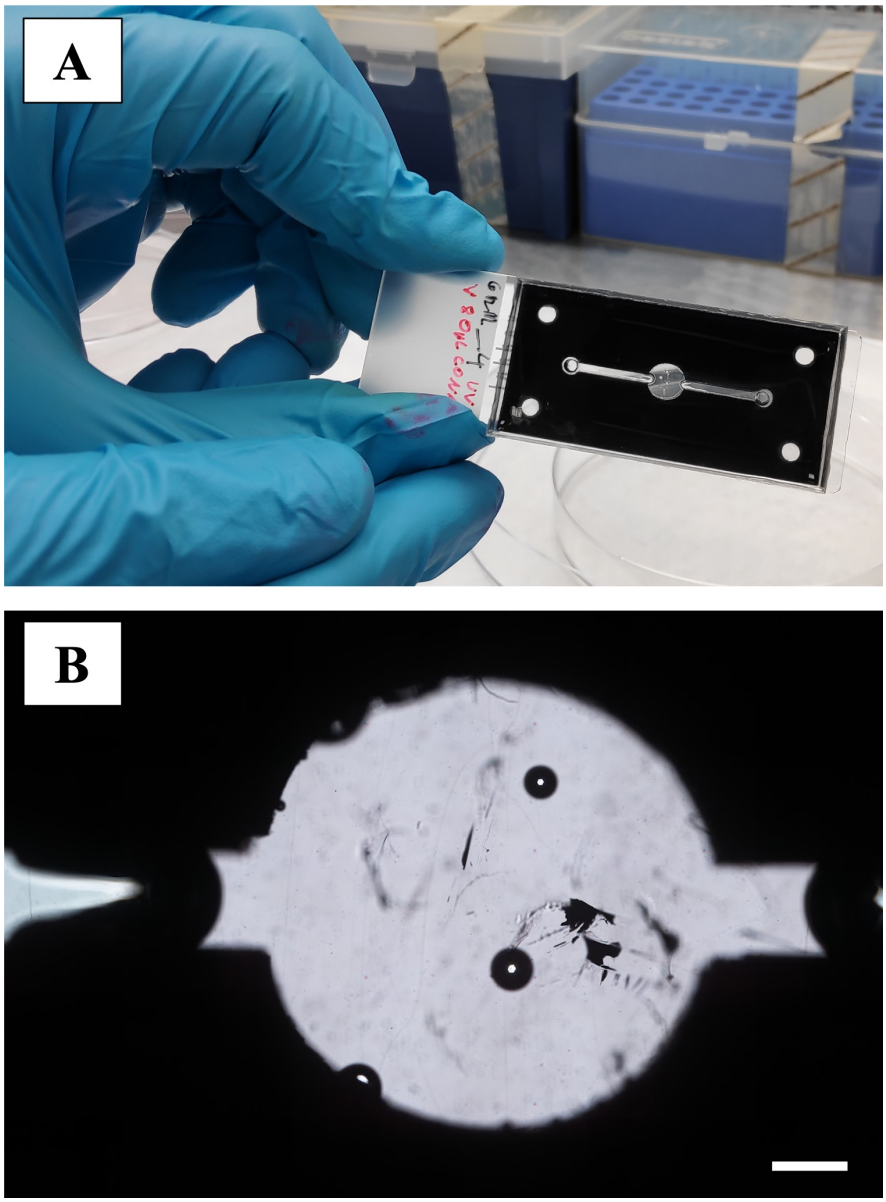

Figure 40. Pictures of the injection test performed on the first neuron-on-a-chip prototype. Scale bar represents 1 mm.

Following this initial test, an experiment was performed using two chips, applying the same biofunctionalization protocol and injecting the cell solution into the chip. Figure 41 illustrates the condition of the chips after 1 day in vitro (DIV 1) and 4 days in vitro (DIV 4).

In the DIV1 images (Figure 41C,D), it is apparent that the central zone exhibited cell dragging, with fewer cells than the region near the circumferential arc. Furthermore, the affected zone closely matched the dimensions of the inlet and outlet microfluidic channels. This suggests that the cell dragging in this central zone is attributable to the flow's influence.

The DIV4 photos revealed a substantial fungal contamination present on both chips (Figure 41E,F). The culture medium within the syringes placed in the perfusion pump showed no signs

of contamination, and the waste reservoir remained uncontaminated. Therefore, the source of this infection was located in the microfluidic chip. Based on these results, the final decision was made to discard the injection method for introducing the coating solution and cells into the chip. Instead of that, this procedure would be performed by pipetting through the tubing ports in the PDMS blocks.

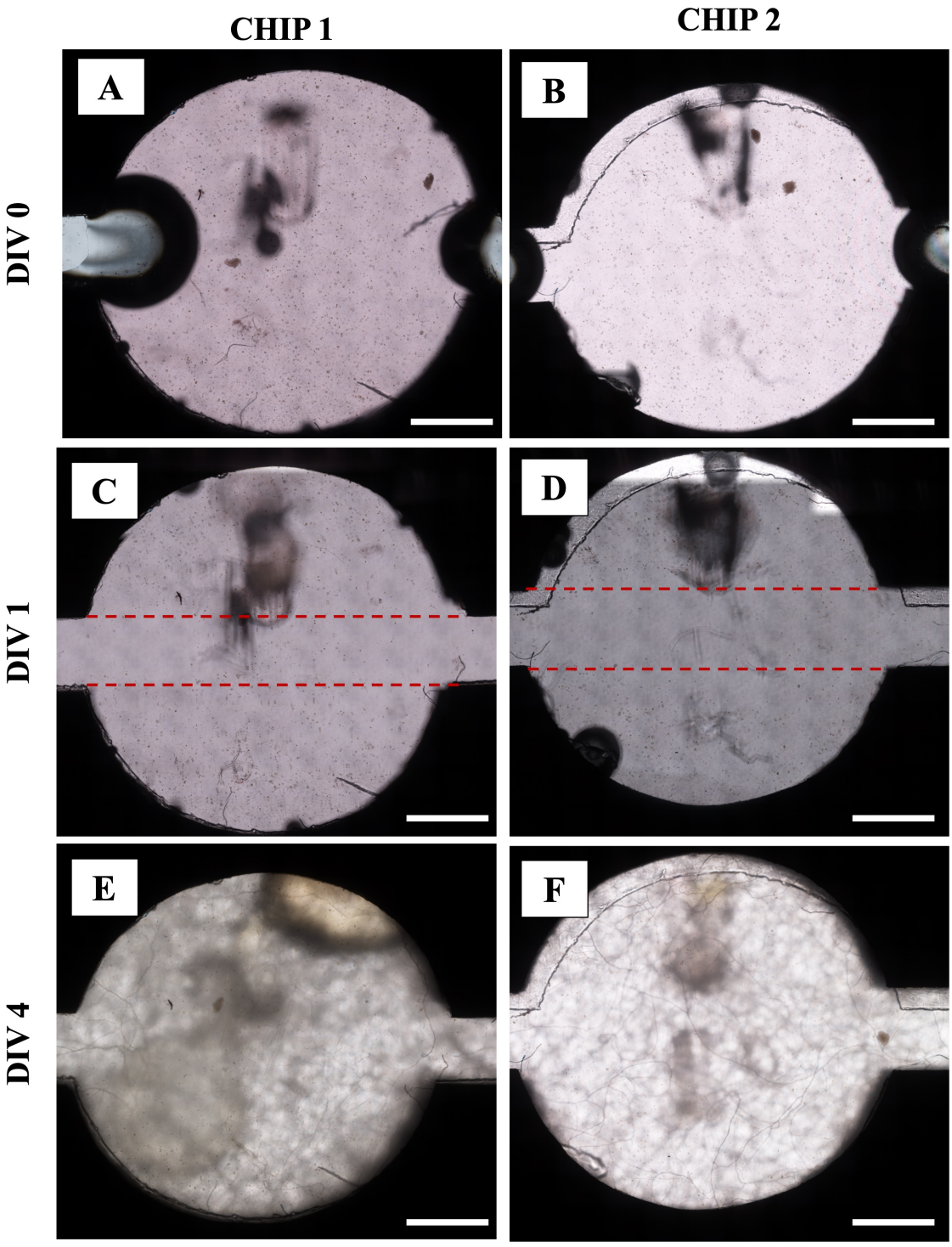

Figure 41. Neuron seeding test on neuron-on-a-chip prototype 1 by injection. In images C and D, the red lines indicate the channel prolongation of the microfluidic channels. Scale bars represent 1 mm.

Due to the outcomes of this test, a significant redesign of the microfluidic geometry became imperative to eliminate the issue of cell entrainment in the central area and ensure a more uniform flow distribution at the chip's inlet and outlet. The redesign involved another inconvenience: the needed volume to fill the culture area had increased compared to the initial concept, due to the need to administrate the dead volume within the chip's inlet and outlet channels. A new layout was developed, emphasizing the minimization of microfluidic channel dimensions and the proximity of the tubing inlets and outlets to the circular region of the fluidic compartment.

An eye-shaped design was chosen as the most suitable solution at this issue in the chip redesign process. With this alternative geometry, the tubing inlets are positioned adjacent to the microfluidic chamber, and the chamber's shape has been tailored at the ends to guide the flow into and out of the chamber via a conical configuration. This design was implemented in a second neuron-on-a-chip prototype. Moreover, a variation of this design was conceived, incorporating an additional vinyl cut beneath the eye-shaped layout. This variant featured a 75-µm vinyl layer designed to protect the cells from potential direct exposure to the flow. Chips constructed with this configuration constitute the third neuron-on-a-chip prototype. An experiment was conducted to compare cell distribution between the second and third prototypes, aiming to determine the necessity of this additional layer.

The results of this test reveal several observations. Firstly, there was no contamination in any of the chips, confirming that the origin of the contamination within the chips was the area where the PDMS block was punctured with the needle.

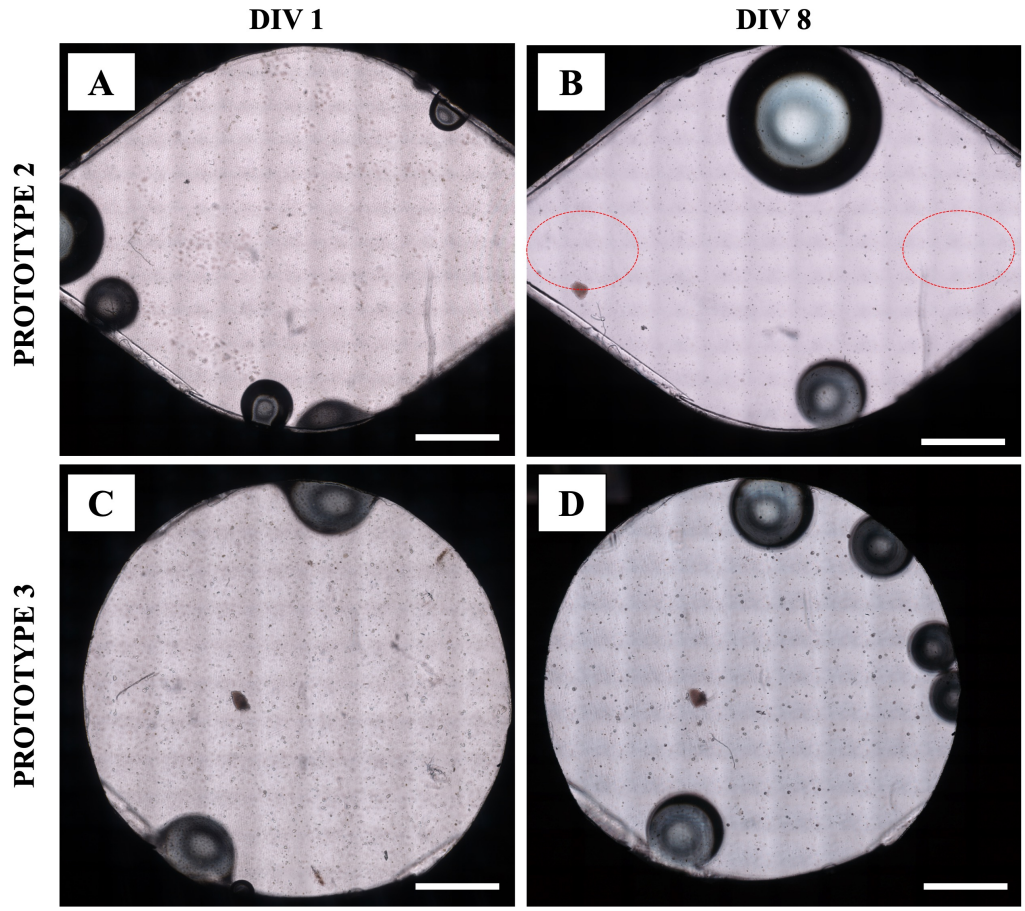

Figure 42. Comparison of cultures performed on neuron-on-a-chip prototype 2 (A,B) and prototype 3 (C,D). Scale bars represent 1 mm.

When comparing prototype 2 with prototype 3, it was possible to identify variations (Figure 42). Firstly, neurons cultured in prototype 3 appear larger, and neurons are more evenly distributed across the culture area. In contrast, prototype 2 exhibits more depopulated regions at the inflow and outflow areas (Figure 42B). In the case of the inlet zone (left side of the picture), the absence of cells can be attributed to the formation of an air bubble during the filling process, preventing cell adhesion in the bubble-occupied area. In contrast, the outflow zone, was free of , yet a small number of cells are still present in that area. Beyond the cell distribution issue, there is a noticeable general decline in cell condition in prototype 2 compared to prototype 3, where the cells exhibit a larger circular appearance.

Based on the analysis of the images obtained from both prototypes, prototype 3 was chosen as the definitive design for studying neural network formation on a chip (Figure 43).

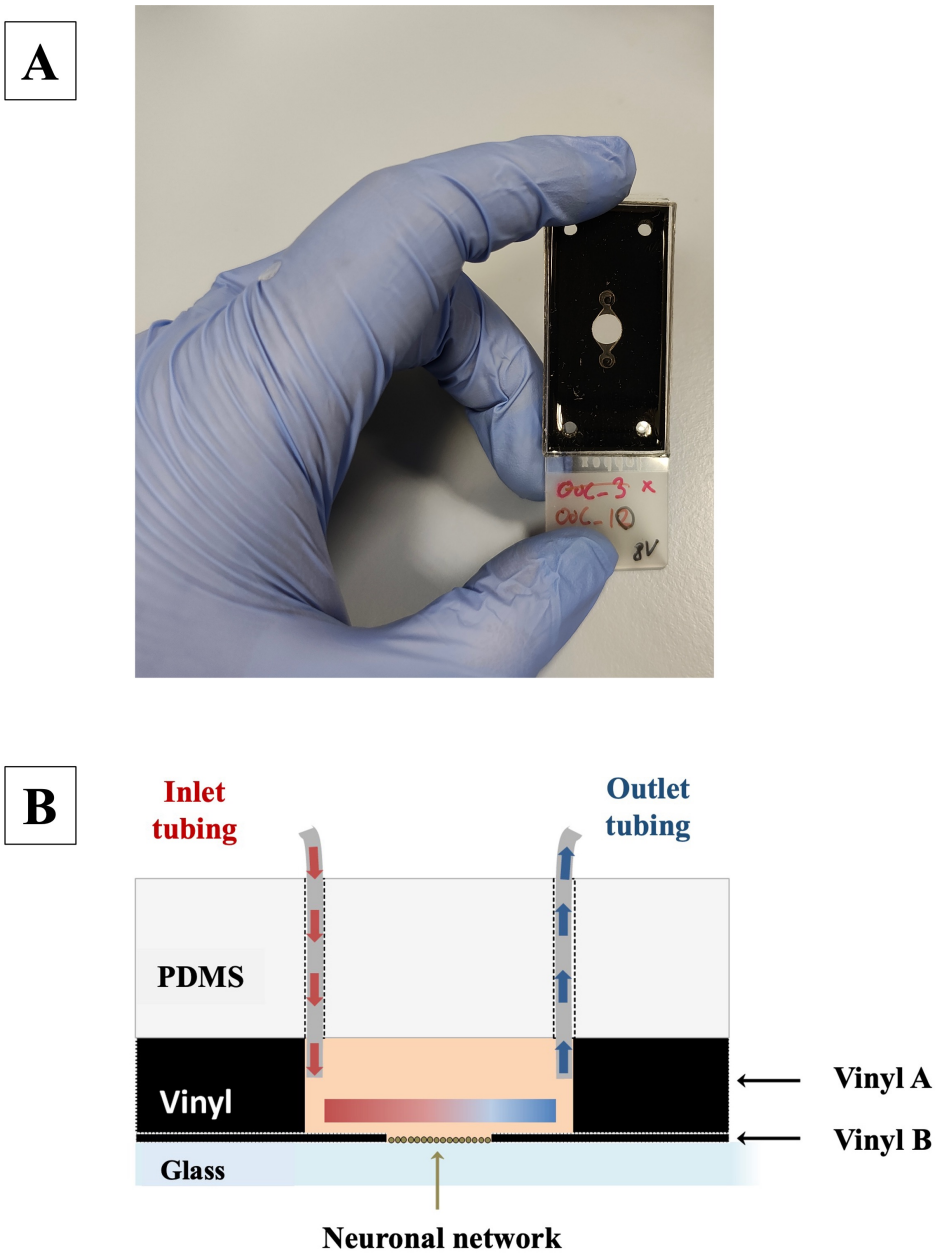

Figure 43. A) Picture of the third and final neuron-on-a-chip prototype. B) Cross-sectional diagram depicting the flow within the chip, extracted from (Herreros et al., 2021).

4.1.5 Cell culture and microfluidic conditions

CNNs were incubated in darkness for 21 days under controlled temperature (30 °C or 37 °C) and humidity (70%). Two sets of experiments were conducted, each with a control group of CNNs grown in Petri dishes under the same conditions as the chip cultures. The dataset for the 30 °C experiments comprised two chips and nine controls, while the dataset for the 37 °C experiments comprised two chips and five controls.

Both types of cultures required medium renewal to ensure cell survival. In chips, the microfluidic system was set with a 1µL/min flowrate in a 1 mL syringe, which it was refilled with a new

syringe after seven days. Half of the medium in the Petri dish controls was replaced weekly with the same volume (1 ml) as in the corresponding chips. The evaluation of the cultures has been explained in section 3.4.1.

4.2 RESULTS

The results of this work are based on the comparison of locust dessert neuron cultures on microfluidic chips against static plate cultures. For this comparative study, from the same mix of disaggregated cells, half of the cells are cultured on a chip and the other half on a culture plate. Both the chip and the culture plates are maintained in the same incubator (Figure 44). Although this detail may seem trivial, introducing more than two pumps inside the incubator increased the internal temperature, exceeding the set temperature established in the incubators. Although this circumstance might appear to be a drawback when it came to increasing the number of chips running simultaneously, it was used to test a new hypothesis. The temperature condition for invertebrate neurons is 30ºC. Comparing the formation of the neuronal network in the chips under non-optimal conditions allows the possibility to hypothesize whether neurons, maintained in adverse conditions, may have a better survival and a more developed network compared to control plates.

Considering these constraints, this study aimed to compare the evolution of CNNs grown in chips and Petri dishes, and to evaluate the effect of temperature on both culture conditions. The network development was monitored by longitudinally evaluating studied graph parameters: the total number of connected nodes, the average clustering coefficient, and the shortest path length. The average clustering coefficient accounts for how densely connected is each local vicinity of the network. The results shown below have been ordered in temporal order.

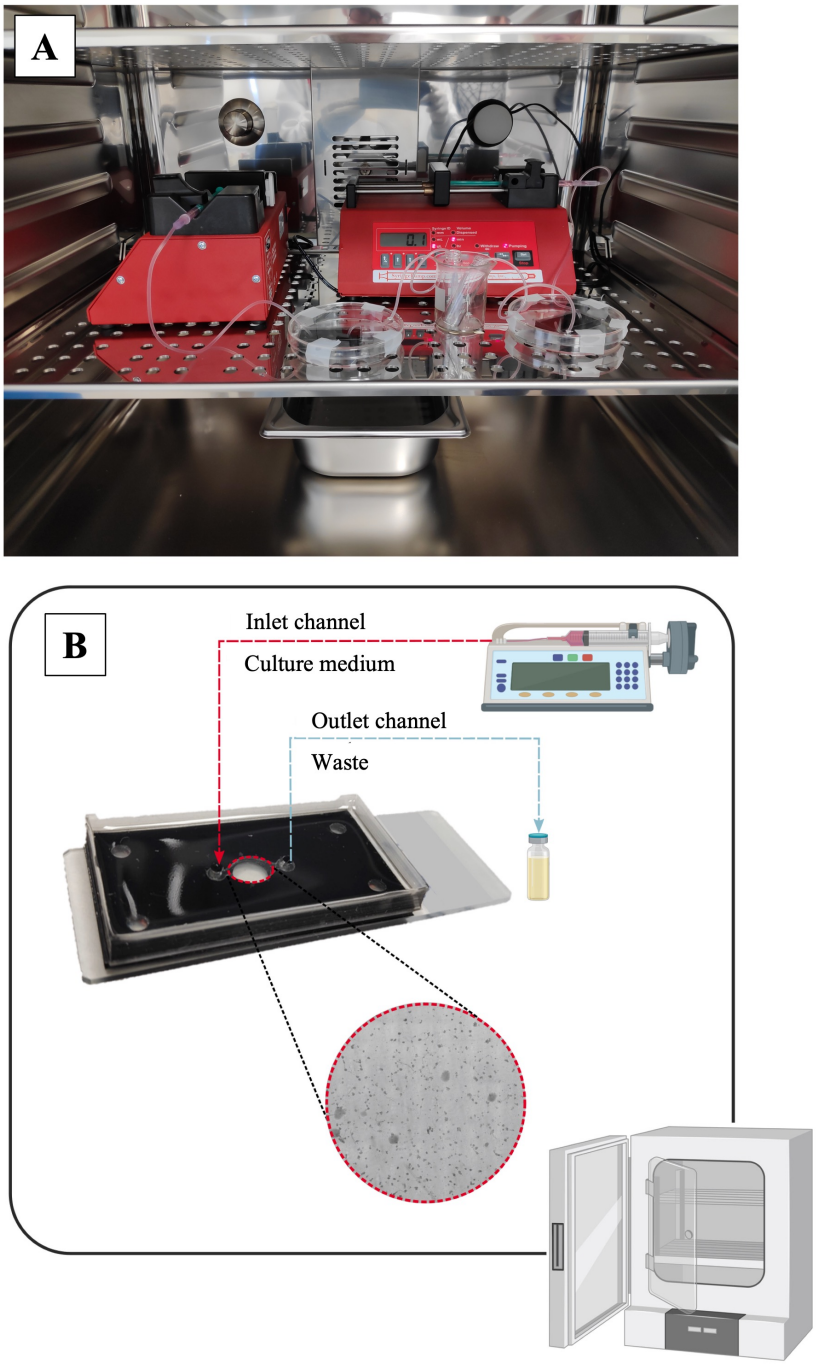

Figure 44. A) Microfluidic set-up for CNN culture inside in the cell incubator composed by the syringe pumps, tubing, neuron-on-a-chips and waste reservoir. B) Schematic view of the set up.

4.2.1 Cell culture 30ºC

The first results of cultured neurons in the OOC device of this chapter are made by two neuron-on-a-chips maintained at 30ºC for 21 days. As expected, the neurons moved slightly to form neuronal aggregates, but they remained heavily attached to the surface. No cell loss or detachment was observed due to coating or flow failures. To demonstrate the non-influence of the flow on the

position of the cells, a study was carried out using an ad hoc image segmentation algorithm to create a graphic that shows the average position of the neurons and neuronal aggregates as a function of the culture age (the paler the color, the older the culture).

Figure 45 shows the distribution of the centroids of the two neuron-on-a-chips cultured at 30ºC, where the distribution of the cell average position does not exhibit any preferential direction due to dragging forces induced by the flow. Furthermore, no greater detachment of cells was observed in the most peripheral areas of the chip, and network processes were also formed in these areas. This fact suggests that the flow was homogeneous throughout the culture volume.

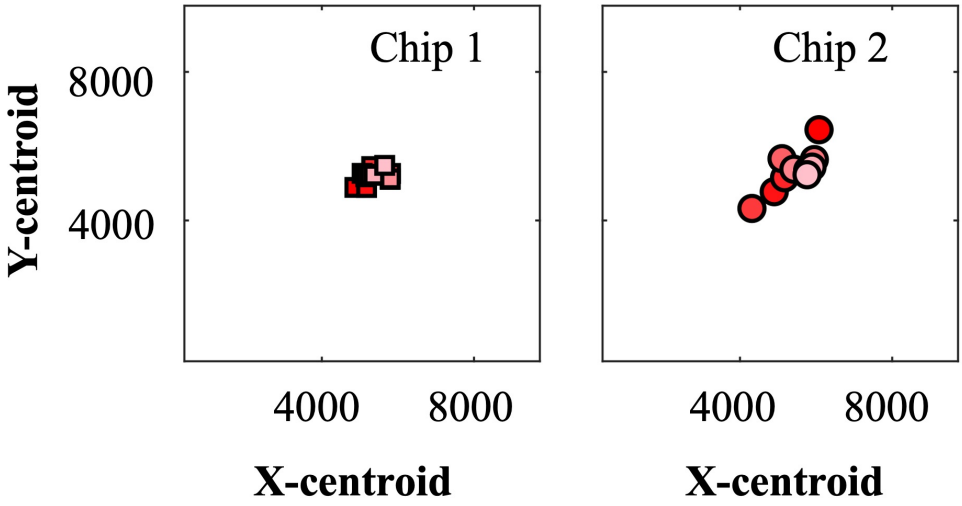

Figure 45. Average cell position of the chip neuronal networks as a function of the culture age (the paler the color, the older the culture).

The continuous flow of culture media was able to remove small particles and debris, but elements with bigger dimensions such as void ganglia capsules, could not be removed. The flow also could wash away the melanin of the culture, which is critical in insect cell cultures due to its detrimental effect at high concentration. As a result, CNNs developed on the chip survived longer than those grown on Petri dishes, where the medium was changed every 7 days.

Isolated neurons in the first day of culture started to grow neurites and form connections with their neighboring neurons around 3-6 days of culture, getting closer to form clusters. At DIV 7, connections among farther neurons are observed, and junctions previously formed are more entrenched. In this step, it was observed an increase in the number of connections, and a more extensive network was settled. After this stage, the networks grew, forming more prominent clusters, until the CNNs settled as a consolidated and mature network on DIV 15. No significant changes in the network were noticed beyond this point. In order to properly quantify the different network states with the tools of graph theory, the resulting graphs from the segmented mosaics were mapped into adjacency matrices (Figure 46). Results of the evolution and development of the graph of the two CNNs grown on chips have similar trends to those grown on Petri dishes

with similar initial density. As shown in Figure 46A, the number of connected nodes, and nodes having at least one connection, increased until DIV 6-7 due to the neurite growth and connections being made. After this stage, the network development was steady. In fact, there was a slight decrease in the number of connected nodes because when connected neurons form clusters, the segmentation algorithm identifies them as a single node.

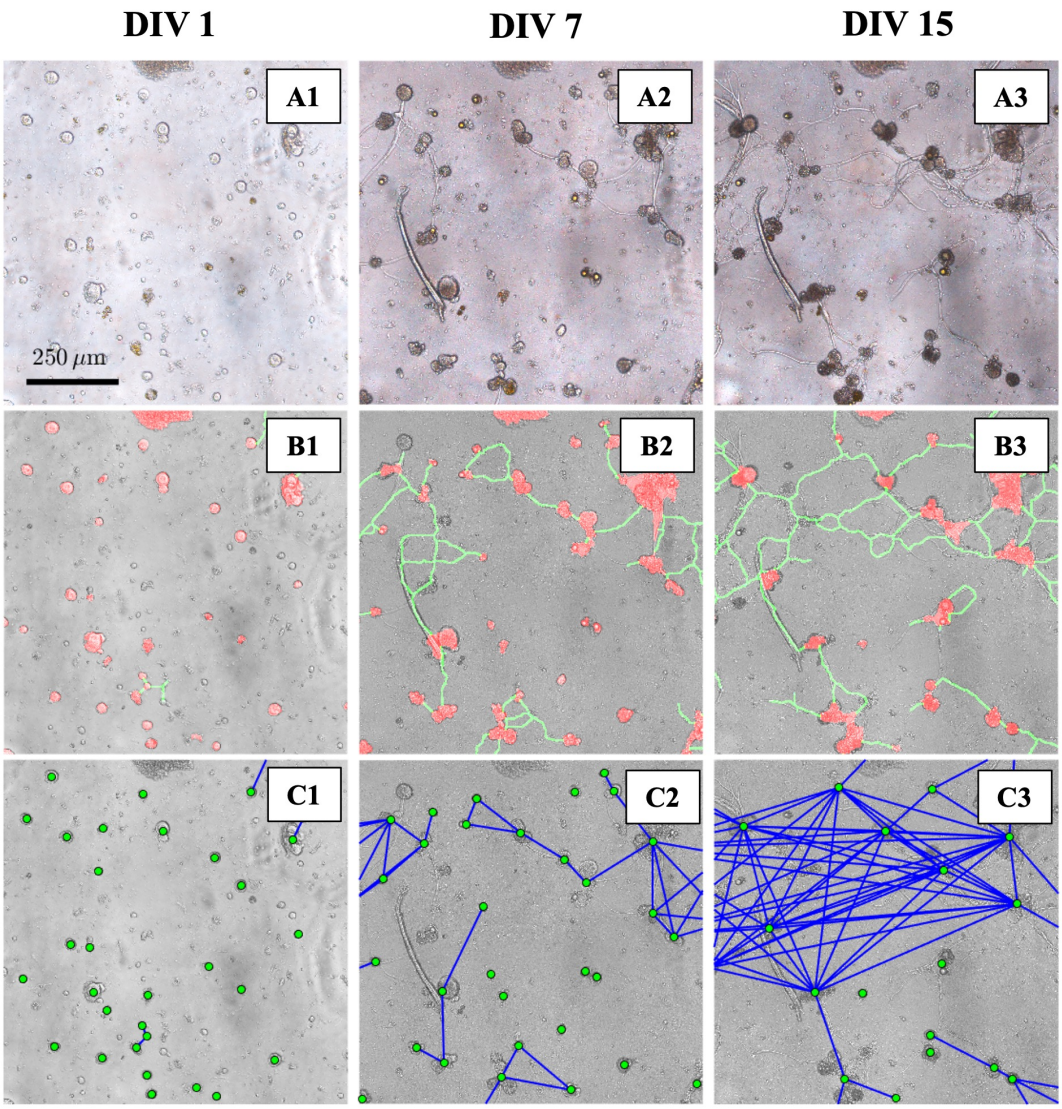

Figure 46. Image segmentation processing steps and extraction of the network graph. A1-3) Cuts of the mosaic image taken at different DIV (days in vitro) during the CNN evolution. B1-3) Output of the segmentation algorithm of the region of interest. C1-3) Graph representing the projection of the full graph into the cluster graph.

Other network properties to analyzed were the longitudinal progression of the averaged clustering coefficient and of the shortest path length (L/SGC), normalized by the size of the largest connected component (Figure 47). Regarding the normalized shortest path, high values were observed at the start of the experiment. This value decreases around DIV 4-6 as links between nodes are formed. Beyond that, L/SGC keeps a low constant value in the more mature stage. As

expected, the clustering coefficient showed near 0 values at the start, with no connections between neurons. In the critical stage of network formation, around DIV 3-6 the clustering coefficient increases, revealing the new connections between neurons. When the mature network is settled, the clustering coefficient value keeps constant at a relatively high value indicating the presence of loop circuits in the network.

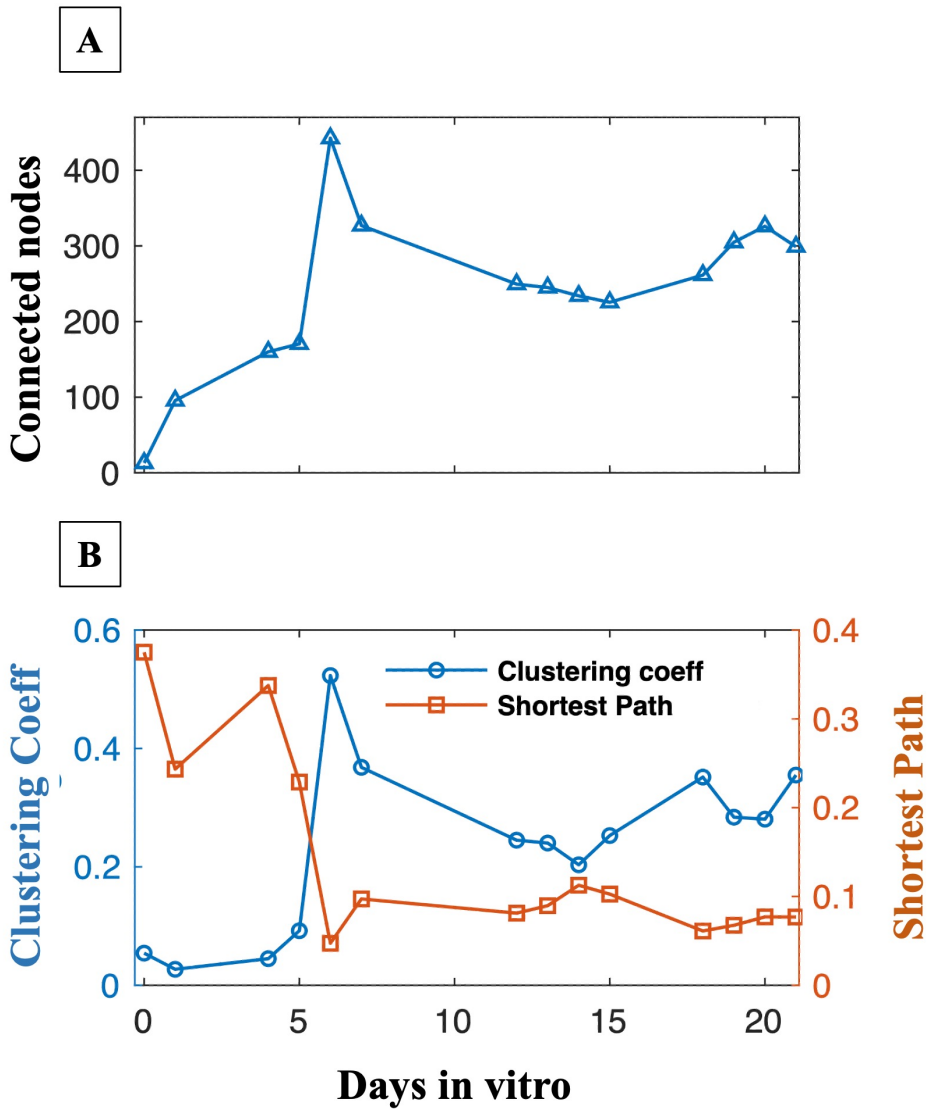

Figure 47. Network properties of the neuronal cultures. (A) Mean values of the number of connected nodes in the CNN as a function of the age of the culture. (B) Mean shortest path length (L/SGC) normalized by the size of the largest connected component (orange) and mean clustering coefficient (blue). Each point is the average over 2 chip experiments.

Both parameters, low shortest path values, and the high clustering coefficient, are studied frequently as characteristics of a small world structure, where the high tendency to form clusters of nodes in highly interconnected subgroups and short distance between them contribute to an optimal functionality in the network based in high efficiency. These results are very similar to the ones obtained in Petri dishes mentioned above, with no significant alteration, so it was confirmed

that the use of the chips to grow optimal functional CNNs with the desired parameters not only does not affect their development, but they promote a more prolonged network survival.

4.2.2 CNN cultures: 30ºC vs 37ºC

After obtaining optimal results in the previous experiment with two neuron-on-a-chips, the next step was to repeat the neuron culture with more microfluidic chips to test the repeatability of the experiment. An unexpected circumstance related to the fluidic set-up occurred in this experimental phase. At this stage of the thesis, the perfusion pumps were placed inside the incubator, as the aim was to have as little dead volume in the tubing as possible. In order to increase the capacity of chips running simultaneously, it was a need to place more perfusion pumps inside the incubator. This change led to an increase in the incubator set-point temperature from 30ºC to 37ºC. Different alternatives were proposed to avoid the rise in temperature. The first was to use another incubator, but the chips behaved differently: the neural networks did not form inside the chips. Because of this, the incubator used for the neuron culture remained the same, even though it involved a variation in the temperature inside. For this reason, the results shown in this section have been reviewed based on the culture method (chip vs. control) and temperature (30ºC vs. 37ºC).

The CNNs exhibited greater longevity in chips compared to the control group. In most cases, the CNNs within the chips remained in optimal condition until DIV 21, demonstrating a stable network structure. Conversely, the networks cultured in Petri dishes began to deteriorate around the end of the second week systematically, and eventually did not survive. Specifically, the CNNs in Petri dishes, where the medium was changed weekly, only survived for 6-8 days at 37ºC.

Figure 48 provides a visual representation of the qualitative distinctions in network development between the chip cultures (A-D) and control cultures (E-H) at both 30ºC and 37ºC. Images captured at DIV 5 and DIV 13 are used for comparison. During the early stages of development, the most notable distinction is the faster growth of neurites in the control cultures than the chips. This accelerated growth in the control group is evident at 30ºC (A, E), but it becomes particularly pronounced at 37ºC (C, G). At 37ºC, while the chip cultures are still in the early stages of development, the control cultures at the same DIV already exhibit a well-established network.

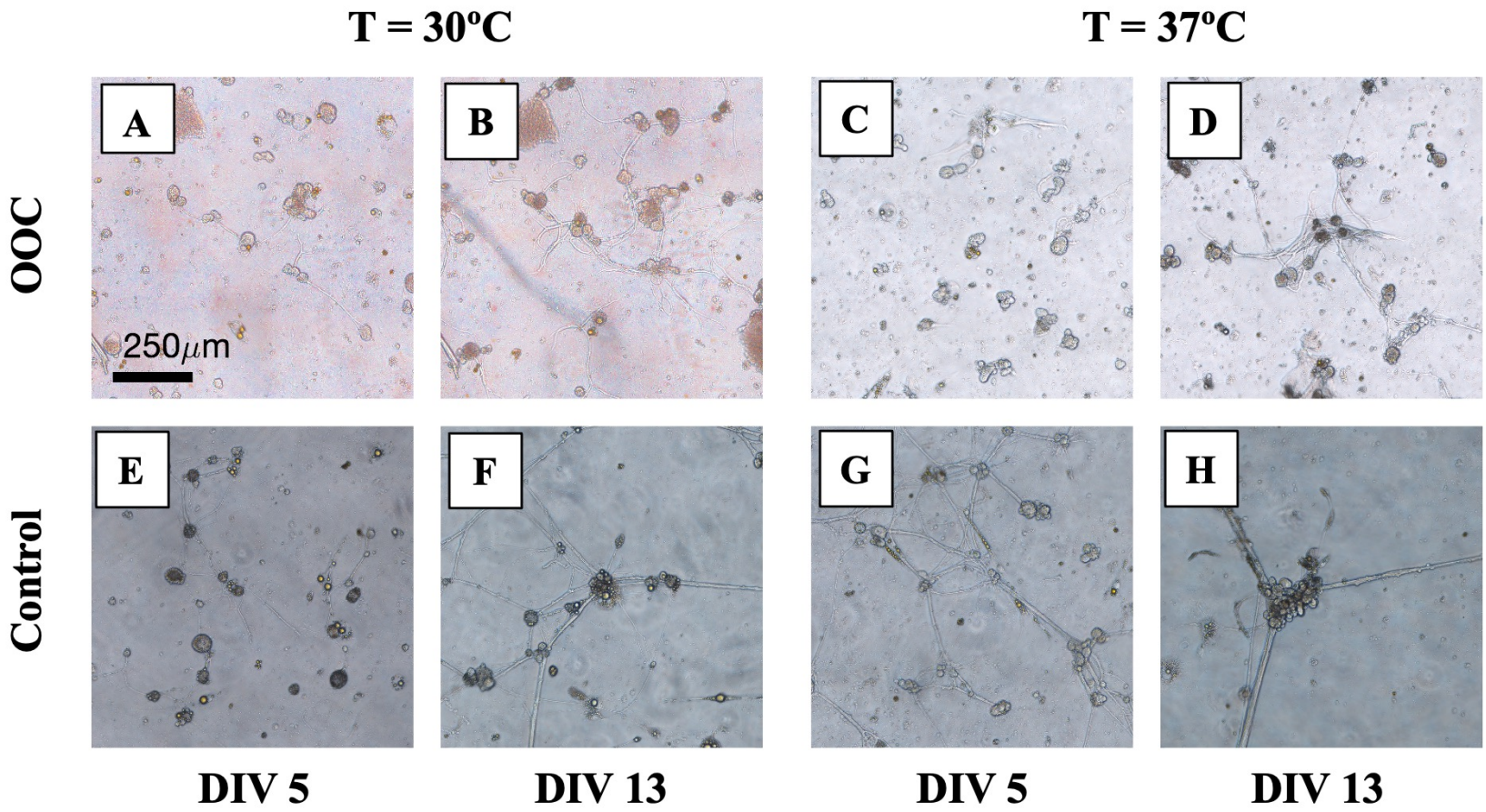

Figure 48. Microscope images of CNNs grown on chips (A-D) and Petri dish controls (E-H) for experiments conducted at 30°C and 37°C on DIV 5 and 13. Extracted from (Herreros et al., 2021)

The fast growth observed in the control cultures extended until DIV 6-8. Beyond this point, both control networks (F and H) experienced a swift deterioration and subsequent collapse at both temperature settings. Conversely, the neuron-on-a-chips (B,D) maintained their networks' integrity, surpassing the control networks' longevity. They continued to grow and mature without signs of degradation until the experiment's conclusion at DIV 21.

Once again, a striking difference in network degradation becomes evident at 37ºC. This is particularly noticeable when comparing the well-formed chip network at DIV 13 (Figure 48D) with the corresponding control network (Figure 48H), which had experienced collapse and partial detachment.

An analysis of the networks was performed to assess these differences systematically, resulting from the segmentation process. Subsequently, various topological metrics were calculated to quantify the disparities in network development and survival observed in the cultures.

The outcomes of this analysis are presented in Figure 49, where several important metrics have been plotted. These metrics include the number of connected nodes (nodes with at least one connection) (A,D), the averaged clustering coefficient, and L/SGC. These metrics are depicted as functions of the number of days in vitro for both chip (Figure 49B,E) and control (Figure 49C,F) experiments conducted at two different temperature settings, 30ºC (Figure 49A-C) and 37ºC (Figure 49D-F). Graphs B in Figure 49 shows the same information as the graphs shown in Figure 47 in the previous section.

The average number of connected nodes (Figure 49A,D) provides quantitative support for the observations made in Figure 48. In the initial days of culture, the number of connected nodes in the control group (green triangles) increased rapidly, reaching its peak on DIV 6 at 30ºC, and DIV 5 at 37ºC. In contrast, the chip cultures (blue squares) exhibited slower development, with peak connectivity occurring on DIV 7 at 30ºC, (Figure 49A) or even as late as DIV 12 at 37ºC (Figure 49D). Following this phase, the number of connected nodes in the control cultures decreased, primarily due to the formation of neuronal aggregates, which the segmentation algorithm identifies as a single node. This decrease was followed by premature network degradation and detachment. In the chip cultures, the number of connected nodes remained stable, except for a minor decline resulting from neuronal aggregation. This data indicates that neuronal networks on control setups mature more quickly than those on the chips. However, these control networks are less stable and tend to disintegrate sooner.

Graphs A and B indicates the temporal evolution of structural parameters in the 30ºC experiments, L/SGC exhibited higher values during the initial days in vitro (Figure 49B,C). There was a consistent decrease in L/SGC values, reaching its lowest point at around DIV 4-6 vitro when the number of connected nodes peaked. After this point, L/SGC maintained a consistently low value

in the mature stage of the chip cultures (Figure 49B). In contrast, in the control cultures (Figure 49C), L/SGC increased due to network collapse.

Experiments conducted at 37ºC, as illustrated in Figure 49E and F, displayed comparable trends in network parameters, although the evolution was not as distinct. This was primarily due to the chips' slower maturation and the rapid degradation of the control cultures. In the chips, an increase in clustering coefficient and a decrease in L/SGC (Figure 49E) can be observed. Even so, the point at which these two metrics intersected occurred later, typically between DIV 12-13, due to the slow pace of network formation. Beyond this point, there was no significant difference between the two metrics.

In the corresponding control cultures (Figure 49F), L/SGC exhibited a continuous decrease up to DIV 5, mirroring the trends observed in the 30ºC experiments. Nevertheless, it increased due to network collapse and neuron cell death after DIV 6-8.

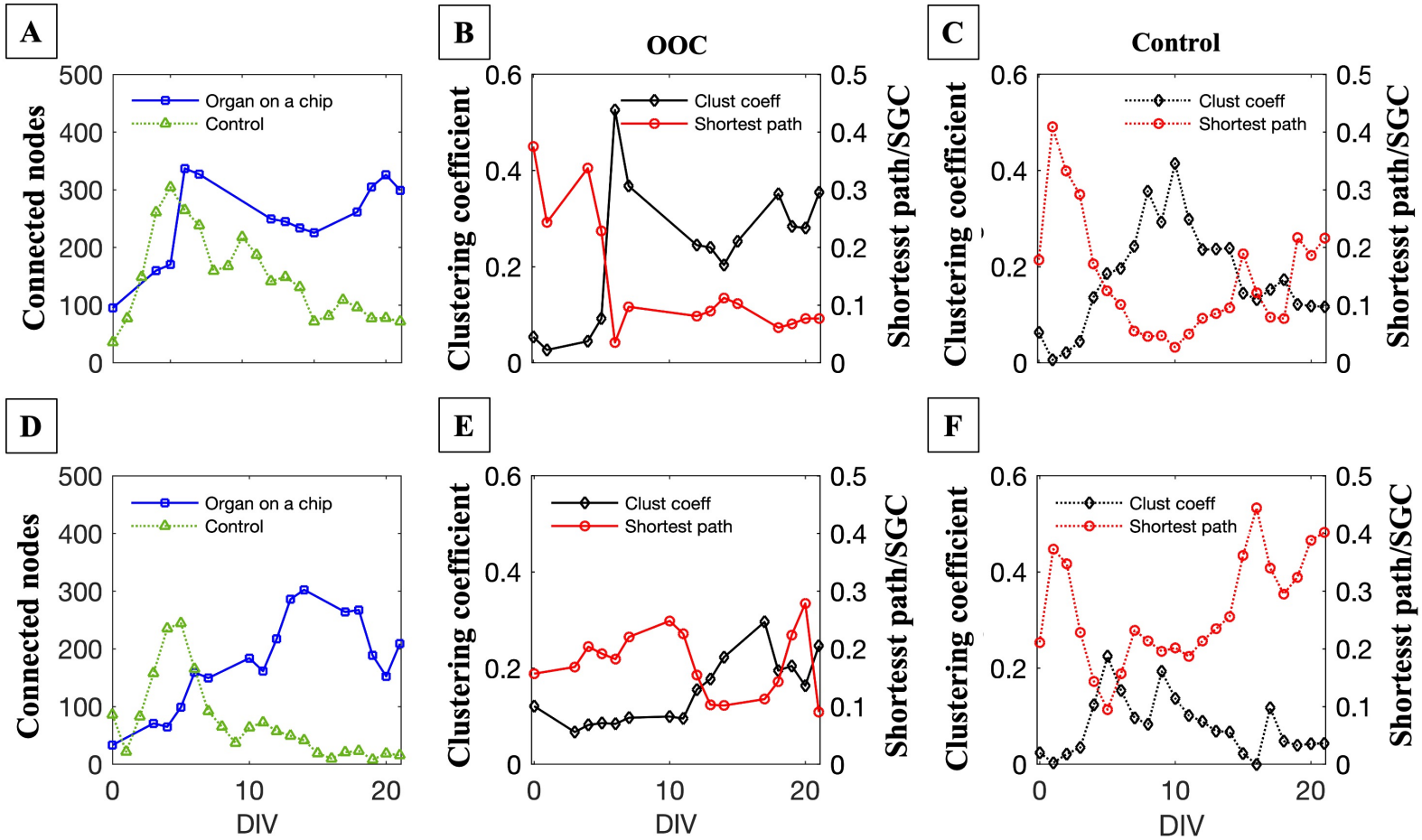

Figure 49. Network properties of neuronal cultures at 30◦ C (A-C) and 37◦ C (D-F). Mean connected nodes versus DIV at 30◦ C (A) and 37◦ C (D). Mean clustering coefficient (black symbols) and average shortest path length L normalized by the size of the largest connected component GSC (red symbols) at 30◦ C in chips (B) and controls (C). From (Herreros et al., 2021).

4.3 CONCLUSIONS

In the work presented in this chapter, the design, manufacturing and cell culture processes of a neuron-on-a-chip have been successfully proved, achieving the next milestones:

1. A reproducible methodology for manufacturing OOC devices made by PDMS, glass, and vinyl was developed. The chip has been demonstrated to be a reliable and helpful system due to its easy handling, renewal of culture medium, contamination avoidance, and control of the culture conditions.
2. The chip complies with essential characteristics for its correct functioning, such as a reliable sealing of the monolithic chip, the verification that the chip compartment geometry does not cause cell dragging inside the chip, and the chip's compatibility with biofunctionalization and sterilization processes.
3. The microfluidic compartment can contain the cells in a delimited area to avoid dispersion and distance between neurons.
4. The results show an improvement in the culture conditions of invertebrate neurons, where a more stable and durable neural network can be observed than in control plate cultures. Although the neural networks formed later than their Petri dishes counterparts, the survival of the CNNs inside the chips was seven days longer. These results were obtained under two different maintenance conditions, which implies a significant improvement in the culture of invertebrate neurons in a microfluidic system compared to the traditional methodology used so far (Herreros et al., 2021).

This neuron-on-a-chip concept has room for improvement in future experiments. The comparative analysis performed in this proof-of-concept analysis was performed only to evaluate the formation of neural networks. MEAs are widely used to study the transmission of electrical impulses from neurons or the stimulation of neurons through microelectrodes. As a future goal, the fabrication of a microfluidic chip integrating microelectrodes inside the microfluidic chamber would imply a significant improvement in OOC devices applied to neuronal culture.

These results were the first demonstration that with the infrastructure of a micro-nanofabrication laboratory, it was possible to integrate the group's expertise with cell culture techniques. All the technological development that has been done in this chapter was established as the starting point for developing the following bioapplications.

5 BRAIN SLICE-ON-A-CHIP

After a first functional OOC, the next step was to adapt the established methodology to enable the production of microfluidic chips with different chamber configurations and geometries.

Within the research setting of the CTB, where this thesis was cattied out, there is another group specializing in the field of neuroscience known as the Cortical Circuits group, which is affiliated with the Cajal Institute. This group possesses extensive expertise in analyzing the organization of the cerebral cortex, employing various techniques such as intracellular injections, histochemical and immunocytochemical methods for optical and electron microscopy, as well as 3D reconstruction techniques.

In this chapter, a novel microfluidic chip has been developed to enhance culture conditions and extend the lifespan of hippocampal slices. This thesis chapter is driven by the necessity for a technique that can maintain hippocampal slices under controlled conditions for extended durations. To assess whether there is a genuine improvement in the brain slice culture status within an OOC compared to a traditional culture, a viability analysis was conducted using fluorescent cell labeling. While administering this tracker is straightforward in culture plates, it presents challenges in a closed system like a microfluidic platform. Therefore, the objectives of this chapter include developing technology for OOC devices that is compatible with local reagent delivery. The specific objectives of this chapter include:

- Designing and fabricating an innovative brain-on-a-chip device composed of PDMS and vinyl, capable of sustaining live mouse brain slices within a microfluidic system.
- Comprehensive characterization of the entire system as an application for OOC, mainly focusing on brain-on-a-chip and validating its capacity to introduce volumes via injection into the microfluidic chip without compromising its integrity.
- Comparing the brain slice-on-a-chip culture with traditional plate culture systems for performance evaluation by fluorescence imaging (Figure 50).

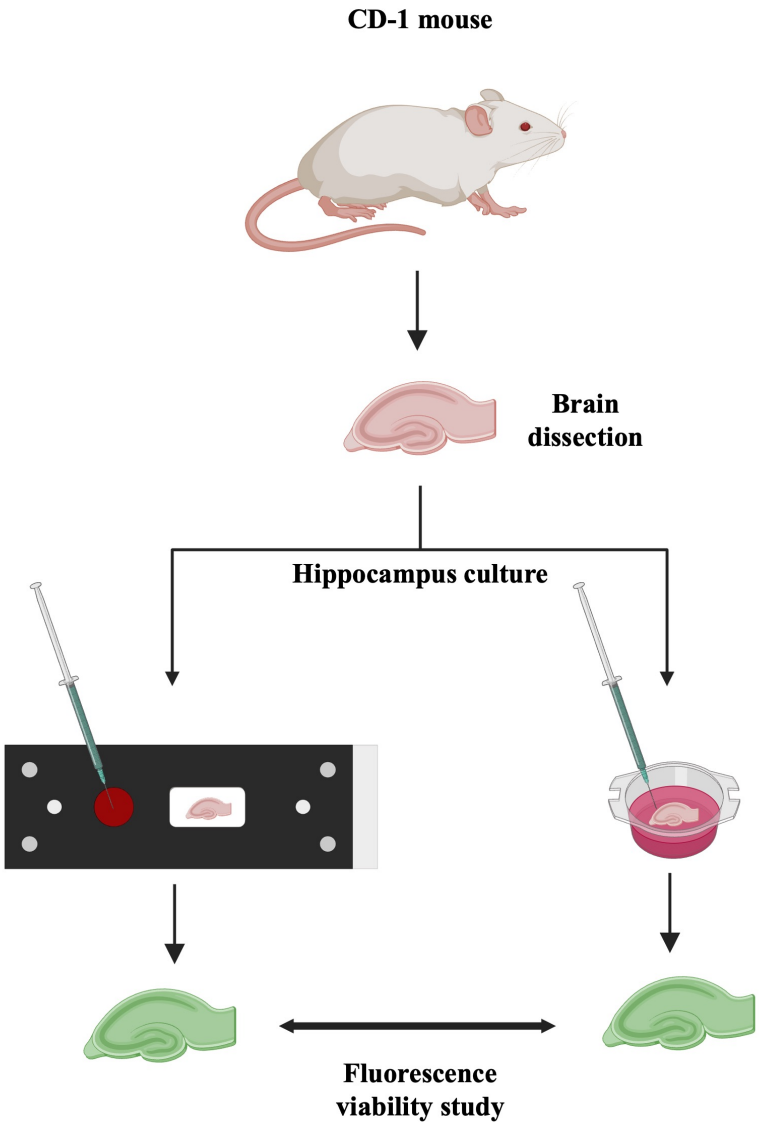

Figure 50. Workflow scheme of Chapter 5 based on the dissection of mouse brain slices, the hippocampal slice culture in organ-on-a-chip devices and membrane inserts and their fluorescent labeling. Created with Biorender.com

5.1 NEW ORGAN-ON-A-CHIP CONCEPT.

In the first stages of defining the microfluidic chip and the culturing method for brain slices, the Cortical Circuits group expressed a keen interest in culturing these tissues with specific requirements to achieve the best possible model replication. The primary and most significant requirement pertained to the choice of the culturing method. In the existing microfluidic literature, two distinct approaches are commonly used: one involves submerging brain slices entirely in culture media, which involves better preservation of the tissue cytoarchitecture but leads to reduced survival due to limited O_2 supply, while the other approach involves interphase cultures, where slices are cultured on a porous membrane, exposing the tissue to air. The latter method garnered the most interest, mainly because the conventional practice for hippocampal slice culture

involves using membrane inserts, so that there was a desire to replicate these conditions within the microfluidic chip.

Furthermore, the method for assessing the culture's status relied on the use of the fluorescent marker Oregon Green Bapta 488. This permeable marker has a high affinity for intracellular calcium, enabling real-time monitoring without harming cells or causing irreversible changes.

As a general principle, microfluidic chips offer a distinct advantage over traditional plate cultures due to their closed-system nature, reducing contamination risk. This property is beneficial but implies that the administration of reagent once the fluidic setup is in place can be challenging. Although options like connectors exist to facilitate reagent injection, one of the core principles guiding this doctoral thesis was to keep the microfluidic setup as basic as possible. This approach aimed to minimize experimental costs and ensure user-friendly chip manipulation.

The chip design phase could begin once the optimal culture conditions were established. Given the necessity to maintain the brain slices exposed to air, a single-chamber chip design was not feasible. Instead, it was imperative to create a microfluidic chip with two compartments: one to perfuse culture media and another to house the biological sample over a membrane. To accomplish this, the conceptual approach involved replicating a culture with membrane inserts inside a chip. Due to this reason, the chip design required the inclusion of a porous membrane that would separate the tissue from the compartment filled with culture media. In contrast, the other compartment would remain entirely empty.

With the chip's structure defined, the subsequent task involved determining the geometries of the microfluidic compartments. The layout of the lower compartment, which did not need to accommodate the tissue and only shared the central microfluidic chamber in contact with the brain slices through the porous membrane, was not critical in its design. Conversely, designing the upper compartment was more complex. The primary criterion for shaping this chamber was the size of the biological sample. For cell cultures, such as the previous bioapplication involving invertebrate neurons, the sample size was determined by the volume of the cell solution and the required observation area, which was based on prior work. In the case of brain slices, there was no standard value, as the size of the slices could vary depending on factors like the age of the mouse and the operator's dissection skills. The only constant dimension was the thickness of the slices, which remained at 400 µm. As a result, the dimensions of the upper layout were set at 15 x 8 mm to facilitate the placement of one with the option of placing an optional second slice. Due to the previous experience with the neuron-on-a-chip devices, there was an awareness of how to increase the number of brain slices without operating all the perfusion pumps simultaneously, which could replicate the temperature rise issue encountered with the incubator. With this

challenge in mind, it was decided that the upper compartment should be spacious enough to accommodate two slices simultaneously, thereby increasing the yield per chip.

Chip version	**Prototype 1**		**Prototype 2**		**Prototype 3**	
Layout	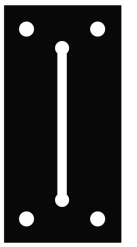		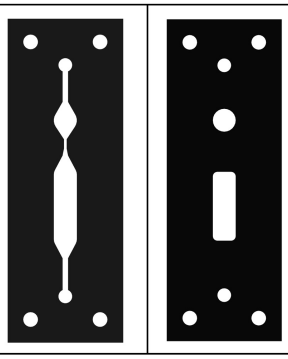		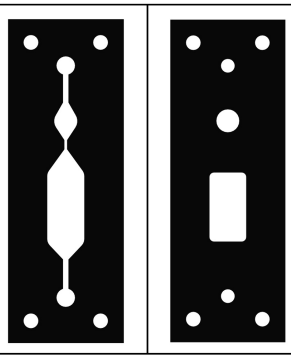	
Vinyl dimension	50 x 25 mm		70 x 25 mm		70 x 25 mm	
Vinyl thickness	600 µm	1500 µm	600 µm	750 µm	600 µm	750 µm
Chip volumen	43.57 µL	193.43 µL	93.89 µL	56.25 µL	135.70 µL	90 µL
Membrane area	42 mm^2	128 mm^2	75 mm^2		120 mm^2	

Table 9. Specifications of the brain slice-on-a-chip prototypes.

Similarly, an idea that had been previously tested with neuron-on-a-chip, the injection of volumes inside the chip, was also revisited. During experiments with neurons, it became evident that puncturing the PDMS block was not an real option without introducing contamination into the culture, as PDMS is not a self-sealing material. As a result, alternative materials were explored to fulfill this sealing requirement and facilitate integration into a microfluidic chip. PTFE emerged as a material capable of fulfilling this role, with PTFE membranes commonly used in reagent bottles to prevent moisture entry.

During the chip design phase, three different designs were proposed to meet the experiment's requirements (Table 9). The first prototype for culturing mouse hippocampal slices was made using 50 x 25 mm vinyl slices, but it lacked an injection pre-chamber due to space limitations caused by the vinyl's dimensions. Due to that, prototype 2 adopted a 70 x 25 mm format and included an injection pre-chamber. Finally, the last prototype (prototype 3) increased the

microfluidic chamber's dimensions from 75 mm² to 120 mm² to facilitate slice placement on the membrane.

5.1.1 Brain slice-on-a-chip design.

The final chip version developed for mouse brain slice culture is an adaptation of the concept of membrane insert plate culture adapted to a microfluidic chip format (Figure 51). This brain slice-on-a-chip prototype consists of PDMS, glass, and vinyl, featuring a single inlet and outlet for parallel flow. This new chip comprises two compartments: a lower one for the culture medium flow and an upper compartment where the brain slices are exposed to the air while staying in contact with fresh media through a porous PC membrane that separates and defines the upper compartment from the lower one. To meet the need for exposing the cultured tissues inside the microfluidic device to a fluorescent marker, the chip structure was designed to enable reagent injection inside the chip. An 8 mm circular PTFE piece was integrated into the top PDMS block to enable this process. Additionally, a pre-chamber was incorporated into the chip design within the lower compartment to retain any potential bubbles generated during the injection process.

Regarding chip construction, the glass slide remains as the base layer upon which the microfluidic chip is assembled, whereas the vinyl and PDMS layers were subjected to modifications. Two vinyl layouts were employed, each designated for a specific microfluidic compartment. The dimensions of the vinyl sheets were expanded to 70 x 25 mm to accommodate larger geometries on the chip.

The lower compartment layout includes an inlet channel, a pre-chamber, a hexagonal microfluidic chamber, and an outlet channel (Figure 51B). Conversely, the upper layout consists of a central rectangular area measuring 15 x 8 mm, designed to accommodate two brain slices simultaneously, along with a circular area for the injection pre-chamber (Figure 51C). The vinyl layers have thicknesses of 600 µm for the lower layout and 1200 µm for the upper layout.

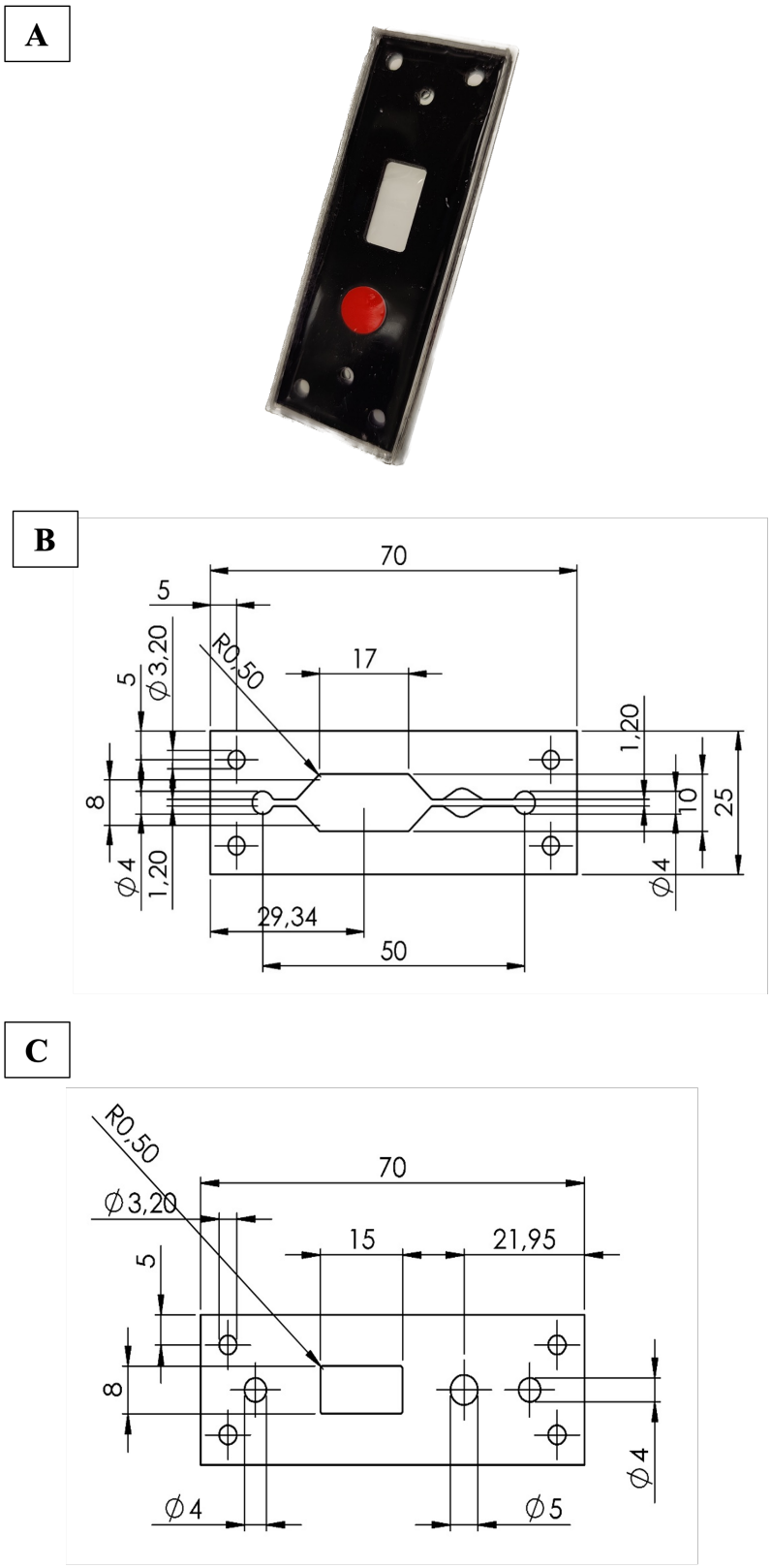

Figure 51. A) Picture of the final brain-slice-on-a-chip prototype. B) Lower layout dimensioned. C) Upper layout B dimensioned. The units of the layouts are represented in mm.

Several considerations influenced this chip structure. Firstly, the lower compartment features a single flow without inlets or outlets in the upper design. This design ensures fresh media is delivered beneath the cut-off, mimicking the approach used in membrane inserts. Furthermore, the absence of inlets and outlets in the upper chamber prevents the issue of having two outlets in a microfluidic chip, which could result in unintended pressure imbalances and unintentional filling of the upper chamber.

The second noteworthy feature is the incorporation of an integrated injection pre-chamber. Unlike the previously manufactured neuron-on-a-chip device, the inclusion of an injection system within the chip is vital due to the need for fluorescent staining for monitoring brain slices. Since the brain slice must remain isolated within its own chamber, the staining agent must be administered through the compartment subjected to the flow. The assumption underlying the chip's design was that by administering the dye through the lower chamber, the solution containing the fluorescent marker would permeate the membrane and label the tissue while keeping the tissue sealed. This approach offers an additional advantage: once the incubation period for staining the sample is completed, the flow can remove any excess stain, thereby reducing background interference in subsequent image capture. To ensure compatibility with the chip, modifications were made to both the upper PDMS block and the vinyl layers adding in the vinyl cuts a circular area (Figure 52). In the lower layout, this area is seamlessly integrated with the rest of the microfluidic architecture, whereas in the upper design, it is isolated to prevent direct interaction between the injected volume and the upper compartment of the chip.

The manufacturing process of the PDMS blocks also undergoes modifications similar to the vinyl cuts, adapting their dimensions to 70 x 25 mm. Due to this change, a new PLA mold had to be manufactured to define the new sizes of the PDMS blocks. The base-curing agent ratio is maintained at 10:1.5. The PTFE plug is integrated into the PDMS block during this curing process. Since the PDMS mix remains liquid, the plug can be positioned inside the 70 x 25 mm rectangles of the PLA mold. Thus, PDMS mix hardens, the plug will remain embedded inside the final cured block without the risk of accidental release.

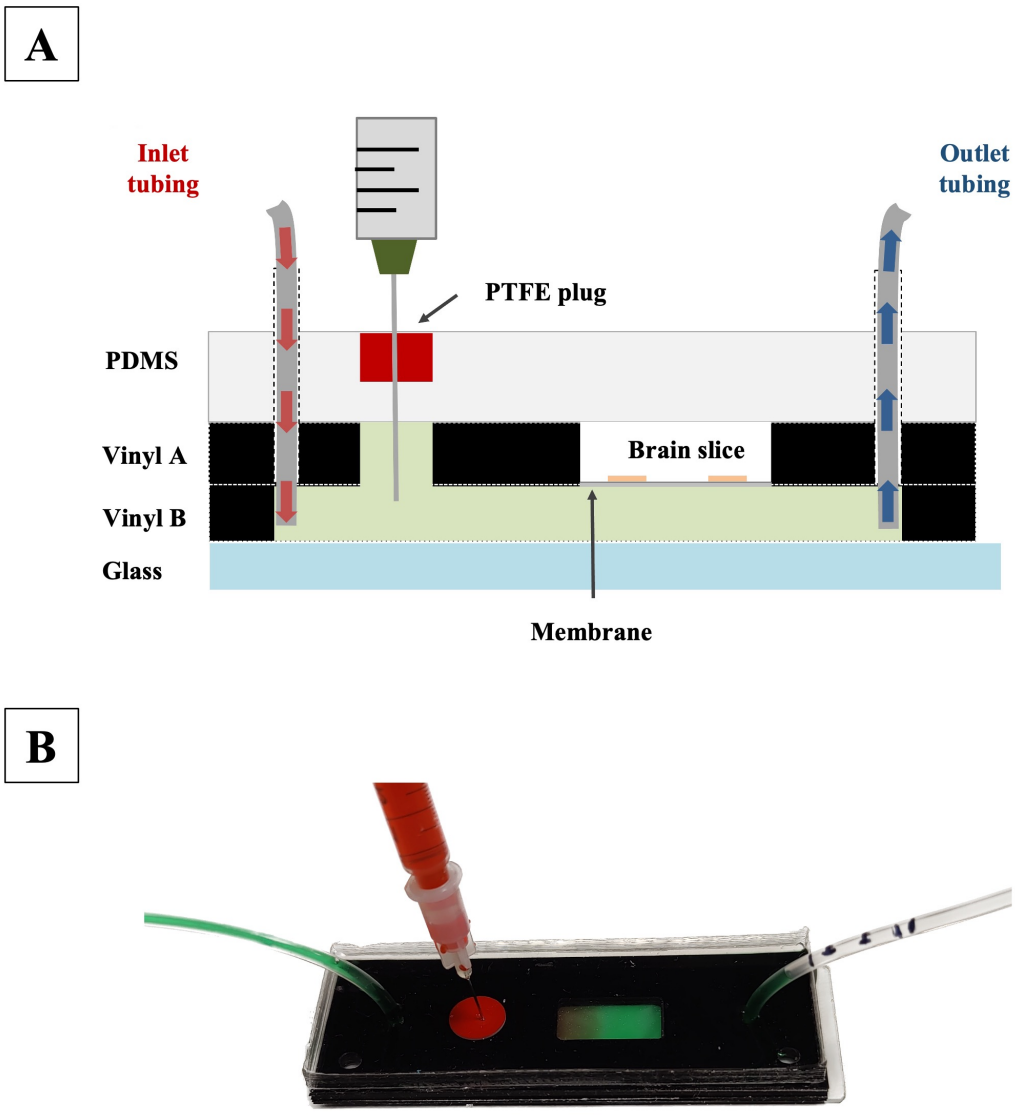

Figure 52. A) Cross section of the brain slice-on-a-chip device and representation of the injection system. B) Real injection test on a brain slice-on-a-chip. Extracted from (Herreros et al., 2022).

5.1.2 Brain slice-on-a-chip alternative chip fabrication process

The inclusion of the polycarbonate membrane as a separator dividing element between the upper and lower compartments necessitates a slightly different vinyl overlapping process. After attaching four vinyl cuts of the lower design, the membrane must be sandwiched between the lower design's last vinyl cut and the upper design's first one. This process, which may appear simple at first glance, is quite intricate. The membrane is extremely thin, measuring only 10 µm in thickness, making it prone to folding easily. Moreover, the membrane as a significant electrostatic charge, causing it to stick to any tool used for handling, such as tweezers. These two factors make it challenging to place the membrane onto the chips without creating folds. To

prevent this issue, a double-sided vinyl with adhesive properties is used to secure the membrane. Afterward, five vinyl sheets of the upper layout are added until the total thickness reaches 750 μm. Including these variations, the modified assembly protocol stands as follows:

1. A protective paper is positioned on the aligner's base, onto which the adhesive side of the first vinyl cut will be adhered. It was decided to begin the overlapping process with the upper layout because it was easier to place the PC membrane over the 15 x 8 mm rectangular area.
2. Four additional upper vinyl cuts are inserted into the guides through the circular notches at each corner of the vinyl cuts.
3. A double-sided vinyl is applied to facilitate the positioning of the PC membrane.
4. The PC membrane is placed onto the double-sided vinyl.
5. Four lower vinyl cuts are overlaid over the PC membrane.
6. A second double-sided vinyl is overlapped to flip the last lower vinyl cut to expose the adhesive side of the vinyl. An additional protective paper is used once the flipped vinyl cut is adhered.
7. The final piece of vinyl that includes both geometries delimited by the PC membrane is removed from the aligner tool and is adhered to a glass slide.
8. The glass-vinyl assembly is positioned on a hot plate and subjected to a heat treatment at 80 degrees Celsius while applying pressure using a weighted plate (5 kg) for 30 minutes. After this step, the glass-vinyl part of the chip is ready to be sealed with a PDMS block.

The primary deviation in the assembly procedure pertains to the introduction of the tissue into the chip. It is not feasible to introduce the tissue through the microfluidic channels. Additionally, even if it were possible to pipette the biological sample, the upper compartment, where the tissue is intended to be cultured, lacks inlets and outlets. Consequently, the only practical method for depositing the brain slices onto the membrane is to conduct this process prior to sealing the chip with the PDMS block.

This alteration in the assembly protocol makes the chip unsuitable for autoclaving before use. Instead, the sterilization protocol involves rinsing the bottom compartment with a 70 % ethanol solution and subjecting the top side of the membrane to 60 minutes of UV radiation exposure. To conclude the assembly process, the PDMS blocks are treated with oxygen plasma before placing the brain slices on the membrane. The plasma treatment conditions entail 80 W for 120 seconds. Following this treatment, the PDMS surface intended for bonding with the vinyl is exposed one more time to UV radiation within a laminar flow cabinet for 20 minutes. During these 20 minutes, the brain slices are placed on the membrane, and subsequently, the chip is sealed with the PDMS block containing the brain slices in the upper compartment.

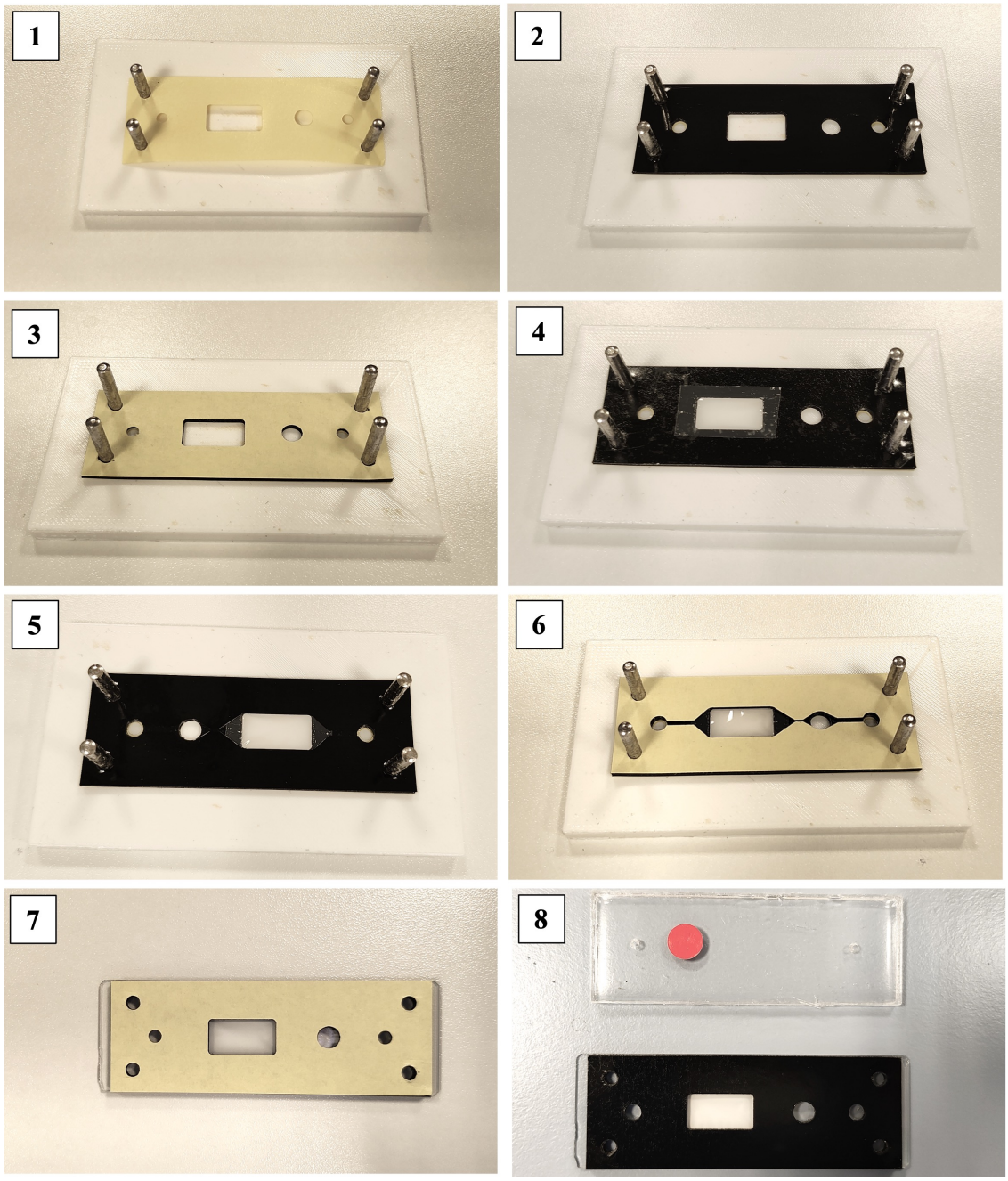

Figure 53. Brain slice-on-a-chip fabrication process. The number of the images are associated with the steps indicated in section 5.1.2.

5.2 SLICE PREPARATION AND CULTURE

After the obtention of the brain sections dissection protocol is explained in section 3.3.2), the slices were positioned onto a chip situated on a PC membrane. Once the slices were situated on the membrane, the chips were hermetically sealed with a PDMS block, and the lower microfluidic compartments were primed with fresh medium. A 1 ml syringe was filled with culture medium (DMEM-high glucose, 20% heat-inactivated horse serum, and 1% antibiotic and antifungal

solution) were connected to the chips and to a perfusion pump, with a flow rate set at 1 µl/min. The chips underwent incubation at 37°C and 5% CO_2 for several days, replacing the syringe every seven days.

Conventional organotypic hippocampal slice culture (OHSC) method was employed as a control. Hippocampal sections were transferred to cell culture PTFE inserts within P24 multiwell plates with 1 mL of medium, which was refreshed every three days.

5.2.1 Image acquisition

Due to the PC membrane's lack of transparency, direct observation of chip sections using an inverted microscope was not possible. Therefore, to capture images of the brain sections within the chips, an Olympus BX51 direct fluorescence microscope was employed. Conversely, the control brain slices, cultured on a hydrophilized PTFE membrane, became transparent when wetted, allowing them to be observed using a Leica DMI3000 B inverted microscope.

Despite the use of different microscopes for each culture methodology, an identical fluorescence labeling procedure using OGB was applied. The staining was administrated into the slices as follows:

- A stock solution of 5 mM OGB was made using a solution of 20% (weight/volume) Pluronic F-127 in absolute dimethyl sulfoxide (DMSO).
- The final volume used was 50 µL of OGB solution (20 µM) per culture.
- After four days since the beginning of the culture, the dye was injected into the pre-chamber of the chip using a 100 µL Hamilton syringe in the chips. In the OHSCs the dye solution was pipetted over the slices.
- The slices were then incubated for one hour in the culture incubator.
- The control membrane inserts were transferred to a new well to decrease the fluorescence background signal. In the brain slice-on-a-chips, a flow of 0.1 µL/min was set for the OGB incubation time to ensure that the dye penetrated the chip correctly.
- To remove excess OGB, the hippocampal slices were visualized one day after.
- During the imaging process, the chip remained sealed, enabling the analysis of the slices inside the chips in real time.
- Photographs were acquired using a direct fluorescence microscope (Olympus BX51) and an inverted fluorescence microscope (Leica DMI3000 B).

5.3 RESULTS

Five rounds of experiments were conducted to achieve these objectives. The initial four rounds involved mouse hippocampal slices, while the final experiment aimed to determine the feasibility

of culturing an entire hemisphere on one of the microfluidic chips. The primary focus of this work, aside from accommodating samples of varying sizes, was to emphasize the process of fluorescence labeling for brain slices. The major technological innovation lay in the integrated injection system, addressing the challenges that rendered this process unviable in the previous chapter of the thesis. Additionally, it aimed to confirm whether the OGB reagent, when administrated in the lower compartment, could effectively diffuse through the membrane, and label the brain slice cells. This hypothesis underpins the functionality of the microfluidic chip, and its validation is critical. Failure to confirm this hypothesis may necessitate reconsidering both chip design and OGB delivery methodology.

The results have been organized into five distinct sections, each corresponding to a different type of experiment. The initial four sections are focused on mouse hippocampal cultures and encompass the development and validation of the chip injection system. In section 5.3.5, the final subheading presents a proof of concept where an entire hemisphere slice was cultured on the chip, departing from the conventional practice of using isolated hippocampal sections.

Throughout the results section, microscopic images of the brain slices within the chips play a pivotal role in supporting the findings. Given that this thesis's primary objective revolves around showcasing a microfluidic chip's technological advancement, the analysis of hippocampal slices and their structural attributes is not exhaustive. It remains pertinent to compare the culture conditions of slices within a microfluidic system versus conventional culture conditions. Thus, a qualitative analysis comparing hippocampal slices cultured within the microfluidic chips to those cultured using standard methodologies in culture plates has been included in section 5.3.4.

5.3.1 Proof-of-concept of hippocampal slice culture on an organ-on-a-chip device.

The initial round of experiments involved the use of the first brain slice-on-a-chip prototype to test if the brain slices could be observe within the chip configuration with the new element, the PC membrane. As previously noted, the PC membrane incorporated into the brain slice-on-a-chip devices presented challenges related to membrane corrugation and opacity. Thus, the primary objective of this initial experiment was to capture microscopic images of the brain slices cultured on the chip. Therefore, this first experiment aimed to obtain microscopic images of the slices grown on the chip to assess whether this polycarbonate membrane could be used or whether it was necessary to use another type of membrane.

The samples were obtained through the manual dissection of a mouse brain, with the slices cut manually using a blade and then positioned within a mold featuring notches spaced 400 μm apart. Although manual cutting did not produce perfectly clean slices, these samples were suitable for

the initial culture as part of the proof of concept. Three microfluidic chips were employed, with two slices being placed in each chip. Images of the cultures are illustrated in Figure 54.

In the first OOC (OOC 1), brain slices were deposited onto the membrane via pipetting through the wider end of a glass Pasteur pipette. After the deposition, any excess culture medium was aspirated to prevent the slices from floating, remaining 20 μL of DMEM medium onto the slices to prevent desiccation. Unfortunately, the slices had overlapped by the time the 20 μL was introduced, rendering separation impossible.

For the second chip (OOC 2), each slice was pipetted individually and positioned at opposing sides of the microfluidic chamber to prevent the overlapping, and 10 μL of medium was pipetted onto each slice. The slice placement process for chip 3 (OOC 3) was the same as OOC 2.

Following the insertion of slices into the three devices, the chips were hermetically sealed using the top PDMS blocks, and the entire lower compartment was filled with culture medium. Subsequently, they were placed inside an incubator at 37°C, maintaining 5% CO_2 and humidity, for a five-hour incubation period. After this time elapsed, the condition of the chips was examined.

In OOC 1, it was observed that the initial drop, pipetted to sustain the humidity of the hippocampal slices, permeated through the membrane, causing the slices to overlap (Figure 54A). In OOC 2, there was a subtle filling of the upper chamber, and the visualization of the slices was impaired due to membrane irregularities (Figure 54B). Conversely, OOC 3 exhibited an empty upper chamber, enabling clear microscopic observation of the slices and facilitating the discernment of hippocampal morphology (Figure 55C).

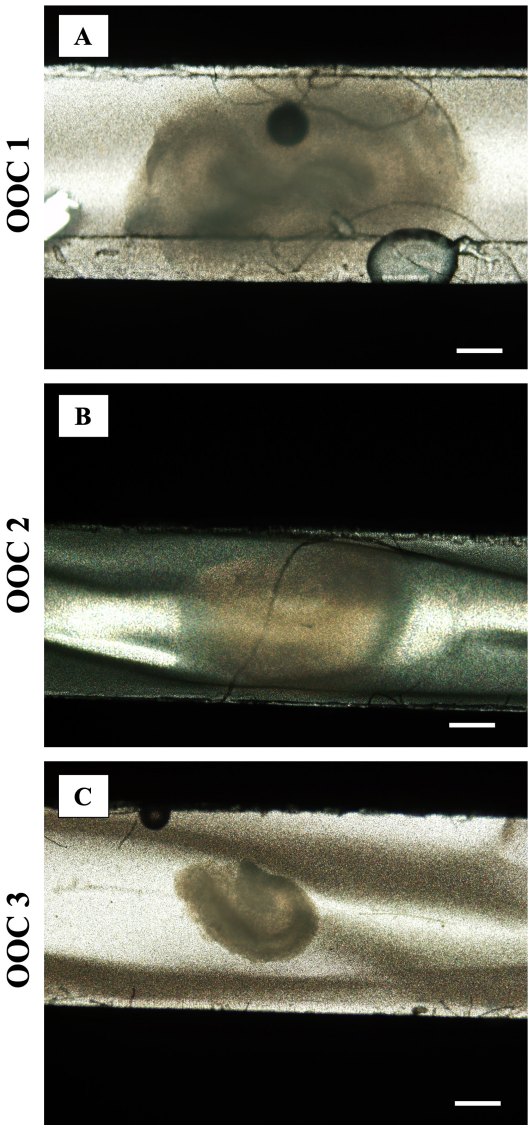

Figure 54. Hippocampal brain slices cultured on the first brain slice-on-a-chip prototype. Scale bars represent 200 µm.

The deductions drawn from this experiment underscored the necessity to increase the dimensions of the upper chamber, expanding the PC area on the chip, thereby mitigating membrane fold occurrences in the central region. Furthermore, it was critcal to introduce greater spacing between slices cultured on the same membrane to avert slice overlap.

5.3.2 Testing of the injection system and the OGB marker.

In the second round of experiments, the objective was to assess the feasibility of applying the OGB marker using the chip's injection system and evaluate whether the introduced staining in the lower compartment via the microfluidic system adequately labeled the tissue cells on the membrane's opposite side. The hippocampal slices were still manually prepared, resulting in slices from the mouse hippocampi that were not perfectly flat. This experiment highlighted two

key issues: the difficulty in evaluate the slices' state due to the membrane's optical characteristics and the impossibility of using an inverted microscope because of membrane opacity.

For this experiment involving OGB administration via injection, two chips with the prototype 2 configuration were employed. After obtaining the hippocampal slices and placing them on opposite areas of the membrane, 10 μL of the medium were pipetted onto each slice. Similar to the previous test, the chips were left stationary for 5 hours without flow, during which the pipetted volume diffused to the lower compartment in all four slices. After the initial 5-hour incubation, the chips were connected to a perfusion pump with a 1 μL/min flow rate. 24 hours later, the chips were examined to assess their condition. The first chip (OOC 4) exhibited leakage around the tubing entrance to the PDMS, resulting in the formation of a significant air bubble in the lower compartment. In contrast, the second chip (OOC 5) maintained a stable appearance with no air bubbles. Following this evaluation, 50 μL of OGB solution (20 μM) were injected into each chip. The perfusion flow rate was temporarily reduced to 0.1 μL/min for one hour to allow the injected volume in the pre-chamber to migrate to the lower microfluidic chamber while preventing complete washout of the lower microfluidic compartment and elution of the fluorescent solution. After 60 minutes, the flow rate was reverted to 1 μL/min, and in the subsequent days, microscopic imaging of the chips was conducted to check the presence of a fluorescence signal in the slices.

On DIV 4, fluorescence was observed in the hippocampal slices on both chips. In the OOC 4, yeast contamination and turbidity appeared in the slice cut, making it impossible to visualize the optical scattering produced by the membrane (Figure 55A,B). Notably, the waste reservoir remained uncontaminated and transparent. As a result, this chip was discarded, and the experiment continued with only OOC 5. Figure 55 illustrates that the fluorescence image provides a clearer view of the hippocampal morphology and various green intensities, offering improved tissue visualization compared to transmitted light photos. By DIV 6, a decline in the fluorescence signal within the slice was evident (Figure 55F), allowing an estimation of the fluorescent marker's duration on the chips.

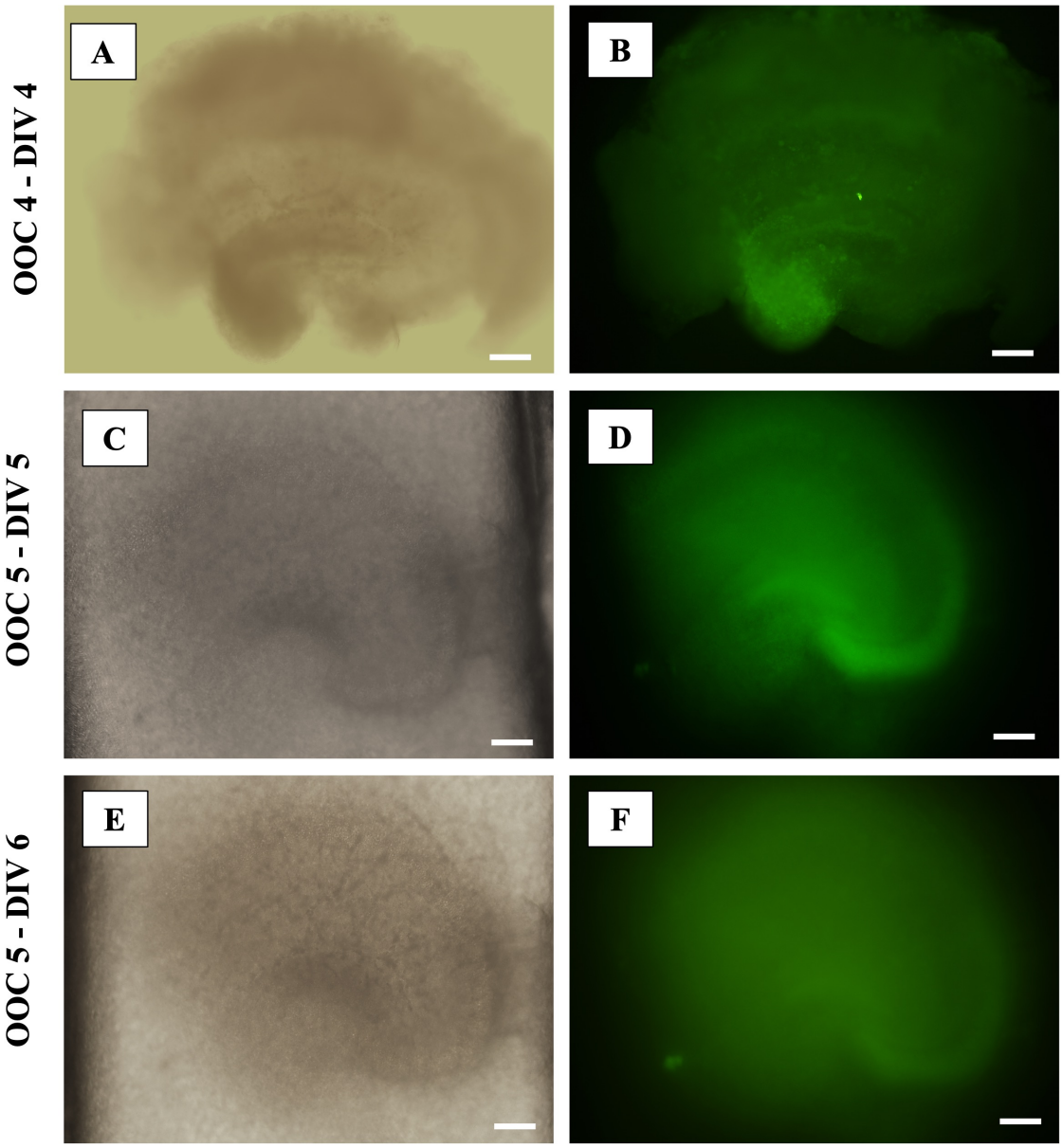

Figure 55 Pictures of hippocampal cultures on microfluidics chips after six days in vitro (DIV 6). Scale bars represent 200 µm.

These results confirmed the viability of the injection method for labeling hippocampal slices with OGB by puncturing the pre-chamber through the PTFE plug. It also demonstrated efficient labeling by introducing the fluorescent marker into the lower compartment without direct contact with the slice. The only concern was the origin of contamination in OOC 4. While OOC 5 remained uncontaminated, the perfused volume in the lower compartment of OOC 4 suggested that tissue contamination may have occurred during the initial dissection process when placing the slices on the membrane. Further replication of the injection process on additional chips was necessary to address these questions.

5.3.3 Long-term hippocampal slice culture assay

The third experiment employed the final chip design, with a single slice cultured on each chip. The primary objective was to maintain the viability of the slices for an extended period within the brain slice-on-a-chip and assess the long-term performance of the chip. By extending hippocampal cultures beyond 20 days from their initial placement on the chip. This extended culture period provided an opportunity to administer the fluorescent marker multiple times, considering the previous test results indicated a signal decline from day 5 onwards. Therefore, if the chip remained free from leakage and contamination, conducting multiple PTFE plug punctures would serve as an excellent opportunity to evaluate the reproducibility of the injection system. The chips used for this round of experiments were designated as OOC 7 and OOC 8.

A noteworthy achievement is the sustained maintenance of fluorescence signal within the chips for the entirety of the 26-day culture period. This extended observation period facilitated the detection of substantial alterations in the cytoarchitecture of the hippocampal slices, which were discernible under both transmitted light and the fluorescence signal of calcium, (Figure 56,57). Throughout the acquisition of fluorescence images spanning from DIV 5 to DIV 26, it is noteworthy that despite a gradual decline in the green signal emitted by the cells as days progressed, minimal background signal was evident within the chips. Furthermore, these findings affirm the OGB marker's efficacy as a robust fluorescence indicator for real-time tissue evolution studies.

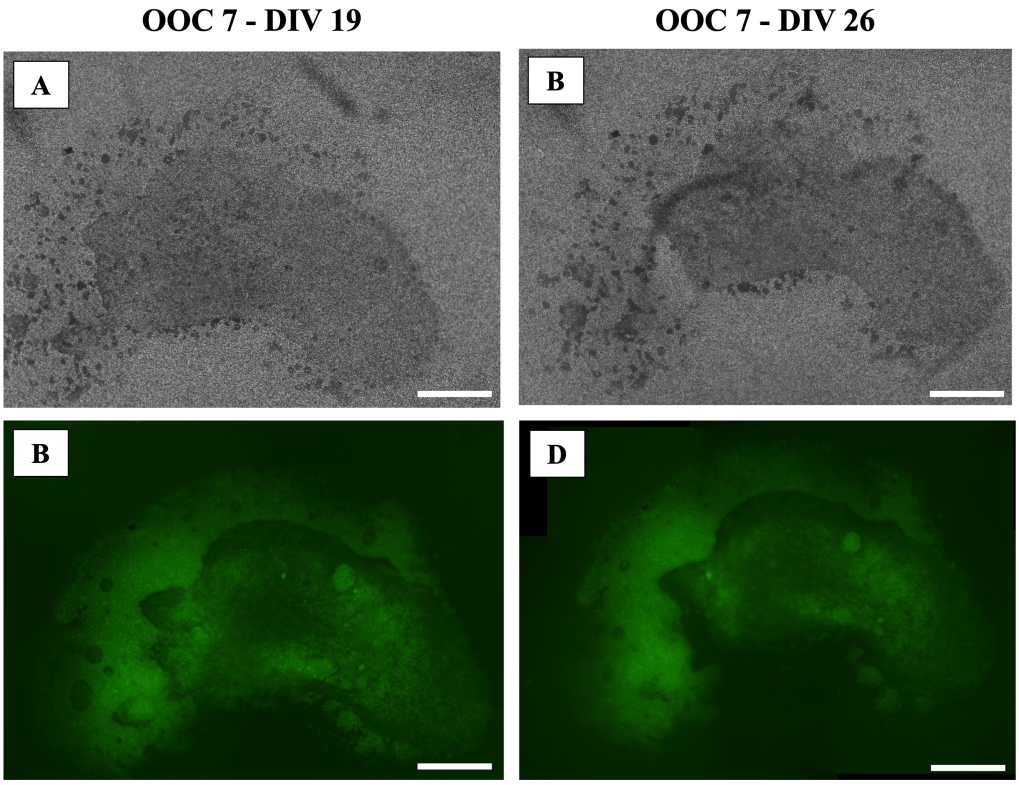

Figure 56. Images of hippocampal slices cultured on OOC 7 in DIV 7 and 26. Scale bars represent 200 µm.

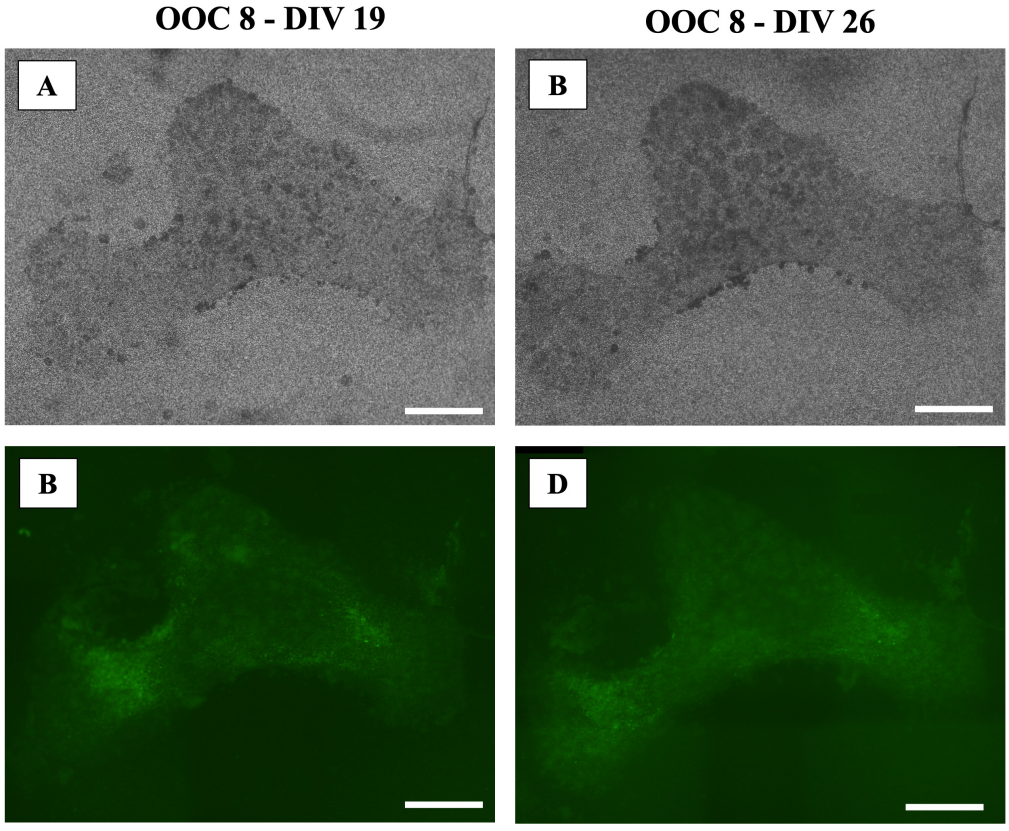

Figure 57. Images of hippocampal slices cultured on OOC 8 in DIV 7 and 26. Scale bars represent 200 µm.

Figure 56 and 57 demonstrated the capacity to evaluate morphological tissue changes over time with fluorescent staining procedures. This experiment confirmed the effectiveness of the OGB marker as a reliable fluorescent indicator for studying the real-time dynamics of tissue evolution.

The behavior of both chips exhibited similarities, including a recurring phenomenon: the gradual filling of the upper chamber within the chips over time. This issue was more pronounced in the OOC 7, with the liquid meniscus consistently positioned to the left of the hippocampal slice (Figure 58). In OOC 8, the filling was less significant, with excess liquid accumulating mainly in the chamber's corners. The cause behind this filling of the upper compartment in both chips was condensation occurring within the chips. Despite the continuous perfusion of culture medium through the lower compartments, the slices remained humidified on the membrane, contributing to the moisture in the upper compartment. Notably, condensation became visibly apparent on the PDMS over the membrane area every time the chips were removed from the incubator. In this test, the chips spent extended periods outside the incubator due to the need for multiple OGB solution injections and longer microscopy sessions, approximately 30 minutes per hippocampal slice daily.

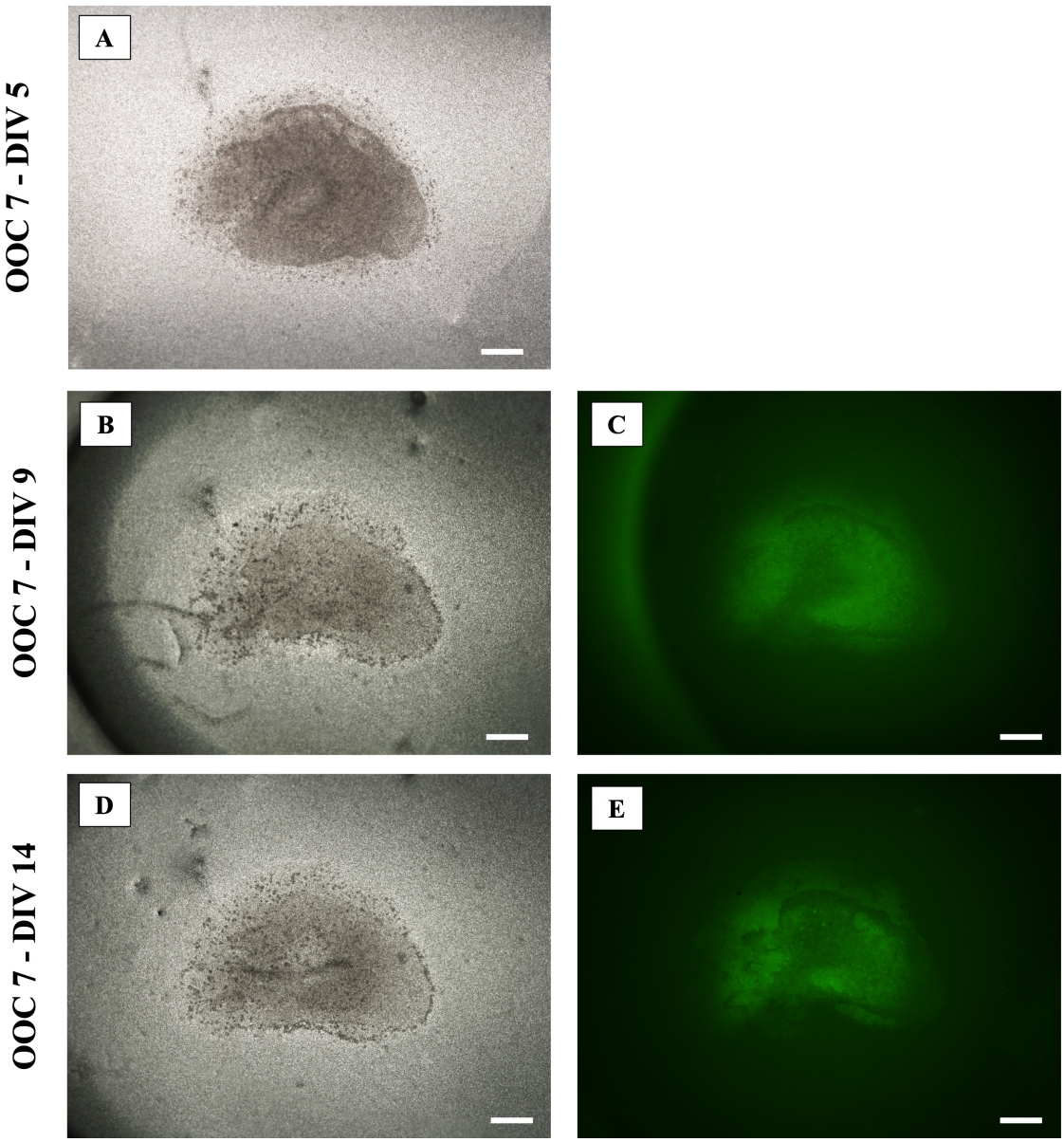

Figure 58. Brain slice culture evolution in OOC 7. Scale bars represent 200 µm.

The evolution of the hippocampal slices differed between the two chips. In the OOC 7 chip, a noticeable loss of cytoarchitecture was observed in the superior zone of the slice cortex, with this phenomenon being more pronounced in the left section. This observation corresponded with the filling of the left portion of the upper chamber due to condensation. In Figure 58B and C, it is evident how the brain section was close to the meniscus of the condensation-induced droplet. Both the transmitted light and fluorescence images depicted this phenomenon. Interestingly, the fluorescence images revealed a green halo with a dotted pattern in the signal, suggesting potential cell migration rather than cell death.

Conversely, the images from the OOC 8 did not display the same tissue behavior (Figure 59). In this case, the hippocampal slice did show some indications of cell migration, primarily in the cerebral cortex region. From DIV 9 onwards, the images indicated a substantial shrinkage of the

slice, resulting in the near-complete loss of its morphology by DIV 14 (Figure 59D,E). The degeneration of the hippocampus persisted until day 26, marking the culture period's end.

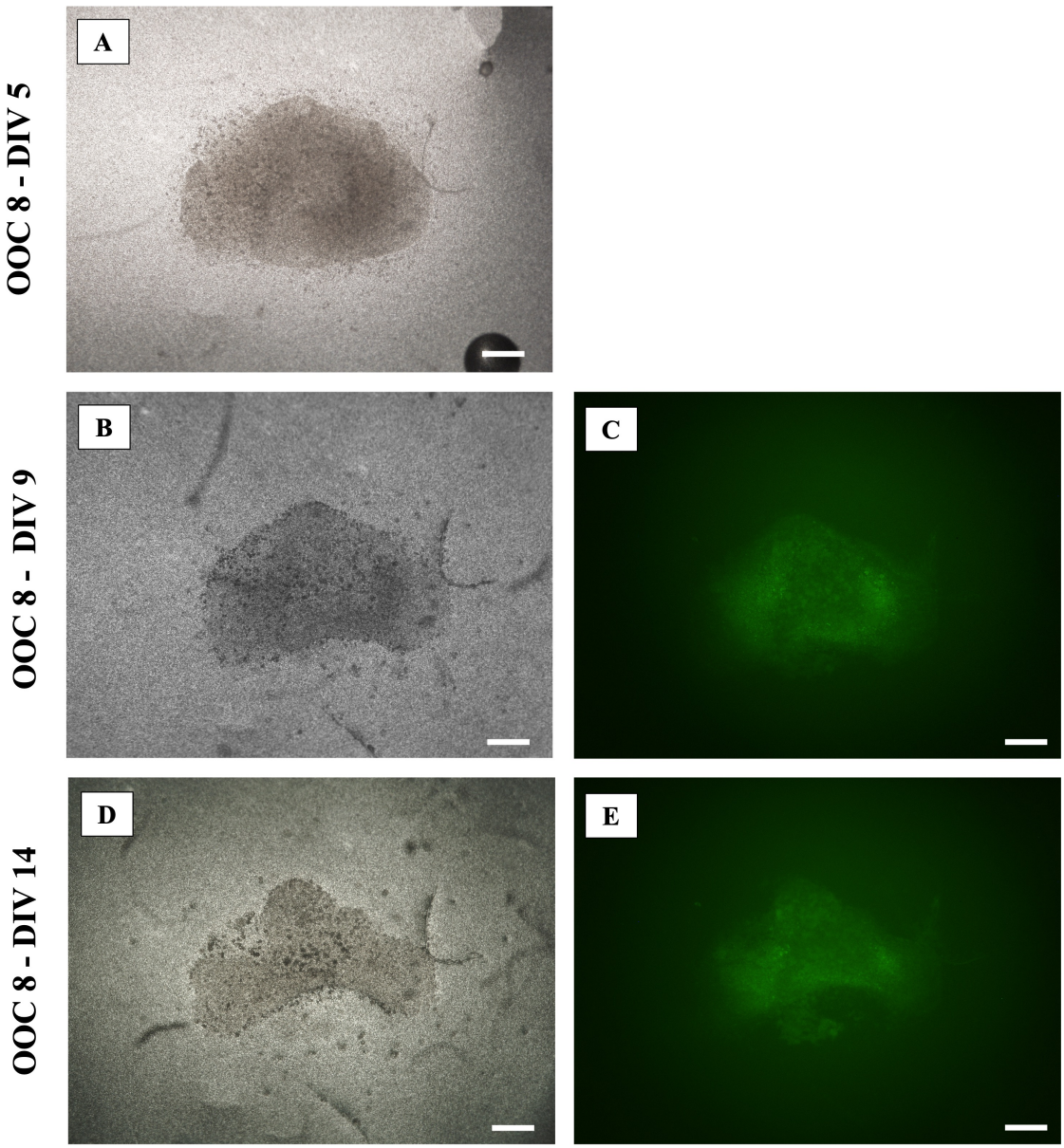

Figure 59. Brain slice culture evolution in OOC 8. Scale bars represent 200 µm.

Following the disconnection of the chips from the microfluidic system, an immunohistochemistry assay was attempted to assess the slices, particularly to stain different cell types within the brain. Using a scalpel, the PDMS and membrane were carefully separated in the upper compartment area. Despite this, once the membrane was removed from the chip and placed in a petri dish with PBS to extract the hippocampal slices, they disintegrated entirely, rendering the analysis impossible.

5.3.4 Hippocampal slices on chip vs culture of hippocampal slices on culture plates

Finally, a final series of experiments was conducted to prepare a second scientific article to showcase the technological advancements achieved with the chip. This article would emphasize the chip's design and development, highlighting the innovations of this brain slice-on-a-chip compared to the neuron-on-a-chip described in Chapter 4. As previously discussed, staining techniques have limitations in detecting minor changes in brain slice cultures, even when using sections from the same hippocampi. To overcome this limitation and identify significant qualitative differences over time, an analysis of the fluorescence labeling pattern of OGB was performed in both the chip and OHSC as control cultures. A total of three brain slice-on-a-chip devices (OOC 9,10, and 11), each containing two hippocampal slices, were employed for these experiments. Brain sections were obtained using a chopper, resulting in straight cuts with a thickness of 400 μm. Every brain slice was administered with 20 μL OGB solution on days 5 and 10 of culture.

All six chip slices remained in good condition during the initial 7 days of culture. After that period, both OOC 9 and OOC 11 chips began to experience partial filling of the upper compartment, leading to water accumulation around the edges of the vinyl. Consequently, the assessment of the slices was based on images captured on DIV 5 and DIV 10 when all hippocampal slices remained exposed to air.

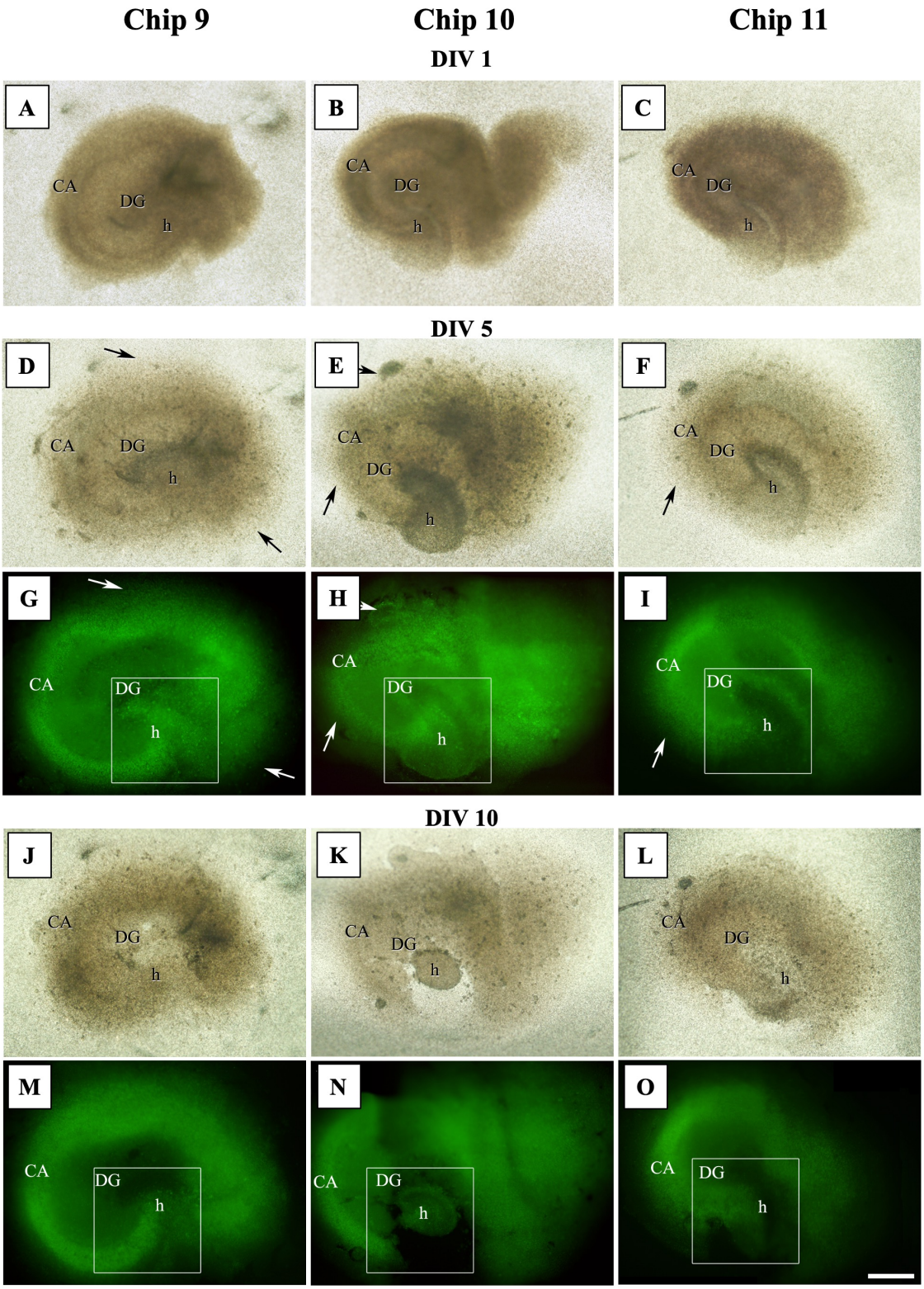

Figure 60. Culture of mouse hippocampal slices on brain slice-on-a-chip devices. The images show brain sections placed into Chip 1 (A, D, G, J, M), Chip 2 (B, E, H, K, N), and Chip 3 (C, F, I, L, O) at 1, 5 and 10 days in vitro (DIV). Scale bars represent 500 µm in (A–F, J–L) and 400 µm in (G–I, M–O). Extracted from (Herreros et al., 2022).

OGB proved highly effective in labeling nearly all living cells, allowing for the clear differentiation of cytoarchitectonic features within various hippocampal subregions, including the

cornu Ammonis subfield (CA), dentate gyrus (DG), and hilus (h) (Figure 60G-I, M-O). Notably, there was a noticeable but gradual reduction in size, particularly in section thickness noticeable in DIV 5 (Figure 60D-F) when compared to DIV 1 (Figure 60A-C), with this reduction becoming more significant by DIV 10 (Figure 60J-O).

The evaluation of OHSC involved two critical criteria: alterations in transparency and cellular distribution. As illustrated in Figure 61, the slices exhibited a general shift in color and transparency, evolving from a brownish opaque appearance at DIV 1 to a light brownish-transparent quality during the first week. Additionally, there was observable cell growth at the section's edge. Comparatively, there were no discernible changes in the overall OGB labeling distribution pattern across hippocampal subregions between the chip slices and the OHSC up to DIV 10 (Figure 61). The progressive reduction in section thickness was less pronounced in the OHSC when compared to the chip slices.

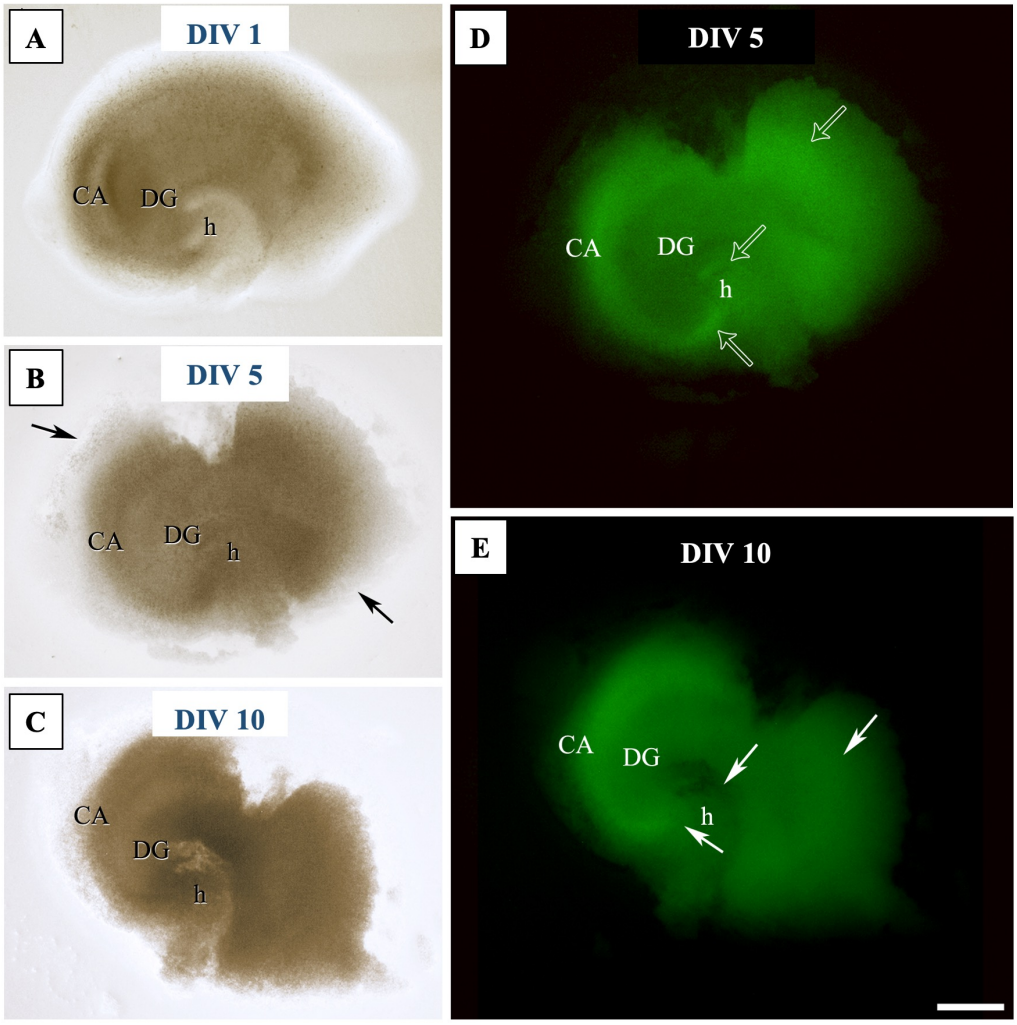

Figure 61. Hippocampal OHSC in P24 well plate controls. Images from a slice placed onto a cell culture insert at 1 (A), 5 (B, D), and 10 days in vitro (DIV) (C, E). Scale bar in E indicates 510 µm in (A–C) and 480 µm in (D, E). Extracted from (Herreros et al., 2022).

Complete attachment of the hippocampal sections to the PC membrane occurred at DIV 7 in the chip, while this process took place at DIV 14 in the PTFE membrane insert. Notably, better preservation of the characteristic hippocampal cytoarchitecture was observed in the chip compared to the OHSC at DIV 5 (Figure 60D-I and Figure 61B,D).

From a technological perspective, integrating an injection system for delivering reagents within the chip goal was successfully fulfilled.

5.3.5 Hemisphere slice culture on the brain slice-on-a-chip device.

During the initial phases of chip design, the primary intention was to cultivate mouse hippocampal slices on the chips, as there was a specific interest in analyzing this particular brain region. While the latest mouse hippocampal cultures were being developed, a final culture possibility was raised for the final brain slice-on-a-chip prototype, the culture of an entire hemisphere in microfluidic chips. This approach aimed to maintain the hippocampus in a more integrated state within the context of the whole brain tissue. Only one experiment was conducted using two microfluidic chips. Sealing was unnecessary in one of these chips as the cut fit neatly within the upper compartment. In the second chip, the sealing process was executed, but the lower region of the hemisphere remained folded along the edge of the upper chamber. Following one day of culture with perfused medium at a flow rate of 1 µL/min, OGB was injected into the hemisphere slice with the same concentration and incubation times as applied to the hippocampal slices. The chip's evolution was monitored over seven days. The results obtained are presented in Figure 62. Similar to the evaluation made in mouse hippocampal slices, there was a notable migration or expansion of cells in the peripheral regions of the hemisphere slice. In this case, the hippocampal region maintained its cytoarchitecture more effectively than the isolated hippocampal slices in the previous tests. Unfortunately, these experiments could not be replicated due to the need to design a new microfluidic chip layout that could seamlessly accommodate hemispheres. Moreover, the primary objective was to design and fabricate a microfluidic chip tailored for the solitary culture of hippocampal slices. Nevertheless, this proof of concept still validates the correct functioning and diffusion of the OGB when administered through the lower compartment of the chip.

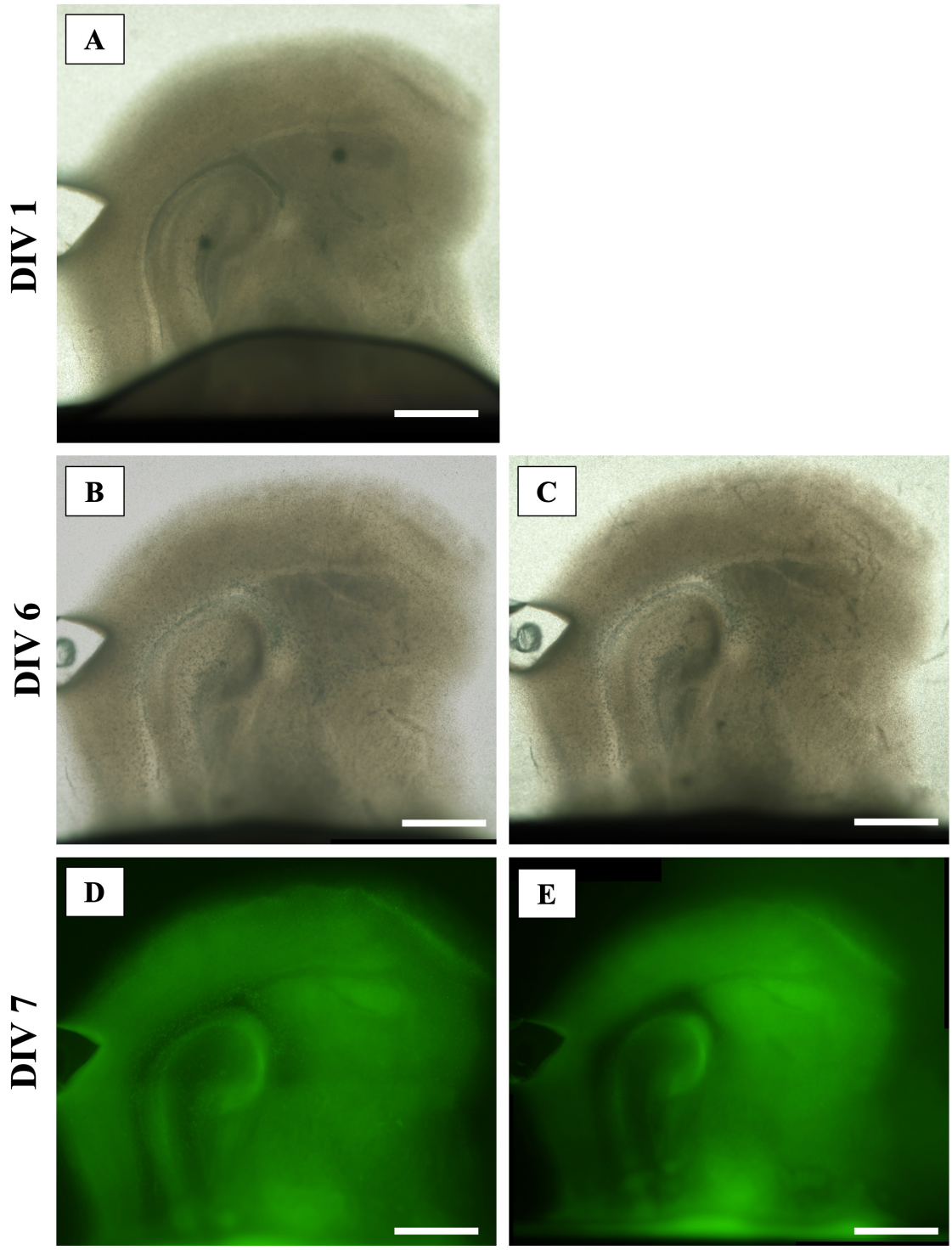

Figure 62. Hemisphere slice culture evolution in OOC 5. Scale bars represent 500 µm.

5.4 CONCLUSIONS

In this chapter, a brain slice-on-a-chip device featuring two microfluidic compartments designed for the culture of mouse brain slices has been designed and manufactured. The fabrication methodology outlined in Chapter 4 of this thesis was adapted to meet the unique requirements of the new tissue culture system. The adaptation of traditional plate culture conditions, employing

membrane inserts, to a microfluidic chip where brain slices remain exposed to air, a critical requirement for this bioapplication, has been achieved. The efforts in this chapter extended beyond the mere culture of brain slices in an OOC:

1. An injection method for the microfluidic device was developed, enabling the administration of a fluorescence marker into one of the chip's compartments, a capability that was not feasible with the prototype designed for neuron culture. Incorporating a piece of PTFE within the PDMS blocks facilitated the ability to inject reagents into the chip.

2. Throughout various cultures conducted in this chapter, the efficacy of this system was rigorously assessed, with the same PTFE piece repeatedly employed without encountering any contamination issues. This new feature of the chip not only permits the injection of fluorescent markers but also offers opportunities for administering various liquids, including drugs for evaluating different therapies in culture, or even seeding cells on the chip using this system.

3. Using this injection methodology, mouse brain slices were successfully fluorescently labeled, with real-time fluorescence images of the slices captured without the need to remove the brain sections from the chip (Herreros et al., 2022).

4. These images of the slices cultured on the chips enabled an assessment of the preservation of tissue cytoarchitecture compared to samples cultured through conventional methods. The results obtained demonstrated a better preservation of brain slice cytoarchitecture when utilizing the microfluidic chip compared to traditional culture methods.

6 SKIN-ON-A-CHIP

At this stage in the thesis, where the fabrication process of OOC devices has achieved a stage of maturity, the next phase involves the design of new OOC models based on a new organ, the skin. This task involved not only determining the chip's layout and configuration but also selecting the specific cell types for culture within the device. This circumstance presented a more significant challenge compared to the two previous bioapplications, which were centered around adapting predefined culture conditions for traditional static plate models. In this context, it became imperative to establish factors such as the cell type to be employed, the initial cell concentration per chip, and the optimal flow rate necessary for sustained, long-term culturing.

From a chip design perspective, a greater reconfiguration was necessary. Given that skin is a stratified tissue (Figure 63), the ideal model for this thesis should manifest as a 3D skin-on-a-chip (SOC) model. To achieve this objective, the design and fabrication protocols underwent final modifications to produce dual-chamber OOC devices capable of concurrently accommodating two parallel flows. In this context, the objectives of Chapter 6 of this thesis encompass the following points:

- Design and fabrication of a skin-on-a-chip device featuring two microfluidic compartments to enable the application of two simultaneous flows.
- Characterization of the microfluidic chip to assess the membrane diffusion capacity and chip well-functioning.
- Recreation of a skin model by co-culturing fibroblasts and keratinocytes on microfluidic chips.
- Integration of immune system cells into the skin-on-a-chip model in a SOC model.
- Establishing a melanoma-on-a-chip model to conduct on-chip drug testing against tumor cells as a proof-of-concept.

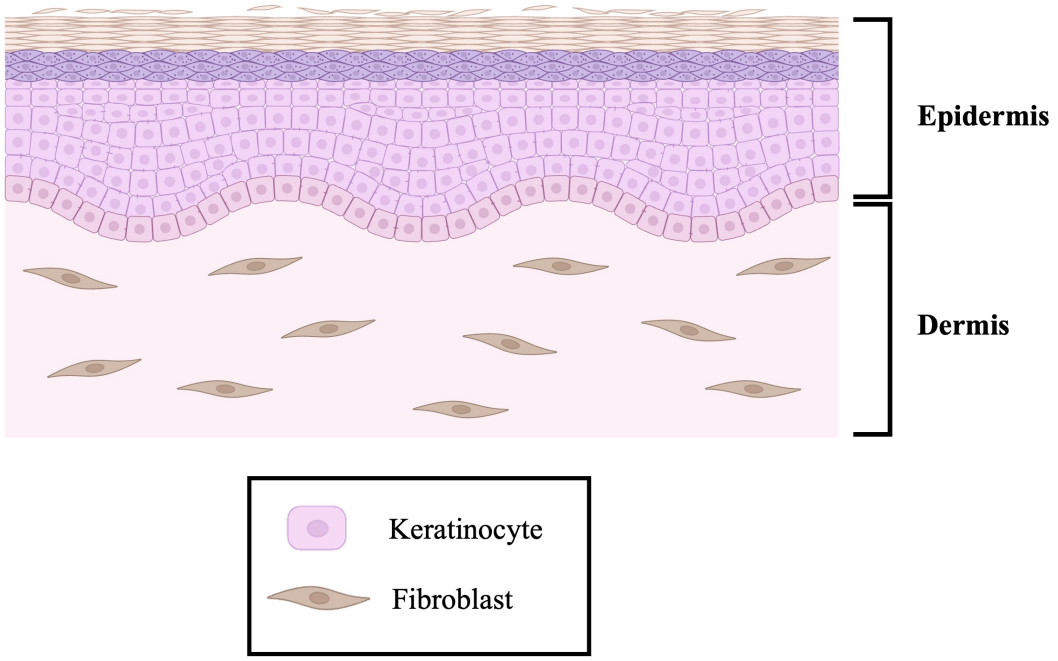

Figure 63. Simplified schematic representation of the skin structure. Created with Biorender.com

6.1 UPGRADED DESIGN.

The skin model to be recreated on the microfluidic chip consists of two compartments separated by a porous membrane at the central area of the chip. This chip design must enable the culture of fibroblasts, keratinocytes, and melanoma cells on the membrane in the upper compartment, while ideally immune system cells are cultured in the lower compartment. In terms of design, after fabricating the brain slice-on-a-chip with two fluidic chambers and flow supply through the lower compartment, the following step was to design a chip capable of supporting simultaneous parallel dual flows in the two geometries.

The chip's structure is maintained using glass as the bottom layer. Vinyl defines the microfluidic geometries, and PDMS blocks with integrated PTFE plugs are used as the top layer. The material that changed from the brain slice-on-a-chip was the PC membrane, which was replaced with a 0.4 µm PET membrane with a thickness of 100 µm. The issues with the previous membrane included poor sample visibility, as it was opaque and unsuitable for use with inverted microscopes, and the presence of corrugation due to its thinness. A literature search was conducted on the types of membranes suitable for skin cell line culture (Ponmozhi et al., 2021; Risueño et al., 2021; Sutterby et al., 2020).

The selected membrane material was PET. Since this specific membrane could not be purchased from a supplier in an individual format, commercial membrane inserts for 6-well plates (Greiner)

were acquired, and the membranes were removed from the inserts and then integrated into the chip.

Design	Layout	Vinyl thickness	Chip volume	Channel size	Channel dead volume
Prototype 1		750 µm	88.73 µL	1 mm	50.23 µL
		750 µm	65.01 µL	1 mm	26.51 µL
Prototype 2		600 µm	76.63 µL	1 mm	45.83 µL
		150 µm	7.70 µL	2.5 mm	-
		600 µm	60.52 µL	-	29.72 µL
Prototype 3		600 µm	76.63 µL	1 mm	45.83 µL
		150 µm	7.70 µL	-	-
		600 µm	70.98 µL	2.5 mm	40.18 µL

Table 10. Specifications of the most relevant skin-on-a-chip prototypes.

The advantages of this PET membrane include its suitability for cell culture, potentially eliminating the need for membrane biofunctionalization when working with adherent cells, and its stiffness. Increasing the thickness of the membranes enhances their stiffness, preventing rippling when placed inside the chip. The downside of having a less flexible membrane is its inability to deform or compress when placed between two vinyl sheets, creating micro-air chambers between the vinyl layers. This issue was problematic as these air zones within the chip are potential points for leaks. To minimize the risk of leakage, the chip configuration is defined by a larger number of vinyl designs.

Table 10 illustrates the three SOC versions used to create a functional device without leakage risks and their technical specifications. During the chip design phase, two specific guidelines

remained unaltered: maintaining vinyl cut dimensions at 70 x 25 mm to increase the working area and accommodate larger geometries and integrating an injection pre-chamber in the upper compartment.

The final SOC device consists in three designed layouts used to fabricate the SOC (Figure 64). In this chip, the pre-chamber located is in the upper compartment, and the dimensions of the microfluidic channels are more extensive in the lower layout compared to the upper one. An additional intermediate design was created to delimitate the common area between the upper and lower layouts. This extra intermediate design is beneficial as it simplifies membrane placement on the chip, requiring coverage only in the central area of the layout, and provides a larger surface for adhering the membrane to the vinyl.